

COMPOSITIONAL AND TOPOGRAPHICAL ANALYSIS OF
ELECTRONIC AND MAGNETIC FILM MATERIALS USING
SCANNING ELECTRON MICROSCOPY

THESIS

Presented to the Graduate Council of
Southwest Texas State University
in Partial Fulfillment of
the Requirements

For the Degree

Master of SCIENCE

By

Michael L. Matheaus, B.S.

San Marcos, Texas
December, 2000

COPYRIGHT

by

Michael Lynn Matheaus

2000

I would like to dedicate this thesis to my friends and loved ones for their kindness and support, who have encouraged and inspired me to complete this endeavor.

ACKNOWLEDGEMENTS

I would like to thank Dr. Carlos J. Gutierrez, for his mentorship, being my thesis advisor, and giving me the opportunity to work on this project. I would also like to thank the former and present graduate students: Charles Watts, Paul Person, Kevin Wiederhold, and Nelson White for their assistance in writing this thesis and their friendship. I would like to extend my gratitude to my committee members, Dr, Victor Michalk, and Dr. David Donnelly, for their participation and additional guidance. I would also like to thank my family for helping me through this time.

December 8, 2000

TABLE OF CONTENTS

LIST OF TABLES.....		viii
LIST OF FIGURES.....		ix
CHAPTER		Page
1	INTRODUCTION	1
1.1	THE IMPORTANCE OF MATERIAL ANALYSIS FOR THE IC INDUSTRY	1
1.2	SURVEY OF SEM/EDS ANALYSIS TO SEMICONDUCTOR	3
1.3	THESIS PROJECT GOALS.....	5
2	THEORY AND OPERATION OF SCANNING ELECTRON MICROSCOPY	7
2.1	SEM HARDWARE.....	7
	2.1.1 ELECTRON GUNS.....	7
	2.1.2 ELECTRON BEAM COLUMN	14
	2.1.3 SAMPLE CHAMBER.....	18
2.2	ELECTRON-SPECIMEN INTERACTION	18
	2.2.1 ELASTIC COLLISIONS	18
	2.2.2 INELASTIC COLLISIONS	19
	2.2.3 TYPES OF ELECTRON SIGNALS RELEASED BY SAMPLE.....	20
	2.2.4 EXCTATION VOLUME.....	24
2.3	DETECTORS	27
	2.3.1 SECONDARY ELECTRON DETECTOR.....	28
	2.3.2 BACKSCATTERED ELECTRON DETECTOR....	30
2.4	ENERGY-DISPERSIVE X-RAY SPECTROMETER	31
	2.4.1 X-RAY DETECTOR.....	32
	2.4.2 DETECTOR ELECTRONICS.....	34
	2.4.3 QUALITATIVE X-RAY ANALYSIS.....	36
2.5	DISPLAY SYSTEM	39
2.6	VACUUM SYSTEM	40
	2.6.1 LOW VACUUM PUMPS	40
	2.6.2 HIGH VACUUM PUMPS	42
	2.6.3 ULTRAHIGH VACUUM PUMPS.....	43

3	SAMPLE DATA AND ANALYSIS	45
3.1	SAMPLE PREPARATION AND ANALYSIS TECHNIQUES	45
3.2	SECONDARY AND BACKSCATTERED ELECTRON IMAGES	54
3.3	EDS IMAGES	72
4	CONCLUSION EDS IMAGES	101
	APPENDICES	105
	APPENDIX A	106
	APPENDIX B	126
	APPENDIX C	128
	APPENDIX D	130
	BIBLIOGRAPHY	131
	VITA	132

LIST OF TABLES

Table 3.1.1. Magnification and scanned sample area relationship. Adopted from Goldstein.	52
Table A.1. Beam current obtained for given accelerating voltages and spot sizes.....	130

LIST OF FIGURES

Figure 2.1.1. Schematic of a tungsten hairpin filament.	9
Figure 2.1.2. Schematic diagram of LaB ₆ direct plug-in replacement for a tungsten hairpin filament. Reference 5.	10
Figure 2.1.3. An example of a FE source, a single crystal wire spot welded to a W wire. Reference 5.	11
Figure 2.1.4. Gun characteristics. Adopted from Gabriel. Reference 4.	12
Figure 2.1.5. Beam current vs. diameter for a W-tungsten filament, LaB ₆ , FE-field emission. Reference 6.	13
Figure 2.1.6. SEM column with electron gun, lens, and specimen emitting data signals.	17
Figure 2.2.1. Creation of characteristic x-rays in the Bohr model atom. Adapted from Gabriel. Reference 4.	24
Figure 2.2.2. Examples of low and high atomic number (Z) sample excitation volume with different accelerating voltages. Reference 6.	25
Figure 2.2.3. Depth of origin of the data signals released by the sample during beam interaction. Reference 6.	27

Figure 2.3.1. A schematic of a SEM chamber with specimen excitation volume, showing relative originating depth of data signal, and common detectors used in their locations. 28

Figure 2.3.2. A schematic of an Everhart-Thornley detector showing the curved path which the secondary electrons due to their attraction to the positively charged Faraday cage. Reference 4. 29

Figure 2.3.3. A schematic of a solid-state backscattered electron detector placed under the optical or final lens. Reference 4. 30

Figure 2.4.1. A schematic of a Li-drift silicon detector. Reference 5. 32

Figure 2.4.2. X-ray counts vs. x-ray energy graph showing overlapping peaks. Reference 6. 35

Figure 2.4.3. X-ray spectra with two ROI chosen. Reference 6... 36

Figure 3.1.1. Electron beam current vs. Accelerating voltage: a) when beam is aligned, b) when beam is misaligned. 51

Figure 3.2.1. Secondary electron images taken using 20 kV, tilt of 45°, at 16X, but different beam diameters. Note that the image in a is sharper and has more resolution than in b. Images a, and b were taken using a spot size of 8 and 2 respectively. 56

Figure 3.2.2. Images a and b are secondary electron images,

while c and d are backscattered images of AFM tips taken at different accelerating voltages at 16X and a tilt of 45°. Images a and c were taken using 5kV, while b and d with 20kV. Notice that all the images are brighter at higher voltages, but this is especially true for the backscattered images. 58

Figure 3.2.3. High magnification secondary images using 5 and 20 keV, of the middle AFM tip in figure 3.2.1. Notice that increases of accelerating voltage, increases the resolution, as well as reduces the shadowing, as more electrons are emitted from deeper in the sample, reducing the effects of surface shape. 59

Figure 3.2.4. Secondary images taken at two different accelerating voltages, a with 5kV and b with 20kV, at a tilt of 67° and at 1500X, of an unknown residue left on the surface of a SiO₂ sample after etching. Notice that the shadowing effect is not noticed, as well as the increase in brightness in the bottom image, as the voltage was increased. 61

Figure 3.2.5. Comparison of tilt has on secondary images taken using 20kV at 16X using a tilt of 45° for a and b using 67°. Notice that the brightness decreases as tilt is increased. 62

Figure 3.2.6. The effect that brightness and contrast levels have on image quality. These images were taken using 5kV with a tilt of 45° at 40X. Image a has the brightness and contrast level set to low while the image b is improved. Note that the darker regions that surround the opening where the wire is placed is due to the presence of conductive carbon impregnation in the polymer. 63

Figure 3.2.7. The effect that brightness and contrast levels have on image quality. These images were taken using 5kV with a tilt of 45° at 40X. Image a has the brightness and contrast level set to low while the image b is improved. Note that the darker regions that surround the opening where the wire is placed is due to the presence of conductive carbon impregnation in the polymer. 65

Figure 3.2.8. The difference of the secondary a, and backscatter image b taken using 20kV, with a tilt of 45° at 16X. Notice how image b shows compositional contrast.... 66

Figure 3.2.9. High magnification of one of the bright dots on the backscattered image in figure 3.2.8. Image a showing secondary image, while b shows the backscattered image using 20kV, a tilt of 45°, at 1000X. 68

Figure 3.2.10. Comparison of tilt has on secondary images a and c, and backscattered images of b and d. Notice that

tilt has more effect on the brightness of the secondary image than on the backscattered image. All of these images were taken using 20kV, at a 16X, while a and b were tilted 45°, and c and d at 65°. 69

Figure 3.2.11. These images were taken using 20kV, with a tilt of 45°, at 16X, but image a was taken using a matrix size of 256X200, while image b used 128X100. Notice how the quality of image a is improved over image b. .. 71

Figure 3.3.1. X-ray spectral graph, where the y-axis is x-ray counts and the x-axis is the x-ray energy, using an accelerating voltage of 10kV, with the Be window closed..... 73

Figure 3.3.2. X-ray spectral graph, where the y-axis is x-ray counts and the x-axis is the x-ray energy, using an accelerating voltage of 5kV, with the Be window open..... 73

Figure 3.3.3. X-ray spectral graph, where the y-axis is x-ray counts and the x-axis is the x-ray energy, using 10 kV with the Be window open. 75

Figure 3.3.4. X-ray spectral graph, where the y-axis is x-ray counts and the x-axis is the x-ray energy, using 20 kV..... 75

Figure 3.3.5. Image of Al, W, Pt coated W, and a Cu wire taken using 20 kV, with a tilt of 45°, at 14.3X, where a is the secondary and b is backscattered electron, c the Al, d the Cu, e the Pt, and f the W x-ray images..... 77

Figure 3.3.6. High magnification at 150X , while using 20 kV with a tilt of 45°, of Pt coated wire in figure 3.3.5 showing a the secondary image; b the Cu, c the Pt, and d the W x-ray images. 79

Figure 3.3.7. Secondary electron image a, and b the Si, c the C, and d the O x-ray images. These images were taken using 10 kV, with a tilt of 45°, at 296X..... 81

Figure 3.3.8. High magnification image taken at 1500X using 5 kV, and a tilt of 67°, of the largest feature on figure 3.3.7. The secondary image in a, and b the Si, c the C, and d the O x-ray maps. 82

Figure 3.3.9. The secondary image in a, and b the C, c and the F x-ray maps, using a magnification of 40X, 5kV, and a tilt of 45°of wire insulation. 84

Figure 3.3.10. X-ray spectral graphs, where the y-axis is x-ray counts and the x-axis is the x-ray energy, using different accelerating voltages showing the elemental composition of a patterned electrical device..... 85

Figure 3.3.11. Images taken using 20 kV, a tilt of 45° at 16X, of a patterned electronic sample containing C, O, Al and Si showing the effect that the acceptance angle of the detector has at low magnifications..... 86

Figure 3.3.12. High magnification images at 1000X using

20 kV and a tilt of 45°, of small Al contact pad of figure 3.3.11.....	87
Figure 3.3.13. Comparison of x-ray spectral graphs, where the y-axis is x-ray counts and the x-axis is the x-ray energy, created using an accelerating 20kV with the Be a) open and b) closed.	89
Figure 3.3.14. X-ray spectral graph, where the y-axis is x-ray counts and the x-axis is the x-ray energy, of several-coated AFM tips using an accelerating voltage of 5kV.....	90
Figure 3.3.15. X-ray spectral graph, where the y-axis is x-ray counts and the x-axis is the x-ray energy, of several-coated AFM tips using an accelerating voltage of 20kV.....	90
Figure 3.3.16. Images taken using 5 kV, with a tilt of 45°, at 16X of several coated AFM tips showing the effects of accelerating voltage. Figure is continued on next page.....	91
Figure 3.3.16. (Continued) Images taken using 5 kV, with a tilt of 45°, at 16X of several coated AFM tips showing the effects of accelerating voltage. Page 2 of 3.....	92
Figure 3.3.16. (Continued) Images taken using 5 kV, with a tilt of 45°, at 16X of several coated AFM tips showing the effects of accelerating voltage. Figure is continuance from previous pages.	93
Figure 3.3.17. Spectral graph, where the y-axis is x-ray	

counts and the x-axis is the x-ray energy, while at high magnification of the left tip in figure 3.3.16.	95
Figure 3.3.18. High magnification images at 7000X showing the effect accelerating voltage at 5 and 20 kV with a tilt of 45° has on the image of the middle tip in figure 3.3.16. Figure is a continued on the next page.	96
Figure 3.3.18. (Continued) High magnification images showing at 7000X the effect accelerating voltage at 5 and 20 kV with a tilt of 45° has on the image of the middle tip in figure 3.3.16. Figure is a continuance of the previous page.	97
Figure 3.3.19. Images taken at 20 kV with a tilt of 6° at 16X of several coated AFM tips using more tilt than figure 3.3.16. Figure is continued on the next page.	98
Figure 3.3.19. (Continued) Images taken at 20 kV with a tilt of 65° at 16X of several coated AFM tips using more tilt than figure 3.3.16. Figure is a continuation of the previous page.	99
Figure A.1. Vacuum control console.	106
Figure A.2. Chamber control vacuum.	107
Figure A.3. SEM column with attached LN ₂ dewar.	108
Figure A.4. Sample stage extended. Note the mounted sample.	109

Figure A.5. Interior of chamber, showing parts of the E-T
and x-ray detectors. 109

Figure A.6. SEM image control and display console..... 110

Figure A.7. Diagram of a cross-section of a Faraday cup
for measuring SEM beam current..... 129

CHAPTER 1

INTRODUCTION

1.1 THE IMPORTANCE OF MATERIAL ANALYSIS FOR THE IC INDUSTRY

Materials analysis in the integrated circuit (IC) industry is very important. It is important in many ways. For a circuit to function properly, the materials used to build the chip must have certain properties. Some of them must have the proper crystal orientations. Other materials must have suitable electrical properties, such as being a conductor or insulator. Another important criteria is their chemical suitability with the other chemicals or materials used in the manufacturing process of the IC.

There are many tools and techniques that exist for analysis of materials, such as x-ray diffraction analysis, x-ray fluorescence (XRF), scanning tunneling microscope (STM), atomic force microscope (AFM), optical microscope, and scanning electron microscopy. Each has its strengths and weaknesses. The simplest of these is the optical microscope.¹

The optical microscope is used to find physical flaws, such as cracks, discontinuities, particles, and misalignment. Over the years, as IC technology advances, the feature sizes of the chips get small. The smallest feature size of current chips is beyond the resolution of optical microscopes. Another one of the optical microscope's limitations is that it can only obtain topographical information of a sample's surface. The scanning electron microscope (SEM) on the other hand has a much higher resolution, and can be used to image the smallest IC features, and at the same time can retrieve information from the surface as well as from several microns below the surface. With x-ray analysis capabilities, this information can include elemental composition of the sample. It is capable of not only a qualitative or "look-see" image, but also able to obtain quantitative information. At the same time, voltage contrast can also be used as a technique for finding electrically defective areas on ICs.^{2,3}

The IC industry needs materials analysis to find suitable materials for construction, and defects. This analysis not only finds the defects, but also determines probable causes for these defects. As mentioned above, there are currently many tools that are needed to properly analyze materials. Each can do something better than the other, but none can do the techniques alone. The SEM on the other hand, with its multiple information gathering

capabilities, is more versatile in the materials analysis, than any other instrument alone.

1.2 SURVEY OF SEM/EDS ANALYSIS TO SEMICONDUCTOR AND MAGNETIC DEVICE MATERIALS

Today, most SEMs are equipped with many different types of detectors. These include the Everhart-Thornley (E-T) secondary electron detector, Solid-State backscattered electron detector, cathodoluminescence detector, and the x-ray detector. Together these detectors give SEMs the ability to obtain topographical as well as elemental data of a sample.⁴

Most of the analysis conducted using a SEM is topographical. One reason why the SEM is so popular with this type of analysis is that the image collected is easy to interpret. The reason for this is that the image collection method is similar to that of the human eye. Therefore the image that the SEM produces looks like the image that an observer would see when looking down at the sample.²

There are several topographical methods that exist. These include secondary electron (SE), and backscattered electron (BS) imaging. The basic SE image detection processes will be discussed in detail in section 2.3.1 and BS 2.3.2. SE image is more popular because it generally gives the better image for showing surface topography of a rough surface.³

There are also several techniques that can be performed on electrical and magnetic devices during SE imaging. If an electrical potential is applied to a semiconductor device, the image will show a contrast where the potential is different, hence the name voltage contrast imaging. A positive charge with respect to ground on a region of a sample produces an electric field that attracts low energy SE back to the sample. This results in a darker region on the image. Similarly, a negative charge on a region causes more SE to escape, causing a bright area on the image. This technique is very useful for failure analysis.¹

Another technique that is useful for magnetic materials is magnetic contrast imaging. This process is similar to that of the voltage contrast. The difference is that a magnetic field exists above the surface of magnetic samples. This field will deflect some of the SE electrons into or away from the detector, which will result in bright or dark areas on the image.¹

The BS image gives different data. Since there is a higher probability for BS electrons in high Z samples, due to their nature which is discussed in detail in section 2.2.2. As a result, BS imaging works well for smooth, high Z samples, in contrast to SE imaging.⁴

Knowing what is in or on semiconductor and magnetic device materials is also important. There are X-rays that atoms

emit during the electron-beam sample interaction, which is discussed in more detail in section 2.2.3. These x-rays have specific energies for each element. Therefore a sample's elemental composition can be obtained by studying these detectable characteristic x-rays. This technique is known as energy-dispersive spectroscopy (EDS).⁵

Once the amount of energy for the detected characteristic x-rays is known, more than just the simple elemental composition of the sample can be found. Not only will the EDS give qualitative data, it will give quantitative data of the sample by the ratios of the amount of the detected elements. Elemental images of samples can also be taken by using only x-rays of a specific energy. These images are useful because they can show elemental location. As mentioned in section 2.2.4, x-rays are generated from the deepest level of the excited volume. Therefore, the x-ray data also gives internal sample information.⁵

1.3 THESIS PROJECT GOALS

This thesis uses scanning electron microscopy to investigate topographical features, as well as the qualitative and the quantitative elemental composition of material samples. Most of which are patterned, and unpatterned microelectronic samples supplied by Lucent Technologies Inc., Thermon Manufacturing

Company, and Southwest Texas Physics department supplied the other samples that were examined.

The experiments were conducted using the Southwest Texas Physics department's Amray model 1400 Scanning Electron Microscope. This SEM was equipped with an Everhart-Thornley secondary electron detector, GW type 133 Solid-State backscattered electron detector, and an EDAX Econ IV x-ray detector.

CHAPTER 2

PRINCIPLES AND OPERATION OF SCANNING ELECTRON MICROSCOPY AND ENERGY DISPERSIVE SPECTROSCOPY

2.1 SEM HARDWARE

The Scanning Electron Microscope (SEM) consists of many components. First, electrons must be produced so that an electron beam can then be formed. Electrons are formed by the electron gun. Once the beam has been formed, its diameter must be reduced and it must be directed onto the sample. A series of lenses in the SEM's column, perform this task. Then the beam needs to be focused on and scanned across the sample. The beam then interacts with the sample. This causes the release of several different types of data signals, which different types of detectors can collect and interpret. This signal is then transferred to a display system. Now the image of the sample can be physically examined.⁴

2.1.1 ELECTRON GUNS

The electron gun consists of a filament (electron source) that is held at a negative potential (cathode); a grid cap that is held at a

slight positive potential with respect with the cathode; and an anode that is held at a high positive potential with respect with the cathode.⁴

Three main types of filaments exist, the tungsten hairpin, lanthanum hexaboride (LaB_6), and the field emission. To produce electrons, most gun's filaments are heated resistively by running a current through them, to a temperature high enough so that some of the free electrons in the filament are able to overcome the work-function and escape, or "boil-off". The tungsten hairpin filament is simply a tungsten wire of about $100\mu\text{m}$ diameter that is bent into a V-shape tip. This helps the electrons leave the filament in only one area, the bottom of the V, to help form a small beam of electrons, which is desired. If the electrons would leave the filament in more than one spot, would result in several undesirable results. First the beam diameter would be much larger than required (a beam diameter of $25,000 - 50,000 \text{ \AA}$ is typical when it leaves the gun assembly), since the smaller the beam is when it leaves the gun assembly, the fewer of the electrons get blocked by the grid cap, which will be discussed later in the section, resulting in a lower beam current, and the easier and smaller it can be made when it reaches the sample. The tip usually has a radius of about $100\mu\text{m}$. The ends of the filament are soldered to two electrodes that are connected to a high-voltage source (10,000 to 20,000 V). As

electrons are emitted from the filament, they are emitted in all directions. So a grid cap that is held with a slightly positive potential with respect to the filament, is placed about 1-2mm below the filament tip which has an aperture on its bottom side. This catches stray electrons that are not in the beam, controls the amount electron emission, and directs and focuses the electrons in the gun toward the anode. As the electrons pass through the aperture of the shield, they are attracted to the anode by the high potential difference that exists between it and the filament. This potential is controlled by the operator, and is called the accelerating voltage. Most SEMs are capable of producing a range of accelerating voltages of 1 to 30keV. Figure 2.1.1 shows a typical tungsten hairpin filament gun.⁴

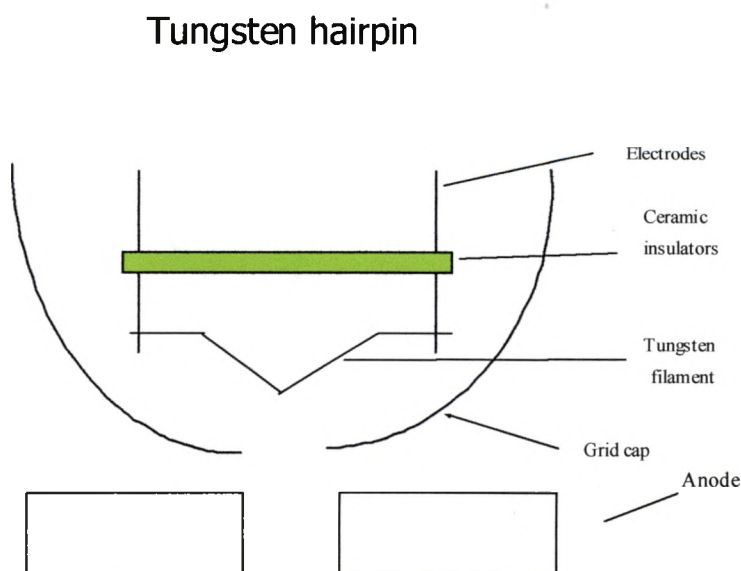


Figure 2.1.1. Schematic of a tungsten hairpin filament.

The LaB_6 gun filament is a sharpened rod of pressed and sintered lanthanum hexaboride powder about 0.5 mm long with a diameter of about $100\mu\text{m}$. It is supported and resistively heated by materials that do not react with LaB_6 , such as carbon or rhenium. It is then attached to stainless steel electrodes such that it can be a direct plug-in replacement for a tungsten filament. Provided that the vacuum in the gun chamber is low enough, the only other changes needed for this modification would be the shape of the grid cap and the bias voltage. The lower vacuum requirements for

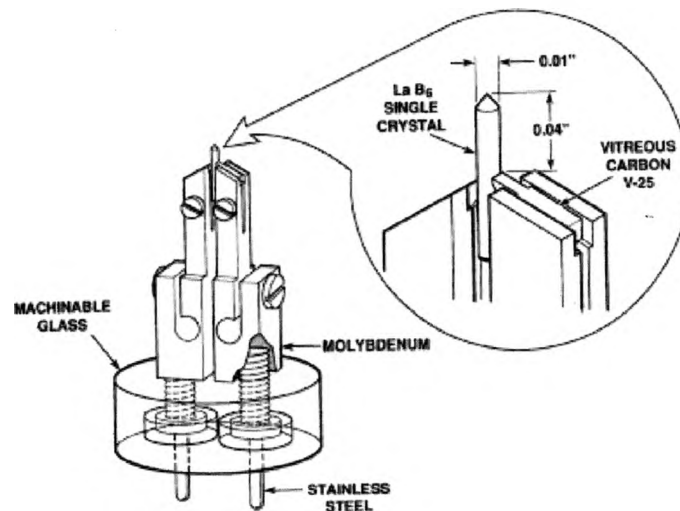


Figure 2.1.2. Schematic diagram of LaB_6 direct plug-in replacement for a tungsten hairpin filament. Reference 5.

the LaB_6 are due to the fact that La and B are volatile and oxides in the presence of oxygen or water vapor which causes loss of emitter material, and that LaB_6 is extremely chemically reactive when hot, therefore it readily forms compounds that “poison” it. This causes

a reduction in its emission. An example of a LaB_6 filament can be seen in the figure 2.1.2.⁵

Field emission (FE) electron guns are different than the ones described above. It does not use high temperatures to “boil-off” electrons from the electron cathode material. Instead it uses a wire of single crystal tungsten, with a sharp point no larger than 100nm that has been spot welded to a tungsten hairpin. Using two anodes, such that the anode closest to the filament is held at a negative potential of 3-5 kV with respect to the filament. Figure 2.1.3 shows a FE electron source. The electric field at the tip is

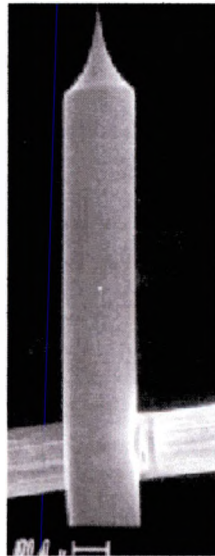


Figure 2.1.3. An example of a FE source, a single crystal wire spot welded to a W wire. Reference 5.

strong enough that electrons can tunnel through the work-function energy barrier instead of using thermal energy to lift them

over as with the hairpin and LaB₆. Field emission is a way of producing electrons without the disadvantages of evaporation of filament material, thermal drift, and relatively low brightness that hinder the other filaments.⁵

Brightness (measured in steradians) is the most important parameter of the electron gun. The brightness, β , is defined as the emitted current/ (area) \times (solid angle of the cone formed by the beam) = $4i_b/\pi^2d^2\alpha^2$, where i_b the beam current, d is the beam diameter of the beam leaving the gun, and α is the beam divergence angle. Brightness is important because the higher the brightness the higher the resolution of the image. As the equation states, the brightness increases as i_b increases, d , and α decreases. For α to get smaller, the convergence of the beam must get smaller,

Characteristics of Electron Guns

Cathode	Vacuum requirement (torr)	Brightness (steradian)	Minimum beam diameter (Å)	Lifetime (hr)
Tungsten hairpin	$>10^{-4}$	10^4 to 10^5	~ 50	40-60
LaB ₆	$>10^{-5}$	10^6	~ 25	~ 3000
Field emission	$>10^{-9}$	10^7 to 10^8	<10	indefinite

Figure 2.1.4 Gun characteristics. Adopted from Gabriel. Reference 4.

which means that the diameter of the beam must be smaller before it is converged. This means the smaller the beam that is being emitted from the gun results in a larger brightness as will higher beam current, which is controlled by the accelerating voltage of the beam. The following table, figure 2.1.4, shows some typical characteristics of different guns.²

The beam diameter is determined by the source size and the demagnification of the lenses, which will be described in section 2.1.2. The more that the beam is diverged, the lower the current that passes through the final aperture. Thus, the largest

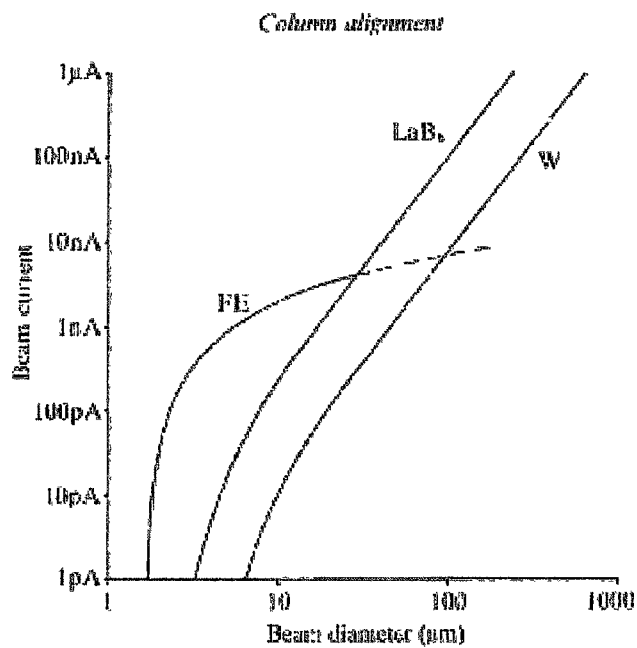


Figure 2.1.5. Beam current vs. diameter for a W-tungsten filament, LaB₆, FE-field emission. Reference 6.

obtainable current varies with the beam diameter, which means that there is a “trade-off” between current and diameter. As can be seen in figure 2.1.5, for a given beam diameter $<50\mu\text{m}$, the field emission gun gives the largest current, but for larger diameters, the LaB_6 is the best choice. This means that the field emission is best gun for high-resolution imaging followed by the LaB_6 , and then the tungsten.^{2,6}

2.1.2 ELECTRON BEAM COLUMN

When the electron beam leaves the gun, it has a diameter between 25,000 – 50,000 Å. The beam needs to have a diameter of around 100 to 500 Å when it reaches the sample. This narrowing of the beam is done by a series of converging or demagnifying lenses. These are magnetic lenses made of copper wire windings inside an iron shell that has the shape of a doughnut, positioned such that the electron beam moves down the center hole. As current is run through the windings, the magnetic flux created in the center of the lenses bend the trajectory of the electrons as they move through the lenses. By adjusting the current running through the windings, the magnitude of the magnetic flux can be controlled, therefore controlling the amount that the beam converges. On most SEMs the current control knob is called spot size. This is because it controls the diameter or size of the beam

that hits the sample. SEMs typically have one to three converging lenses.⁵

Once the spot size of the beam has been created, it must then be focused on and scanned across an area of the sample. This is done by the objective lens. Similar in design to the converging lenses, except that it incorporates scan coils and stigmator, which will be defined below.⁴

The objective lens is the most powerful of the SEM's lenses. This is simply because more current is passed through it. As a result, enough heat is generated in the lens that requires it to be liquid cooled. The current in this lens is controlled with the focus knobs. There are several levels of focus sensitivity available, from coarse to very fine focus. By adjusting the current through this lens, the electron trajectory is bent so that the beam convergence point is controlled along the optic axis or z-axis of the microscope's column.⁵

Now the electron beam needs to be scanned over the sample. It is scanned over a rectangular area by the scan coils. These are controlled by a scan generator, which runs a current through these coils. The scan generator is synchronized with the CRT screen, so the electron beam's position on the sample is the same as the position seen on the CRT. The ratio of the CRT display area to the distance the electron beam is scanned, is called the

magnification. Only changing the scan area changes the magnification. As a result, once the image has been properly focused, it will remain in focus as magnification is changed.⁴

The rate at which the beam passes over the specimen is called the scan rate. This can be varied from 100 – 100,000 lines/scan. Image clarity improves with lower scan rates because the beam electrons have sufficient time to interact with the sample. This results in the release of more data from the sample. The type of data that the sample releases during electron beam-sample interaction will be discussed in section 2.2.3. A general rule is that fast scans are used to select regions of interest to be scanned, focusing and column alignment, and slower scans are used for image recording.⁴

Flaws in the coils of the magnetic lens may cause the lens to focus more strongly along one axis than the other. This causes a distortion or change in shape of an object as the focus is adjusted, and is observed at magnifications above 1000X. This effect is called astigmatism. These flaws can be compensated for by the use of a weak magnetic lens called a stigmator. The stigmator is located inside of the objective lens, and exerts a magnetic field in the opposite direction and having a magnitude equal to the nonsymmetric field created by the objective lens. The procedures

for the proper operation of the stigmator can be found in Appendix A.5

The final aperture is beneath the objective lens. These apertures are made of platinum or molybdenum and normally have a single hole with a diameter of 100 - 300 μm . This aperture's function is to block stray electrons that are not part of the imaging beam. Smaller apertures are used when higher resolution, or large depth of field is desired. Since small apertures block out some of the imaging beam as well, they also decrease the beam current that strikes the sample. This lowers the amount of backscattered electrons, and x-rays that are created during electron beam-

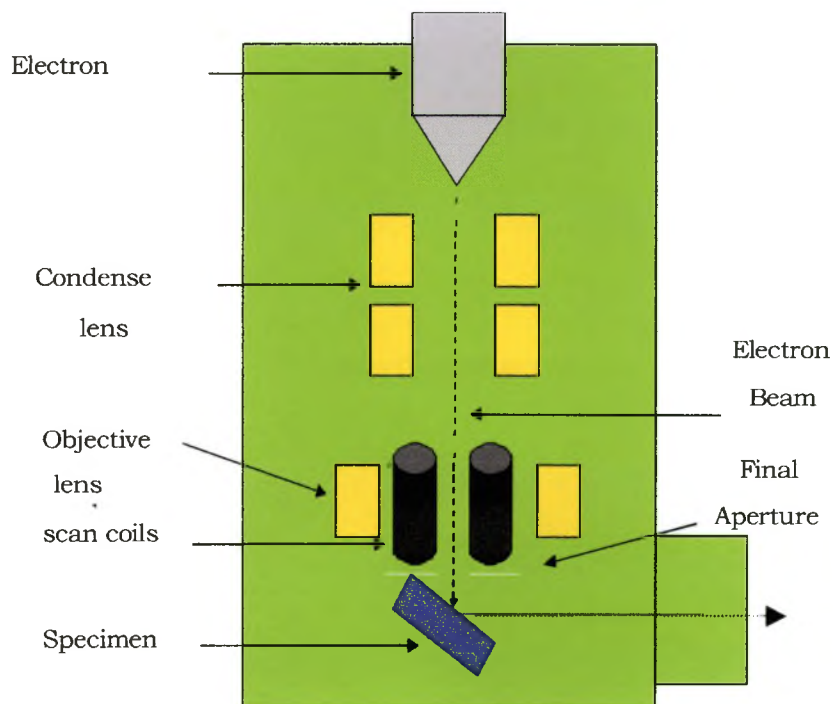


Figure 2.1.6. SEM column with electron gun, lens, and specimen emitting data signals.

specimen interaction, which will be discussed in more detail in section 2.2.3. As a result, a larger aperture is used when conducting backscatter and x-ray analysis. An example of a SEM column can be seen in figure 2.1.6.⁵

2.1.3 SAMPLE CHAMBER

The sample is mounted on an aluminum stub that is then secured to the SEM's sample stage. The stage controls the sample positioning (see Appendix A for sample positioning control of an Amray model 1400) and gives it a pathway to electrical ground.²

2.2 ELECTRON BEAM-SPECIMEN INTERACTION

As the sample undergoes electrical bombardment, the beam electrons interact with either sample atom electrons or nucleus. Electron-nucleus interaction results in elastic collisions, and electron-electron interaction results in inelastic collisions.⁷

2.2.1 ELASTIC COLLISIONS

Elastic collisions result in the change in direction of the beam electron but has little effect on its velocity. As a result, the electrons kinetic energy, $E = m_e v^2 / 2$ is almost unchanged. It will lose less than 1eV, which is much less than the beam energy, which is normally more than 1 keV. At the same time, the electron is deflected or scattered by angles of 0° to 180° . The electron is scattered by Coulomb interactions between the beam electron and

both the sample atoms nucleus and all of its electrons, known as Rutherford scattering.⁵

2.2.2 INELASTIC COLLISIONS

Elastic collisions result in little loss of beam electron's kinetic energy. In inelastic collisions on the other hand, a beam electron may lose anywhere from a fraction of a keV to all of the electron's energy, which is the accelerating voltage of the beam, and can be up to 30 keV. The amount of energy loss is determined by which process occurs, since there are several processes that cause energy to be transferred from the beam electron to the electrons or atoms of the sample. This is in contrast to elastic collisions in which there is only one type of interaction process. The most common processes are discussed below, in order of increasing energy loss.⁵

Phonon excitation is caused by a beam electron, which deposits energy into the sample and transfers this energy in energy loss events, of $<1\text{eV}$. These loss events, excite the lattice oscillations. This causes the sample to heat.⁵

Metallic samples that have weakly bound outer electrons in the conduction band are so loosely bound, that in a solid sample, these electrons are no longer localized to a specific atom, but form a "sea" of electrons. The moving beam electron can excite the free electron "sea", creating waves in the "sea".⁵

When a loosely bonded valence band electron of an insulator or a semiconductor can be excited to the conduction band with enough kinetic energy so that the electron can move in the sample. Similar effects can happen in metals, except that the electrons are promoted straight from the conduction band.¹

A Coulombic field of the sample atoms can cause the beam electron to undergo deceleration. This deceleration causes an energy loss of the electron. The energy loss can have a value of a fraction of an eV to the total energy of the beam. This loss is converted into a photon of electromagnetic energy, as the sample atom relaxes. This “braking radiation” is known as bremsstrahlung.⁵

2.2.3 TYPES OF ELECTRON SIGNALS RELEASED BY SAMPLE

Section 2.2.2 discusses that several different types of inelastic collisions are possible. The sample releases different types of data when it undergoes inelastic collisions. As the electron beam transfers kinetic energy to the sample, which can then raise the sample atom to an excited state. As that sample atom relaxes to the ground energy state it releases energy. Depending on the amount of the released energy, it can be in the form of a secondary electron, or photon (light, which is called cathodoluminescence or x-ray).⁷

During inelastic collisions the sample atom is excited to a higher energy state. This, results in the atom releasing one of its shell electrons as the atom goes back to its ground state and is emitted from the sample. This electron is called a secondary electron. A secondary electron can also be produced after a beam electron undergoes several interactions, which cause it to lose enough of its energy and its trajectory takes it back out of the sample.⁵

Secondary electrons are electrons that escape from the sample during electron beam bombardment which have energies below 50 eV. The term is not very accurate because they could be from either the beam, after many collisions inside the sample, but more likely from sample atoms a short distance under the surface. Secondary electrons are the most abundant data that the sample releases.⁵

When beam electron raises the outer-shell electrons of sample atoms to higher energy states, which causes the atoms to emit the surplus energy as it relaxes back to its original state, this energy appears as light. This low energy process is known as cathodoluminescence. For opaque samples, this type of data is released from the surface of the sample, but for non-opaque samples, this data can originate from any part of the excited volume. The excited volume will be discussed in section 2.2.4.⁴

As discussed earlier, during electron bombardment, as the Coulombic field of the sample atoms can cause electrons from the beam to undergo deceleration. This creates bremsstrahlung x-rays. Since bremsstrahlung x-rays are independent from the elemental composition of the sample it forms a continuous spectrum from zero to the beam energy. Since most of the electrons are decelerated with little energy loss, and fewer lose more energy, which approaches the beam energy, most of the bremsstrahlung x-rays are from 1 to 5 keV. The x-ray count versus energy graph, called x-ray spectra, would have an asymmetric curve that is highest at the low energies and gradually slopes down at higher energies.⁵

Bremsstrahlung x-rays are not the only x-rays produced during electron bombardment. When a beam electron with high enough energy, interacts with an inner-shell atomic electron, this atomic electron can be ejected. This leaves the atom in an excited state. An upper shell electron then falls to fill the vacancy left by the ejected electron. This dropping from a higher energy shell to a lower energy shell causes the atom to release a high energy quanta. For example, if a K-shell electron was ejected and an L-shell electron dropped to fill the vacancy, this would result in the emission of a $K\alpha$ x-ray. If an M-shell electron would drop instead, it would be a $K\beta$ x-ray. An ejection of a L-shell electron would

result in a M-shell dropping, which emits an $L\alpha$ x-ray. If the electron that dropped did not come from the highest shell, then a higher shell electron can also drop into the newly created hole, releasing yet another quanta. For example, if a K-shell electron was ejected and an L-shell electron dropped to fill it, this leaves a vacancy in the L-shell, while it emits a $K\alpha$ x-ray. But if the atom has a higher shell such as an M-shell, one of these electrons can fall and fill the vacancy, which causes an $L\alpha$ x-ray to be released. The magnitude of these energy quanta is equal to the difference in energy of the two shells involved. Since energy levels of the different shells are unique to atoms of each element, the emitted x-rays are then uniquely characteristic for each element that undergoes electron beam interaction. Therefore these quanta are called characteristic x-rays. This type of x-ray emission has energies ranging up to the accelerating voltage. When a sample is examined, and an x-ray spectrum is produced as mentioned above, it will have peaks, which coincide with energy levels of samples major elemental composition. Figure 2.2.1 shows the formation of characteristic x-rays. These x-rays will also appear on an x-ray spectrum mentioned above. When large numbers of characteristic x-rays of a given atom are detected, these x-rays appear as peaks on the spectra graph. Actually the characteristic peaks sit on top of the bremsstrahlung x-ray spectral graph.⁴

Creation of X-Rays

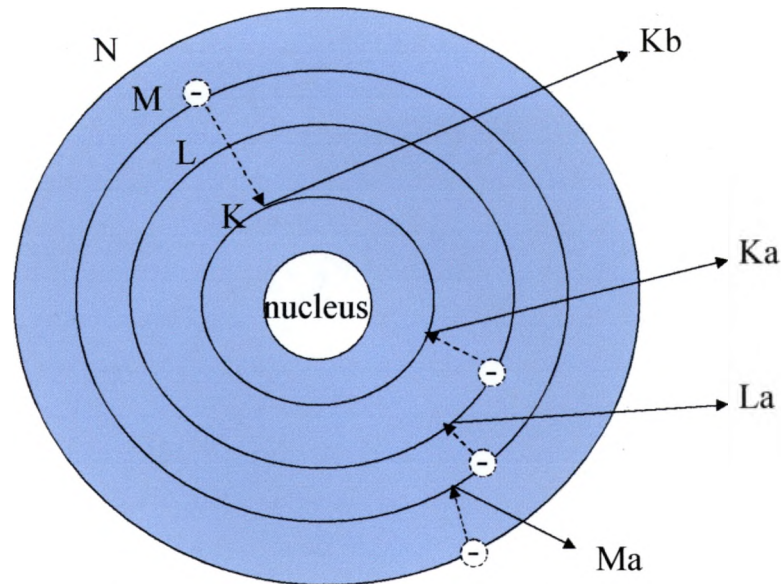


Figure 2.2.1. Creation of characteristic x-rays in the Bohr model atom. Adapted from Gabriel. Reference 4.

As mentioned in section 2.2.1, elastic collisions result in scattering of angles ranging from 0° to 180° with very little loss of a beam electron's kinetic energy, so they will retain energy of more than 1 keV. When the resulting angle is such that after one or more consecutive elastic collisions, the beam electron emerges back out of the sample, it is known as a backscattered electron (BSE). Since the electron is scattered by Rutherford scattering therefore it is more probable for this type of scattering with higher Z elements.⁵

2.2.4 EXCITATION VOLUME

The excitation volume or depth of penetration is defined as

the volume of the sample where data signals originate. The depth of penetration is several microns (generally $>5\mu\text{m}$). It is a function of acceleration voltage of the beam and the atomic density of the specimen. This is because the high Z samples offer more

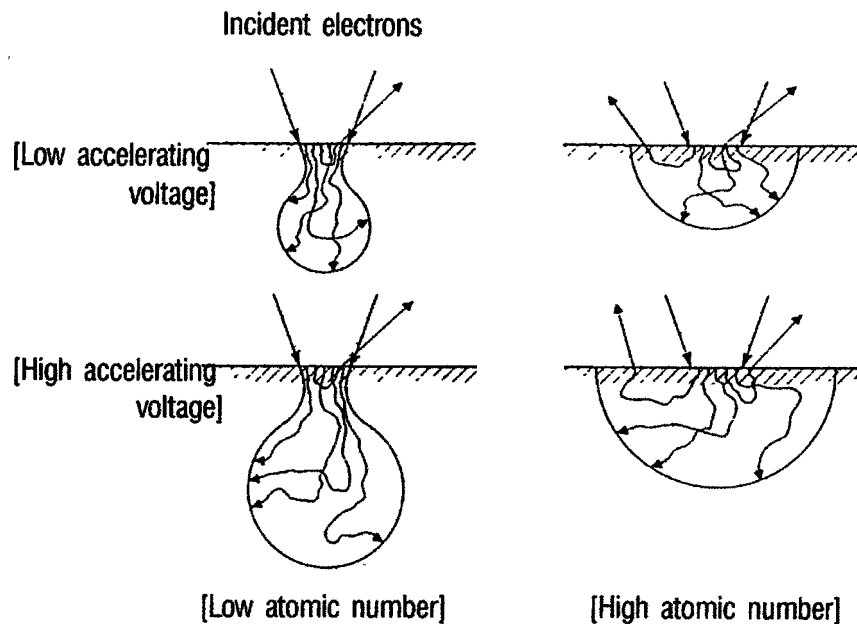


Figure 2.2.2. Examples of low and high atomic number (Z) sample excitation volume with different accelerating voltages. Reference 6.

resistance to the penetration of beam electrons. For increasing Z reduces the penetration depth for a given voltage. This also causes the excitation volume to have a semi-circle shape. Lower Z materials offer less resistance. This allows for more penetration in every direction, resulting in a pear shape volume, as shown in figure 2.2.2.⁵

Tilting the sample causes an increase in the lateral dimension (dimension parallel to the surface) with respect to normal incidence, and no change in the depth in the dimension, which is parallel to the beam. This can have an effect on the amount of sample data emission. For example, as mentioned in section 2.2.1, elastically scattered particles, typically result in little change of direction. Generally after elastic collisions, the particles continue moving in the same general direction. When the sample is not tilted, there is a higher probability that the particle continues downward into the sample. But tilting the sample increases chance that a beam electron will emerge out of the sample, because it will take less of a scattered angle to cause backscattering.⁵

No matter what the composition or orientation of the sample, an increase in beam voltage always increases the excitation volume. With the nature of different types of scattering, which occur from the particle collisions and the data signals that are then released, which are discussed in sections 2.2.1-2.2.3, are emitted by the sample from different depths of the excitation volume. Figure 2.2.3 and 2.3.1 show examples of the relative depths of the volume at which the different signals originate, and the positions that different detectors should be placed in the SEM to detect them.⁴

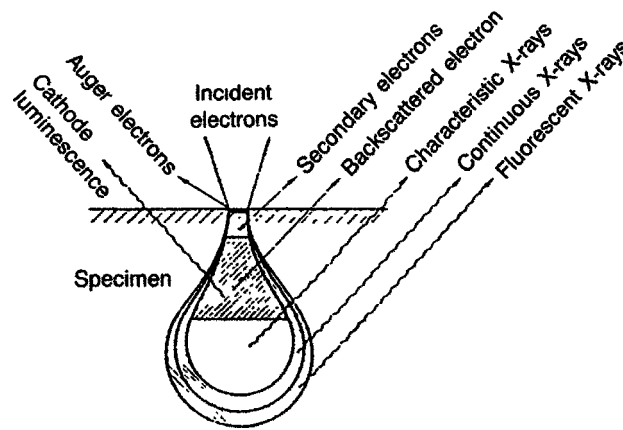


Figure 2.2.3. Depth of origin of the data signals released by the sample during beam interaction. Reference 6.

2.3 DETECTORS

As mentioned in section 2.2.3, the sample releases several different types of data signals whose energies range from a few eV to the accelerating voltage of the beam, which can be up to 30 keV. To get a higher understanding of the sample, several of the different signals should be obtained since they give different characteristics of the sample. To accomplish this, several different types of detectors are required. This includes secondary and backscattered electron detectors. Since x-rays are also produced during electron bombardment of the sample, the SEM may also be equipped with an x-ray detector. X-ray detection and analysis will be discussed in section 2.4. Figure 2.3.1 shows an example of the most used detectors and their positions in the typical SEM chamber.⁴

Origin and detection of data

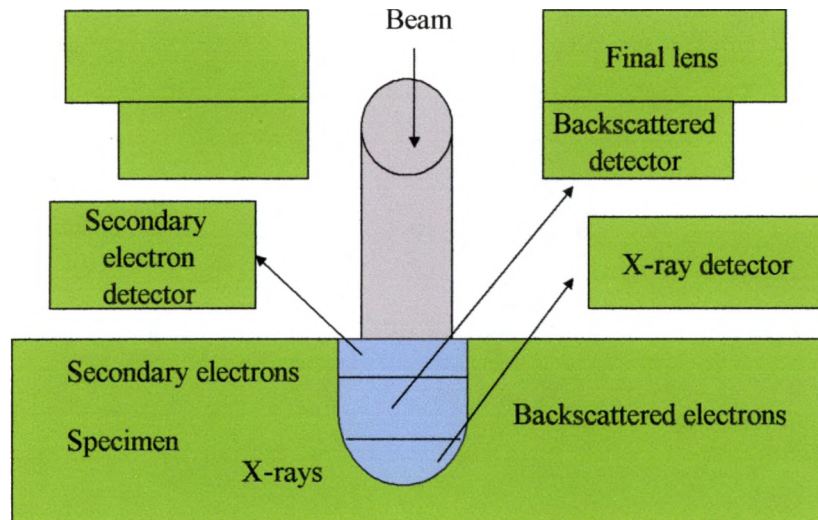


Figure 2.3.1. A schematic of a SEM chamber with specimen excitation volume, showing relative originating depth of data signal, and common detectors used in their locations.

2.3.1 SECONDARY ELECTRON DETECTOR

The basic form of the SEM image comes from the secondary electrons. The most widely used secondary electron detector is the Everhart-Thornley (E-T). The E-T is so widely used that often it is mistakenly believed to be the only secondary electron detector, but it will be the only one discussed.⁴

The E-T detector is mounted inside the chamber at a right angle to the electron beam. The sample can be tilted to increase the number of electrons entering the detector and thereby improving the image. Secondary electrons with energy of 1-5 eV

are attracted to the detector by a Faraday cage, which has a positive charge of ~ 200 V. This causes the trajectory of the electrons to curve toward the detector. Figure 2.3.2 shows a schematic of a typical E-T detector.⁴

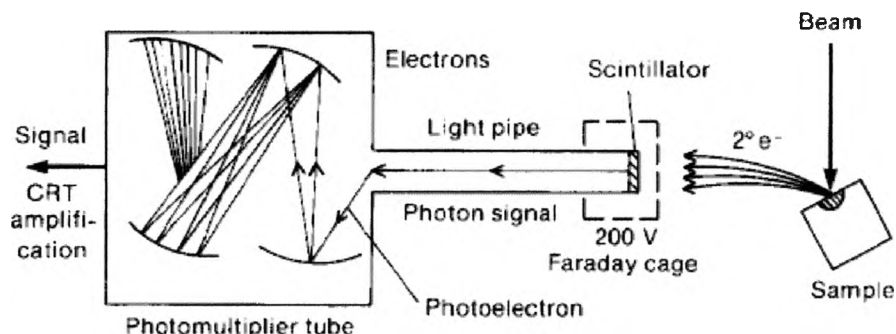


Figure 2.3.2. A schematic of an Everhart-Thornley detector showing the curved path which the secondary electrons due to their attraction to the positively charged Faraday cage. Reference 4.

The Faraday cage surrounds a scintillator from made of aluminum, which has a positive 10-20 V applied to its face. This causes the secondary electrons to be sufficiently accelerated so that they produce photons when they strike and interact with the scintillator. The photons then are totally and internally reflected through a light pipe (made of glass) to a photomultiplier. The photons now strike the first electrode of the photomultiplier, which converts the photon back to an electron current. The electrons are then accelerated onto successive electrodes in the multiplier, which produces many electrons. The gain that the multiplier

provides is $10^5 - 10^6$. It has a response that is high enough to operate a CRT.⁴

2.3.2 BACKSCATTERED ELECTRON DETECTOR

As with the secondary electron detectors, there are several backscattered electron detectors that exist, but only the solid-state diode detector will be discussed. Solid-state detectors are made from flat silicon wafers several millimeters thick, with a depletion zone, which is created by applying a positive potential to a thin gold outer layer. They can be annularly shaped and are generally placed under the objective lens. Figure 2.3.3 shows a solid-state backscattered electron detector.⁸

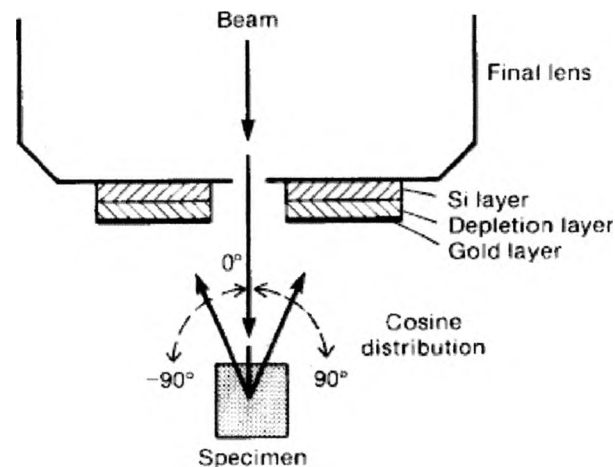


Figure 2.3.3. A schematic of a solid-state backscattered electron detector placed under the optical or final lens. Reference 4.

The detector operates by electron-hole pair production by the energetic backscattered electrons. The semiconductor has an

empty conduction band, which is separated from the filled valence band by a band gap. As the backscattered electrons strike the detector, some of them scatter inelastically in the semiconductor material. This transfers some of the energy to the valence electrons, causing them to be promoted up to the conduction band. This leaves a hole in the valence band, since there is an external potential applied to the detector, the electrons and holes do not recombine as they move in opposite directions. The collection of charge is used to as input to a current amplifier. The gain that the amplifier provides is around 1000. This is a low enough to compromise the performance of a CRT, because the detector produces a high capacitance, which in return, produces a large time constant. The time constant affects the detector by not accurately following the rapid change in signal that occurs across sharp edge. As a result, the image looks blurred for high scan rates, but improves somewhat for lower rates.⁴

2.4 ENERGY-DISPERSIVE X-RAY SPECTROMETER

As discussed in section 2.3, some SEMs use only secondary and backscattered electron detectors, but some have x-ray analysis capabilities. The energy-dispersive x-ray spectrometer (EDS) gives the SEM this compositional analysis capability. It consists of an x-ray detector, amplifier, analog-to-digital converter and a multi-channel analyzer.⁵

2.4.1 X-RAY DETECTOR

The x-ray detector is a lithium-drift silicon diode. Putting together two pieces of pure silicon, one doped with Li, and the other with B, produces this diode. This creates an equal amount of B^- acceptors and Li^+ donors evenly distributed in a drift zone. A thin gold film covers the front of the diode. Applying 1000 V in reversed bias produces a depletion zone in the diode. This removes the electron-hole pairs. Then an x-ray passes through a beryllium window, which isolates the detector from its surroundings allowing the detector to remain in vacuum when the chamber is vented and protects it from stray light and contamination, which can include condensation. This window also blocks out x-rays of less than 1 keV, but can sometimes be opened to let them pass as well. Opening this window can be dangerous for the detector because it is no longer protected from losing its vacuum if the chamber is

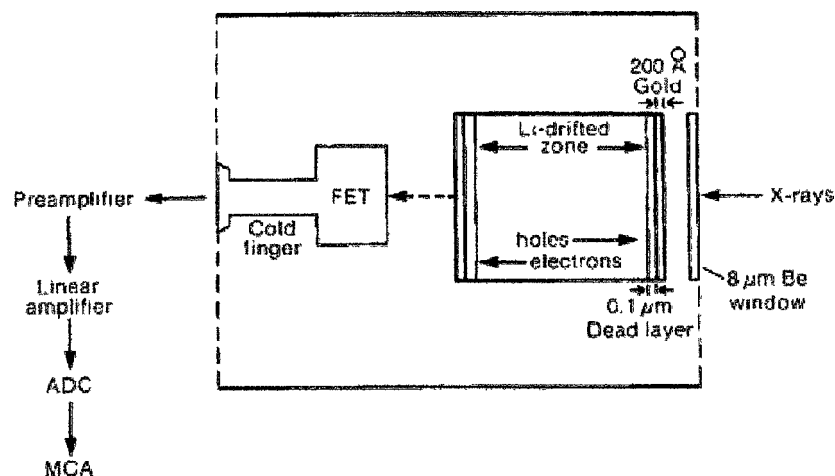


Figure 2.4.1. A schematic of a Li-drift silicon detector. Reference 5.

vented or in case of a vacuum leak. The x-ray then enters the depletion zone, and produces electron-hole pairs. These pairs are now swept out by the bias, and appear as a charge pulse on the backside of the diode. The magnitude of this pulse corresponds to the x-ray energy. Figure 2.4.1 shows a lithium-drift silicon detector. A field-effect transistor (FET) is located behind the SiLi detector.⁵

The FET, which is a preamplifier, converts the charge pulse into a voltage signal. This is the first step in amplifying the signal. To reduce electronic noise and prevent free diffusion of lithium through the semiconductor, the FET and the semiconductor are kept at liquid nitrogen temperatures (LN₂) through the cold finger that is attached to a dewar filled with LN₂. If it were not kept at this low temperature, the Li, which is mobile in Si, can migrate through the Si, especially with a current flowing through it. This could destroy the detector. The high voltage bias of the diode must then be removed before the detector can be raised from LN₂ temperatures.⁵

The Southwest Texas Physics Department's SEM is equipped with an EDAX ECON IV x-ray detector. The ECON IV has the cold finger, detector diode, and FET are enclosed in metal tube called an end cap. The Be window closes this cap. A collimator is placed over the end of the end cap and window. The collimator is for

reducing the chance of an extraneous x-ray from reaching the detector; keep stray x-rays from parts of the chamber, which are produced as backscattered electrons emitted from the sample strike portions of the chamber walls and sample stage. But this collimator also only allows x-rays that leave the sample from a certain angle range, called an acceptance angle, to be detected. This phenomenon can be noticed at low magnifications.⁹

2.4.2 DETECTOR ELECTRONICS

After the x-ray has been converted to a voltage signal, it must be counted and displayed. This is the role of the detector electronics.⁵

After leaving the preamplifier of the detector, the pulse is amplified by the main amplifier, where it is electronically modulated to enhance the signal-to-noise ratio. Since the amplification is a time dependent function. This may cause a “pile-up” of pulses if the count rate is too high. “Pile-up” occurs when the pulses are being created faster than the amplifier can process them. This is known as dead time, which is defined as the probability that at least two x-rays will enter the detector at the same time, causing both signals to overlap. Overlapping causes the formation of sum peaks; the resulting energy is a sum of the energies of the overlapping peaks. The spectrometer rejects both of the overlap pulses if the second peak arrives before the first peak

reaches its maximum value or rejects only the second peak when the first peak has been processed but the signal has not yet returned to its base line, and the SEM operator should maintain moderate count rates to lower the dead time and the resulting overlapping. Figure 2.4.2 shows an example of overlapping.⁶

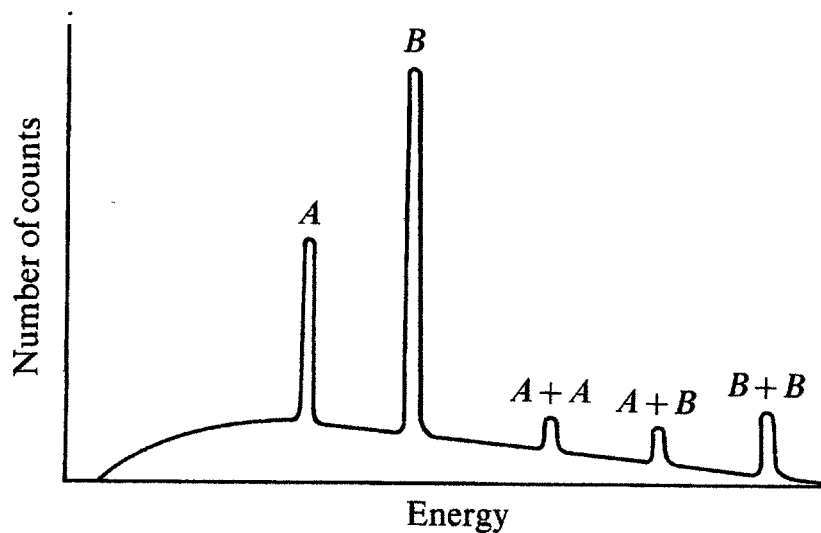


Figure 2.4.2. X-ray counts vs. x-ray energy graph showing overlapping peaks. Reference 6.

Now the amplified signal is converted to a digital signal by the analog-to-digital converter (ADC) and sorted, stored as a histogram of voltage intensity or counts per energy, and displayed by the multi-channel analyzer (MCA) or computer x-ray analyzer (CXA) as its known today as most MCAs functions have been integrated into software and computer displays. As pulses enter,

they are sorted by energy levels by the magnitude of the pulses, and stored in a channel, which corresponds to its energy.⁵

2.4.3 QUALITATIVE X-RAY ANALYSIS

Qualitative analysis is the identification of elements present in a sample. Creating an x-ray spectra graph as discussed in section 2.2.3 will show the samples elemental composition. Some of the most powerful features of modern energy-dispersive spectrometers for qualitative analysis are region-of-interest (ROI) and automatic peak-identification routines. By selecting the energy range that corresponds to particular x-ray peak of the x-ray spectra graph. The ROI can be created. Figure 2.4.3 shows an x-ray spectra graph where two ROIs have been chosen. The ROI for the

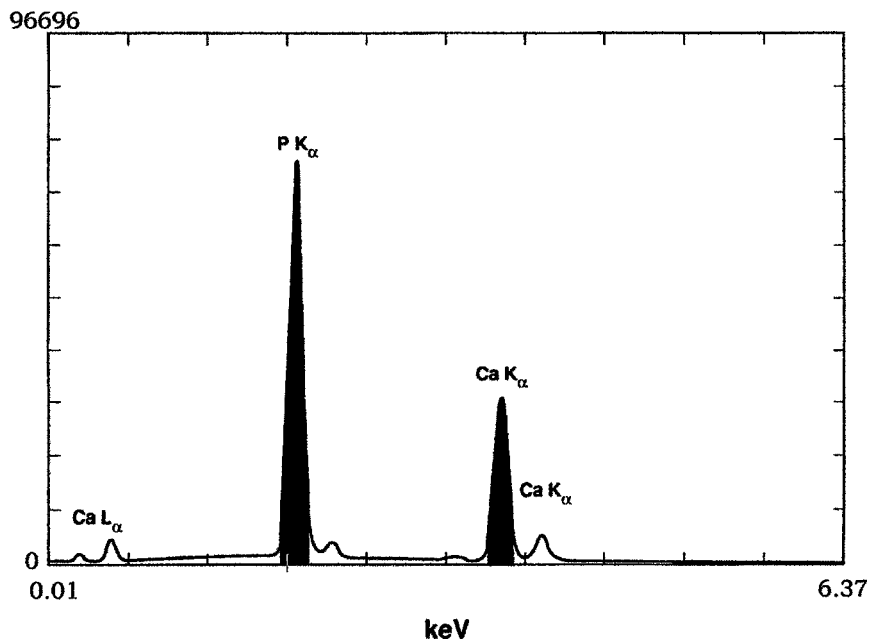


Figure 2.4.3. X-ray spectra with two ROI chosen. Reference 6.

P K_{α} has a starting energy of 1.89 keV and an ending energy of 2.10keV. This range covers the P K_{α} x-ray energy of 2.013 keV. Likewise a range of 3.50 – 3.875 keV was chosen for the 3.69 keV Ca K_{α} .⁶

The peak-identification allows the operator to place the cursor on a peak of the x-ray spectra, which corresponds to the energy of the x-ray. The computer database will identify elements, which emit x-rays of the same energy. After the automatic peak-identification has been used to determine elemental composition of the sample, the ROI lets the operator define energy bands for which to record the intensities. As figure 2.4.3 shows bands that if the ROI are chosen to correspond with the energy of the elements' characteristic x-rays. The sample's x-ray map can be taken, but the map can only be made, by using one energy range. As discussed in section 2.2.3, an element can produce several different characteristic x-rays. Figure 2.4.3 shows that three different Ca x-rays have been detected, but get a higher quality map, only the peak with the most counts should be selected For the ROI.⁵

X-ray dot maps are important to electron microscopy since it can show the elemental composition of the sample, as well as the location and relative concentration of the elements. After a ROI has been selected, the EDS system records the location every time

an x-ray has been detected and analyzed by the method described in section 2.4, and displays the x-ray with a dot in the corresponding location on the monitor. Since the beam is scanned across the sample in coordination with the monitor, the density of the dots seen on the screen shows variations of the concentration of the selected x-ray energy. In real time the electron spot is only on one point of the sample for a fraction of a second. As the beam interacts with the sample atoms at these points, only a small amount of x-rays are released, and have large fluctuations in the number of counts from point to point. Also as can be seen in figure 2.2.3, x-rays are created from deep in the excitation volume and as discussed in section 2.2.4 the excitation volume can have a larger diameter below the surface than the beam itself. This can result in x-rays being emitted not from the point where the beam is but next to it, but the EDS does not know where an x-ray originated but where the beam was. These result in an image that appears fuzzy or noisy. This can be improved by taking a slower scan, to obtain a higher statistics; a really good image should be taken over a period of several minutes to several hours, and may still look noisy.⁵

Qualitative x-ray analysis using an EDS is a powerful tool for scanning electron microscopy. The elemental composition from atoms whose characteristic x-rays range from 1 to around the

beam energy (up to 30 keV) can be determined if the x-ray detector's window is closed. If it is windowless or is opened, the range is lowered to around 0.65 keV. Composition of a sample may be found in less than two minutes. But the ability to create an elemental image or map is useful. The location of the sample elements can then be found.⁵

2.5 DISPLAY SYSTEM

The image of the sample is displayed on a cathode ray tube (CRT) or a computer monitor. The electron beam is scanned across the sample by the scan coils that are controlled by the scan generator. As the beam is scanned in a rectangular area, there is a one-to-one correspondence between its x and y coordinate and of the spot on the CRT, which is also controlled by the same scan generator. The signal is sent from one of the SEMs detectors to the amplifier, which controls the brightness of the CRT. The more intense the signal detected from the sample (the more data the sample releases) the brighter or more intense the image. The information signal in the CRT is not just x and y but also i, where i is the intensity coordinate.⁴

Digital imaging is similar to imaging with a CRT as discussed above. The digital image consists of a numerical array (x, y, i), where x and y are for the position and i is the intensity of the signal. Each position is created as a digital address and then

converted to a voltage to drive the scan circuit by a digital-to-analog converter. The positions correspond to a matrix array in the computers memory. The number of discrete positions controls the digital resolution; the more positions the higher the resolution. Once the beam position has been assigned an address, the detector measures the intensity. The voltage signal is converted to a digital value for i , and is stored as (x, y, i) , and a hard copy can then be printed. The numerical values are then switched back to an analog signal to be viewed on the monitor.⁴

2.6 VACUUM SYSTEM

There are several reasons why a SEM can only be operated under vacuum. As discussed in section 2.1.1, the electron filaments react with oxygen and water vapor. This would greatly decrease the lifetime or cause them to fail immediately. If the electron gun could produce electrons, they would collide with the much heavier atoms in atmosphere. This would cause them to be deflected in all directions. Section 2.4.1 states that since the x-ray detector, is kept at LN_2 temperatures, without a vacuum, water vapor would condense and freeze on it. After time, ice would build up on the detector, which would absorb lower energy x-rays. So a vacuum is required for proper and long term SEM operation.⁷

2.6.1 LOW VACUUM PUMPS

A mechanical or rotary vane pump is used to achieve low

vacuum ($\sim 10^{-2}$ torr). This type of pump works by simply displacing the air. The rotary pump consists of a round chamber with a rotor, with spring-loaded vanes that keep the vanes in constant contact with the chamber wall. The rotor is eccentrically mounted in the chamber and spun by an electric motor that is connected to the rotor on the other side. The vanes are positioned such that an air inlet allows air to enter the space between the two vanes, the rotor, and the chamber wall. As the rotor is turned the air inlet is now blocked, trapping the air in the pump chamber. As the rotor continues to turn, it moves the trapped air as the other vane passes the exhaust outlet, which allows the trapped air to escape through the exhaust outlet. At low vacuum pressures, oil from the pump can escape through the air inlet and travel to the evacuated areas of the SEM, because there are not enough gas molecules to stop the diffusion or “knock” the oil molecules back in the pump. If this would happen, this vapor would polymerize when the electron beam hits it. This would contaminate the inside of the SEM. To prevent this from happening, molecular sieve traps are used between the pump and the SEM. The sieve is made of a material that absorbs oil and water. The Southwest Texas Physics Departments SEM uses two mechanical pumps. A Leybold pump is used rough pump the chamber and column, and an Alcatel

pump is used to back up the turbomolecular pump, which will be discussed next.

2.6.2 HIGH VACUUM PUMPS

Roughing pumps work well for pumping large volumes of gas at pressures above 10^{-2} torr. But, the vacuum requirements to minimize electron beam scattering, and filament and x-ray detector damage, are higher than that of which a low vacuum pump can achieve. A high vacuum pump must be used, but these pumps cannot operate at atmospheric pressures, so it requires that a mechanical pump to rough pump the SEM.

Once a low vacuum exists, a high vacuum pump, like a turbomolecular (turbo) pump can be used. A turbo pump consists of a chamber, which contains alternating rows of stationary slotted disks, called stators and rotating blades that are attached to a rotor. The rotor is turned at high speeds (70,000 rpm) by an electric motor. This assembly resembles a turbine engine. As the blades are spun, they strike gas particles, propelling the molecules down towards the next disk, where the process continues. The stators help create a high pressure inside the chamber as gas molecules accumulate there. The pressure created at this portion of the pump is high enough for a roughing pump to pump. Therefore a roughing pump is used to pump out the exhaust of, or

to back up the turbo pump. Turbo pumps can achieve a vacuum pressure of $\sim 10^{-7}$ torr.¹⁰

Turbo pumps will achieve a vacuum suitable for a tungsten filament, LaB₆, and the rest of the SEM for proper operation, but does not reach the requirement for a field emission gun. Figure 2.1.4 shows the vacuum requirements for the different electron sources. This requires a very high vacuum $>10^{-9}$ torr. To get this type of vacuum, an ion pump is attached to the top of the SEM's column near the electron gun. The Southwest Texas Physics Departments SEM is equipped with a Leybold turbomolecular pump. Turbomolecular pumps are popular on SEMs because they have a lower chance of contamination due to the backstreaming as discussed in section 2.6.1 than other high vacuum pumps.

2.6.3 ULTRAHIGH VACUUM PUMPS

As discussed in section 2.1.1, the electron source oxidizes at high temperatures. This oxidation gradually destroys the source. The lower the vacuum, the less oxidation will occur, which prolongs the sources lifetime, as shown in figure 2.1.4. To insure the long lifetime of the filament, the vacuum of the electron gun region is kept as low as possible. To reduce the pressure in this region an ion pump is attached to the upper area of the SEM's column.¹⁰

When the pressure is below 10^{-5} torr, an ion pump can be used. It consists of an anode that attracts free electrons. As the electrons are moving to the anode, they collide with gas atoms, which ionizes the atoms. Now there is more than one electron moving towards the anode to ionize more gas atoms. At the same time the positive atom is accelerated towards the cathode with such force that it sticks to the cathode, trapping the gas molecules. As a result, ion pumps “get full” and have to be recharged. The Southwest Texas Physics Departments SEM is equipped with a Leybold ion pump.¹⁰

CHAPTER 3

SAMPLE DATA AND ANAYLSIS

3.1 SAMPLE PREPARATION AND ANALYSIS TECHNIQUES

General knowledge of what type of SEM analysis is to be conducted (high resolution secondary electron, and backscatter electron, and/or x-ray), and general electrical characteristic (conductive or nonconductive) of the sample is useful for proper sample preparation. Before any preparation, the analyst should study the sample with the naked eye or even an optical microscope. This allows the identification of possible areas of interest (areas that will be scanned) for mounting placement. Sample movement in the SWT Amray 1400 SEM is limited, although more modern SEMs may have may have 200 mm wafer capability. Some areas of large samples may not be viewable because of this limited movement. Hence, care needs to be taken to mount the sample so that the areas of interest can be viewed. Also, the sample size cannot exceed a maximum size. This size varies for different SEM stages, but it must allow for total movement of the sample (X, Y, Z, tilt, and rotate), so the desired

sample position can be obtained. See appendix A for sample positioning.⁶

If the sample is too large, the area of interest needs to be removed so that it is the proper size. This can be done by different techniques depending on the material. If the sample has a crystalline structure it can be cleaved. Other samples should be cut with a low speed diamond saw. Some geological samples may even be chipped off with a hammer. For the SWT Physics Department's Amray 1400 SEM, the largest sample that can be examined is 1½ inches in diameter.²

Debris or contamination should be removed from the sample. The method of cleaning depends on the type of analysis to be conducted. For example, if just electron imaging is desired, the sample should be blown off with compressed gas. Acetone, ethanol, and methanol should also be used to remove organic contaminants if x-ray analysis is being performed for low Z samples, because these contaminants may also emit characteristic x-rays. However, it will be shown in this thesis that the use of organic solvents can leave behind surface residue features.⁶

As discussed in section 2.2, the sample absorbs beam electrons. Conducting samples can easily carry the resulting electric charge to a sample stub to which it is mounted (which will be discussed later), which is then secured to the SEM's sample

stage that is grounded. This gives a path to ground, which prevents sample charging, which appears as bright flashes (like lightning deep inside clouds during a thunderstorm).

Nonconductive samples are susceptible to charging, especially for high accelerating voltages. This can be a problem because low voltages limit the resolution, x-ray counts, and will not create high energy x-rays, so the SEM will not detect high Z materials. As mentioned in section 2.2.4, low accelerating voltages decrease the depth from which x-rays are emitted. If the sample has an insulating layer on the surface, and elemental analysis from the lower layer is desired, a low voltage may not be able to penetrate the outer layer. To avoid this a thin coating of a conductive material should be applied to the sample after being mounted to a stub, which will be discussed later. This coating can be applied by evaporative or sputter coating techniques. The film is either gold or carbon, typically $< 100 \text{ \AA}$. Gold is used when secondary imaging is desired and carbon is used when backscattered and x-ray analysis is conducted. This is because Gold blocks low energy x-rays, and gives off characteristic x-rays itself, while carbon is more transparent to low energy x-rays because of its low Z ($Z = 6$).⁶

Once the sample has been sized and cleaned, it needs to be mounted on a sample stub, which is usually made of aluminum. The sample is secured to the stub with double-sided conductive

carbon tape and/or silver paint. Sample stability is important during SEM analysis because any movement other than normal positioning will result in a shift in the field of view, which interferes with image recording and x-ray analysis.⁶

The disadvantage of carbon tape and silver paint is that they both can give off characteristic x-rays, which could interfere with x-ray analysis. Silver paint must also dry before being exposed to vacuum, because it will outgas. This is because silver paint is essentially a colloidal mixture of Ag particles suspended in an organic solvent that must be evaporated. The advantage silver paint has over carbon tape is that it can provide some conductive contact to the stub by its capillary action of the liquid. This is useful if a sputter coater is not available.^{6,11}

After the sample has been properly prepared and scanned, the data need to be analyzed. This data may include secondary and backscattered electron topographical images and x-ray spectral graphs and images. Several parameters help control the data released by the sample. These include beam accelerating voltage, current, diameter, scan rate, and length of scan, as well as sample position. These must be taken into consideration during analysis.¹²

One of the characteristics of the SEM that make it one of the most popular analyzing instruments, is the apparent ease with

which its images can be interpreted. This is due to the fact that SEM images appear to be similar to what the human eye produces, especially its three-dimensionality and the high depth of field (compared to an optical microscope) although the two imaging processes differ greatly.²

For the human eye, the more light an object surface reflects, the brighter it appears, with a particular type of SEM image, the more of that type of data signal is being detected originating from a particular area of the sample, the brighter the area. The amount of data being detected by the detectors is the result of more data being emitted by the sample, and the position (particularly the tilt of the sample) and shape (sharp edges emit more signals, which is known as edge effect) of that area of the sample cause a larger number of the data signals to be emitted to the detector. The amount of data emitted is affected by the elemental composition of the sample and the beam current.^{2,5}

A higher beam current, means that more electrons are available to interact with the sample, results in a greater sample signal that is easier to distinguish from “noise electrons”. This generally results in a higher quality image. Several parameters affect the current. These are the beam voltage, beam diameter, filament emission, and beam alignment. While the emission should never exceed 100 μA , to prevent filament damage, the

others can be adjusted. These should be set to maximize the current unless other conditions warrant it. As mentioned earlier, the voltage will be determined by whether x-ray analysis will be conducted (depth of analysis and energy of x-rays to be detected) and if the sample suffers from charging effects. The higher voltage causes an increase in the beam current. By decreasing the beam diameter current is reduced, which may be needed during x-ray mapping to control the x-ray counts per second which controls the dead time as explained in section 2.4.2. Also, making the diameter smaller increases the resolution. The smallest feature that can be imaged is at best the same size as the beam (a SEM can never “see” a feature smaller than the diameter of its beam). So, for high-resolution topographic imaging, the smallest beam diameter should be used that will still give a good image.⁴

To measure the beam current, a Faraday cup was made by the procedures in appendix C. Figures 3.1. 1 shows the beam current versus accelerating voltage using the largest beam diameter of the SWT Physics department’s Amray 1400 SEM, when the beam is misaligned and when it is properly aligned. As can be seen, beam misalignment results in low beam current. Low beam current results in low x-ray counts and a grainy image. This shows the importance of imaging with a properly aligned beam.

As mentioned in section 2.2.3, the elemental composition of

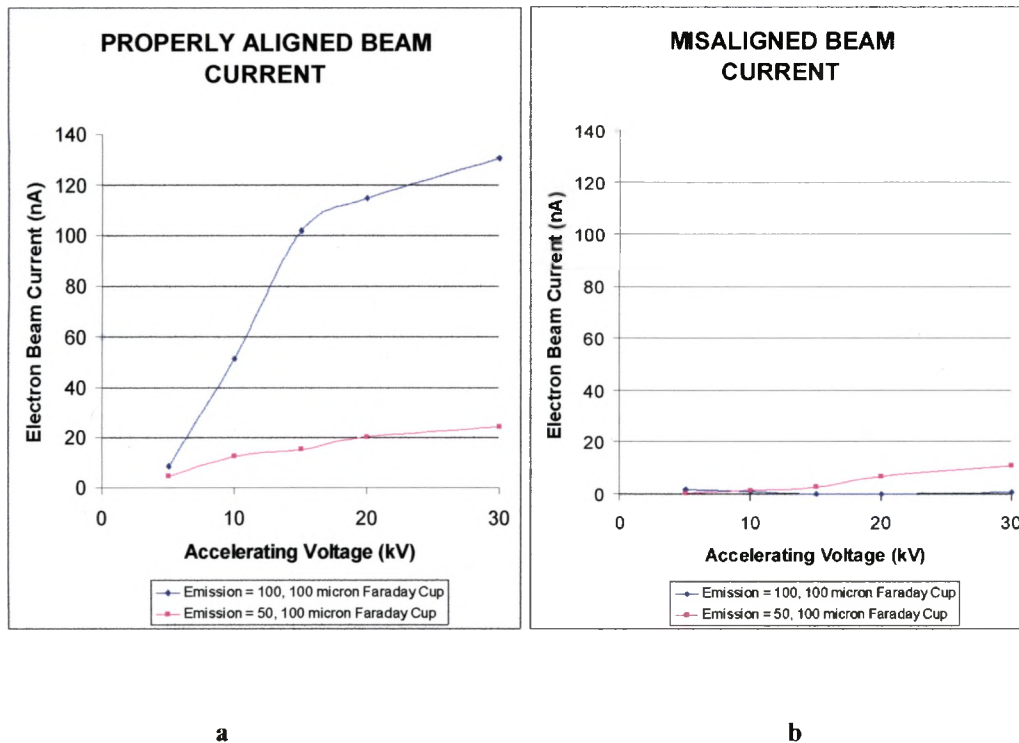


Figure 3.1.1. Electron beam current vs. Accelerating voltage:
a) when beam is aligned, b) when beam is misaligned.

the sample affects the amount of signals emitted. This is most obvious with backscattered electrons. As a result, a sample with localized concentrations of higher or lower Z atoms will result in bright or dark areas respectably. This will not give the identification of specific elements of the sample, but just show a contrast between higher and lower Z areas. This will be discussed in more detail in section 3.2.²

The shape and positioning of the sample also affects the direction that the emitted data is released. A flat sample can easily

be positioned so that a maximum amount of signal can be detected. But a non-flat or rounded sample releases its data in a more evenly distributed volume.²

Other than the shape of the sample surface, the size of its features can be found, by using the fact that the area of the sample that is scanned controls the magnification of the image. The relationship between the magnification and the scanned area can be seen in table 3.1.1.⁵

Table 3.1.1. Magnification and scanned sample area relationship. Adopted from Goldstein.

Magnification	Scanned area of sample
10X	$(0.01\text{m})_2 = (1\text{cm})_2$
100X	$(0.001\text{m})_2 = (1\text{mm})_2$
1,000X	$(0.0001\text{m})_2 = (100\text{micron})_2$
10,000X	$(0.00001\text{m})_2 = (10\text{micron})_2$

As discussed in section 2.4.3, x-ray spectral graphs can be found which show the relative concentration peaks of the detected characteristic x-rays on top of the Bremsstrahlung x-ray background curve. Examples of spectral graphs can be seen in section 3.3.

Since x-rays originate towards the bottom of the excitation volume, and the beam accelerating voltage affects the depth of this volume, the SEM operator has some control of the depth of x-ray origin. As mentioned earlier in this chapter, higher accelerating voltages increase the beam current. This results in a sharper and

brighter image, but more x-rays will be created from deeper in the sample. For bulk samples this is not a problem, but for elemental analysis of only the top layer for samples with a coating on the surface, this is a problem. This requires a lower voltage. On the other hand, lower voltages may not supply sufficient energy to excite higher energy characteristic x-rays in the sample. The highest energy x-rays that can be produced during beam sample interaction is just slightly less than that of the beam. For example, if a voltage of approximately 5 keV is used, there will be no creation of x-rays of 5 keV or higher. In fact, there is a reduction of x-rays produced that have energies approaching the accelerating voltage, which is discussed in more detail in section 2.2.3.

There are five main parameters that affect the quality of SEM data collection. This must be taken in balance of each other to give the desired data.^{5,12}

- 1 Higher accelerating voltages gives higher resolution but also gives unclear surface structure, more edge, and charging effects. While lower voltages have low resolution, the surface structures are clearer (because beam penetration into the sample is reduced), there are less edge effects, and there is less charging.
- 2 Larger probe current gives more signal, and a smoother image, but decreases the resolution. Less current gives

higher resolution (because the incident beam diameter is reduced), but the image looks grainy.

- 3 Smaller working distance gives greater depth of field, and a higher resolution. Increases in the working distance give smaller depth of field and less resolution, but are often useful for x-ray imaging.
- 4 Large beam diameter gives a larger current. This results in more x-rays and backscattered data. Which increases the quality of this type of data. But it also reduces the resolution and the depth of field. Small beam diameters (lower beam current) give higher resolution, and greater depth of field but a grainy image.
- 5 Longer x-ray exposure time, the more x-rays will be detected, which produces higher quality of x-ray images.

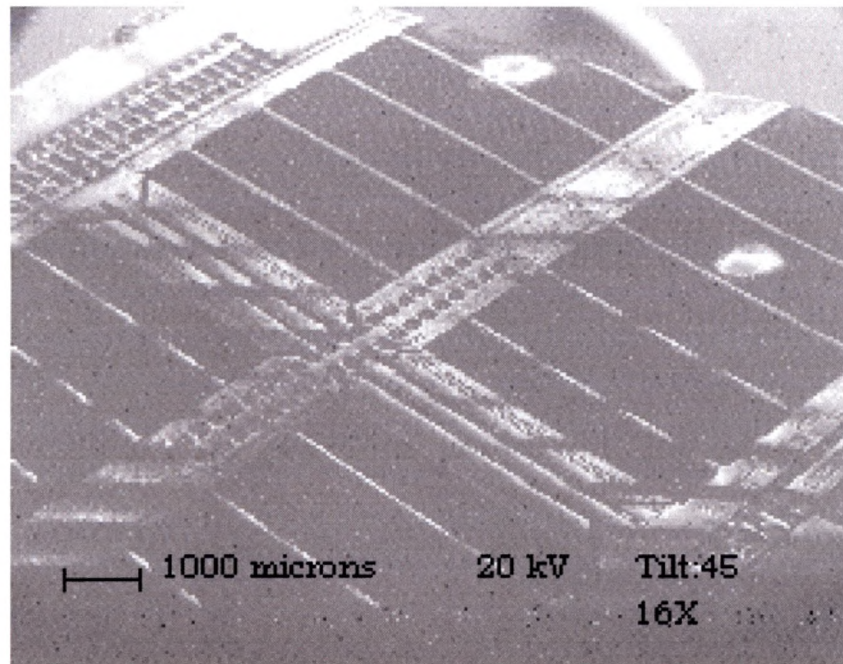
3.2 SECONDARY AND BACKSCATTERED ELECTRON IMAGES

One of the primary functions of the SEM is to produce images of three-dimensional objects. Both secondary and backscattered electron images exhibit topographic contrast. By far the largest number of data signals released by the sample during electron bombardment is secondary electrons. As mentioned in section 3.1, the more data signals released by the sample results in an image of higher resolution. Therefore secondary images are generally used for topographical imaging, and backscattered

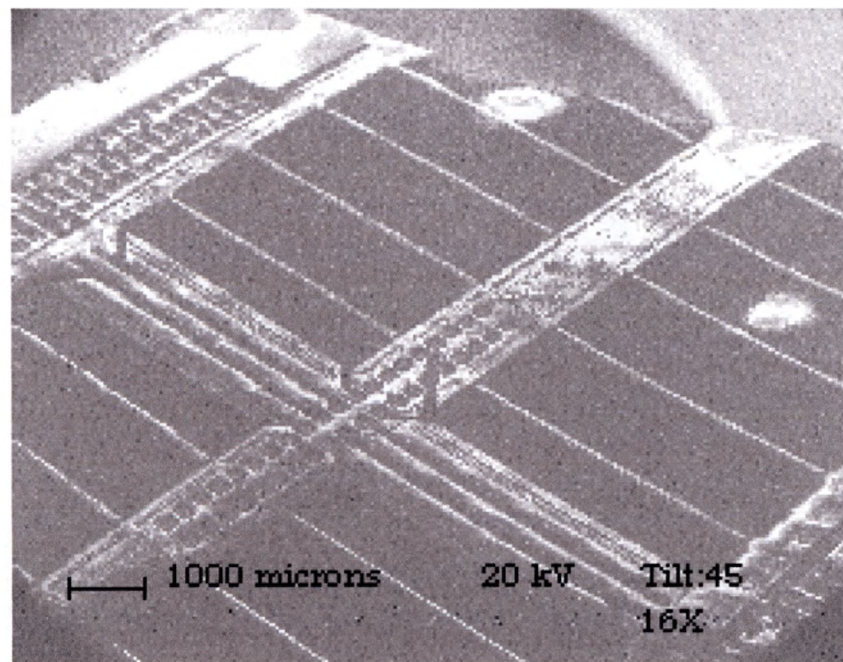
images are used to show compositional contrast. Together these two types of images can give valuable sample information.²

The smallest feature that can be imaged is at best the same size as the diameter of the beam. So, for high-resolution topographic imaging, it was found that the smallest beam diameter should be used that will still give a good image, before the image becomes grainy. Figure 3.2.1 shows the difference when a larger and smaller beam was used on a patterned microelectronic sample provided by Dr. Daniel Chesire of Lucent Technology. The images show that the smaller beam gave a sharper image. On the Amray model 1400 SEM, the beam diameter is controlled by the spot size knob. This control is labeled such that the smaller the spot size, the larger the beam diameter, 0 being the smallest and 10 the largest. The reason the smallest beam diameter is not always used is because, as discussed in section 3.1, the smaller the diameter, the lower the current. This affects the amount of signal the sample emits, resulting in a darker image. Less data signal emitted by the sample is not as important for secondary images because there are much more of this type of signals given off, but backscattered electrons and x-rays are emitted in much lower amounts.⁴

Acceleration voltage of the electron beam also affects the images produced. As the voltage is increased, the beam current is increased. This causes more beam sample interactions. As a



a) secondary electron image



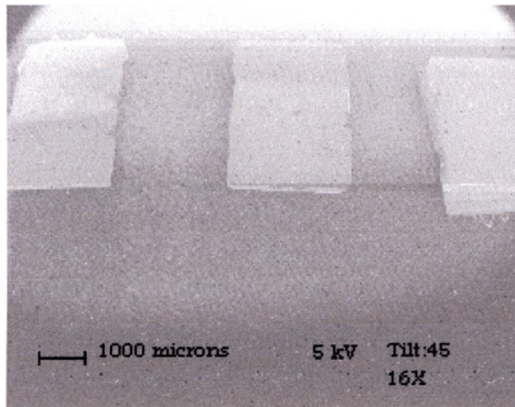
b) secondary electron image

Figure 3.2.1. Secondary electron images taken using 20 kV, tilt of 45°, at 16X, but different beam diameters. Note that the image in a is sharper and has more resolution than in b. Images a, and b were taken using a spot size of 8 and 2 respectively.

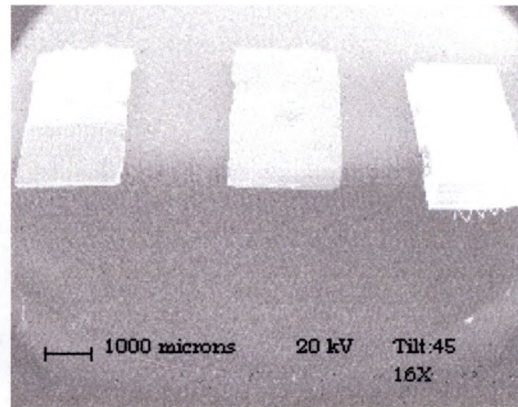
result of the increase in interactions, more data signals are released by the sample, and a brighter area of the image is caused. Figure 3.2.2 shows the contrast of secondary and backscattered electron images when two different accelerating voltages are used. It is seen that the secondary image always gives a higher quality topographical image. These images are of three different Atomic Force Microscope (AFM) tips that were provided by Dr. Heather Galloway of the Southwest Texas State University Physics department. Southwest Texas State University Graduate student Kevin P. Wiederhold mounted and coated all of tips. The right most was tip that was mounted upside down.

Increasing the accelerating voltages was also found to increase the resolution of images. This is more obvious at higher magnifications. Figure 3.2.3 shows a higher magnification image of the middle tip in Figure 3.2.2. The point of the tip can be seen easier, as well as a sharper overall image as the voltage is increased. Note the shadowing effect seen on the tip at the lower voltage and the absences of this effect at the higher voltage. This phenomenon will be discussed next.

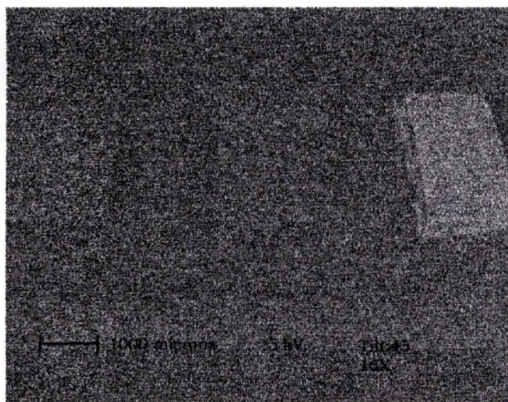
Higher voltages also result in the deeper penetration of the excitation volume as discussed in chapter 2.2.4. This obviously results in more data emission from deeper inside the sample. This



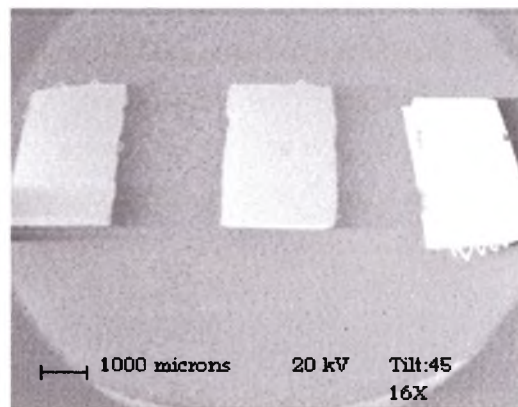
a) secondary electron image



b) backscattered electron image

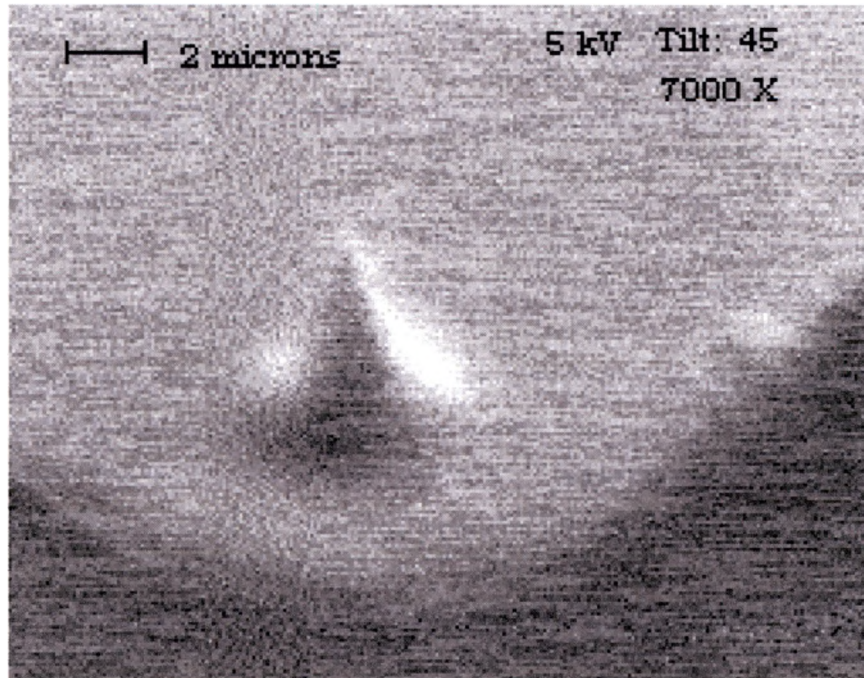


c) secondary electron image

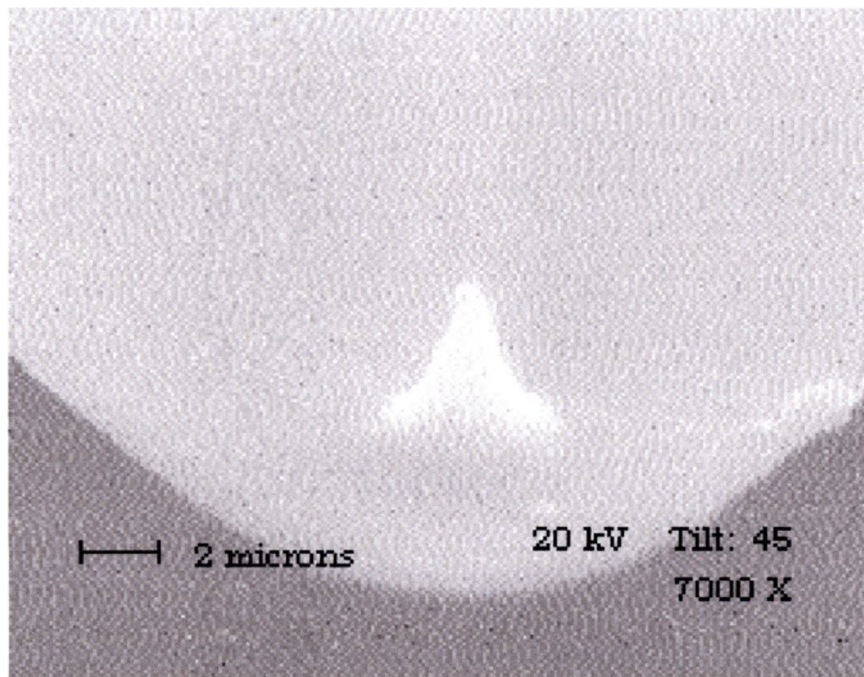


d) backscattered electron image

Figure 3.2.2. Images a and b are secondary electron images, while c and d are backscattered images of AFM tips taken at different accelerating voltages at 16X and a tilt of 45° . Images a and c were taken using 5kV, while b and d with 20kV. Notice that all the images are brighter at higher voltages, but this is especially true for the backscattered images.



a) secondary electron image



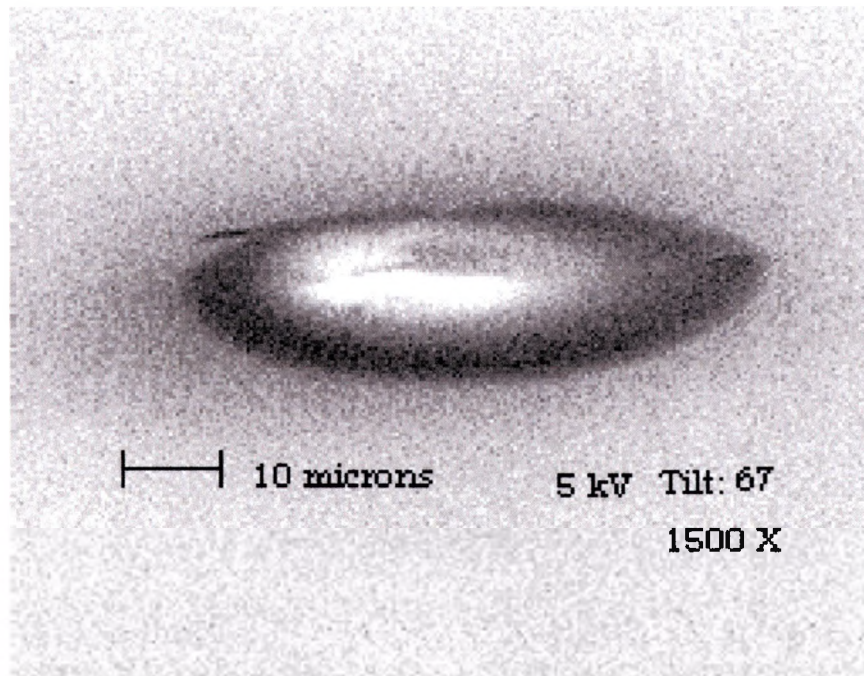
b) secondary electron image

Figure 3.2.3. High magnification secondary images using 5 and 20 keV, of the middle AFM tip in figure 3.2.1. Notice that increases of accelerating voltage, increases the resolution, as well as reduces the shadowing, as more electrons are emitted from deeper in the sample, reducing the effects of surface shape.

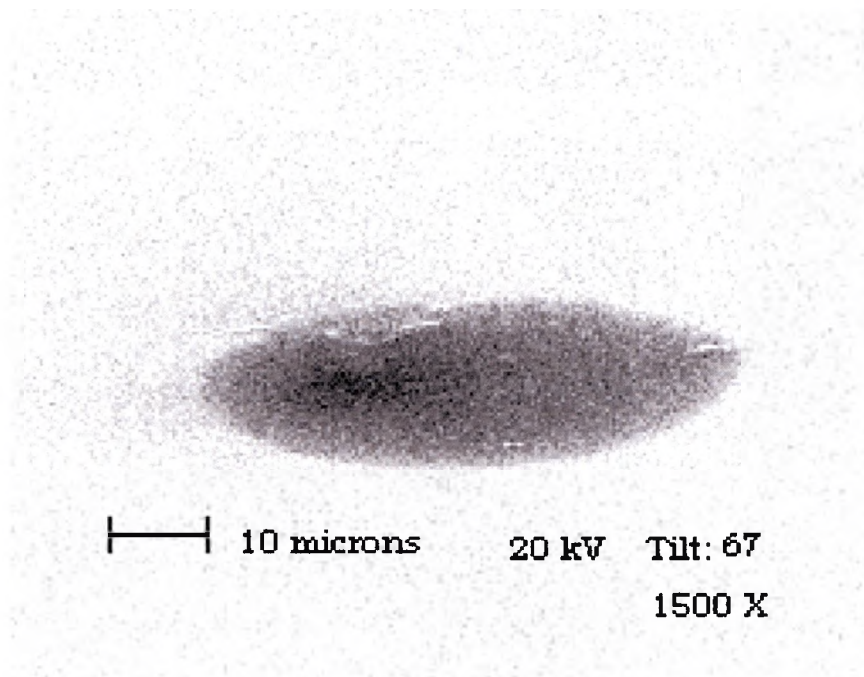
can be useful when a non-flat surface feature is being imaged, since more data is detected from the surface at certain angles with respect to the beam. Figure 3.2.4 are images of a hill like feature, which was produced by etching a SiO₂ sample that was also supplied by Dr. Daniel Chesire of Lucent Technology, in an HF acid bath by Southwest Texas State University Graduate student Matt Langendorf. These images show how using a low voltage can cause a bright area or shine on the sample surface as more of the signal is originating closer to the surface, but higher voltages cause an increase in the origin of signals from deeper in the sample. This causes more data to be acquired from an area that is less like the shape of the feature, which reduces the shine from the image.

Figures 3.2.5 show the effect of increasing tilt has on the sample. As the sample tilt angle increases from 45° to 65°, the number of secondary electrons detected from the top surface to decrease.

As images are displayed, the brightness and contrast controls are important to the quality of the image seen by the observer. These controls should be properly adjusted so that a good image is seen. Figure 3.2.6 is an image of carbon-impregnated polymer wire insulation (used for pipe heating applications) provided by Thermon Manufacturing Inc. (100 Thermon Dr. San Marcos, Tx.) where the brightness and contrast

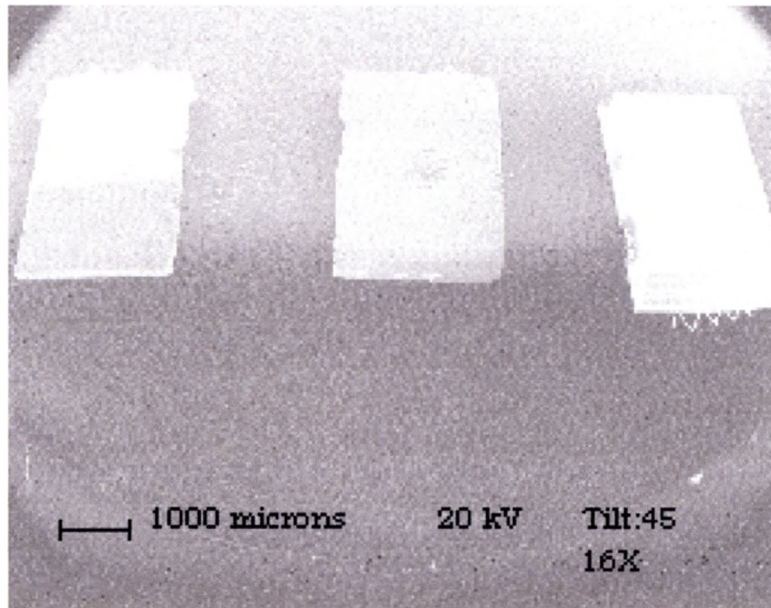


a) secondary electron image

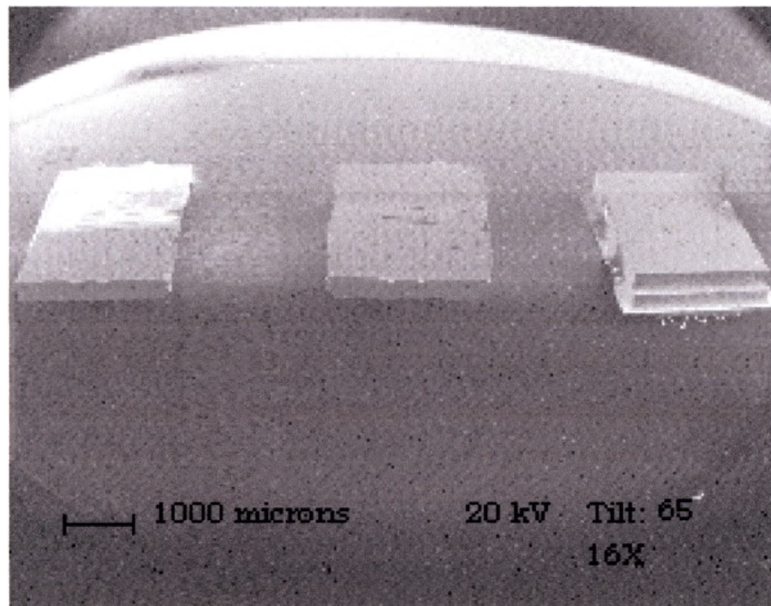


b) secondary electron image

Figure 3.2.4. Secondary images taken at two different accelerating voltages, a with 5kV and b with 20kV, at a tilt of 67° and at 1500X, of an unknown residue left on the surface of a SiO_2 sample after etching. Notice that the shadowing effect is not noticed, as well as the increase in brightness in the bottom image, as the voltage was increased.

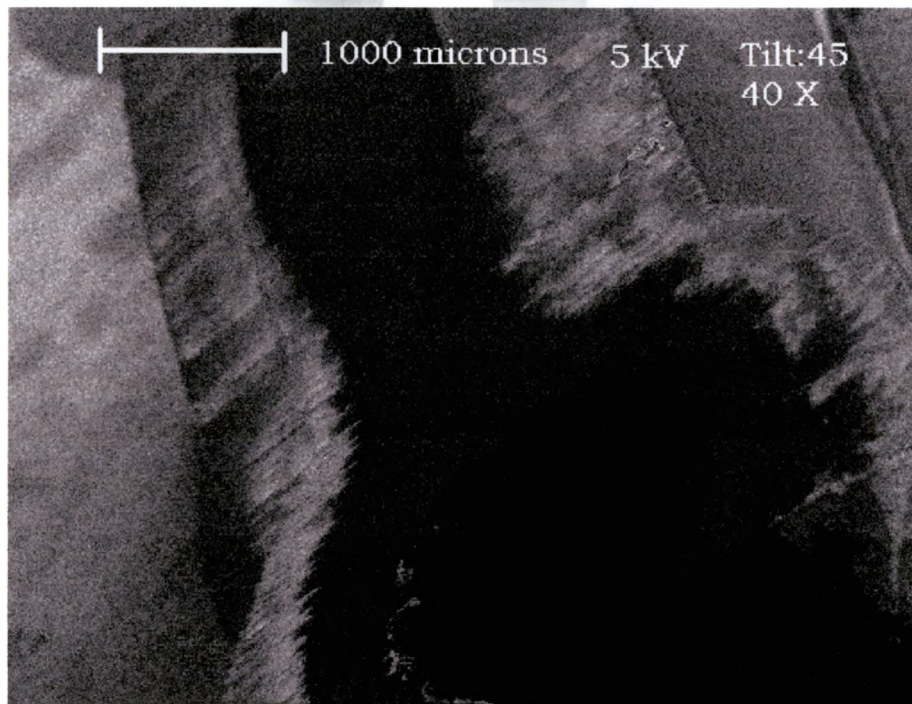


a) secondary electron image

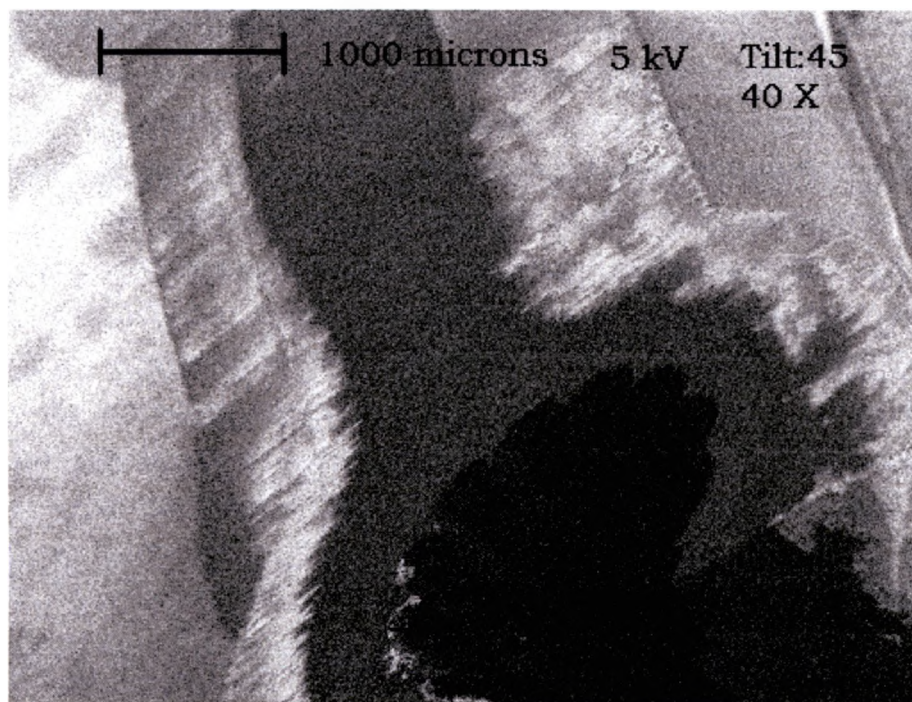


b) secondary electron image

Figure 3.2.5. Comparison of tilt has on secondary images taken using 20kV at 16X using a tilt of 45° for a and b using 67° . Notice that the brightness decreases as tilt is increased.



a) secondary electron image

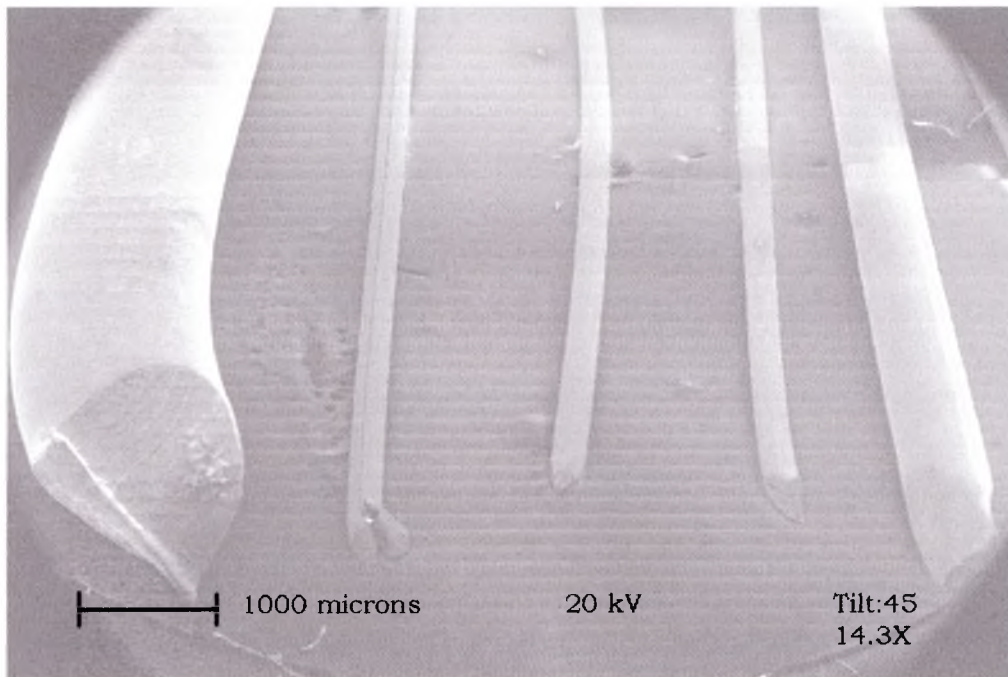


b) secondary electron image

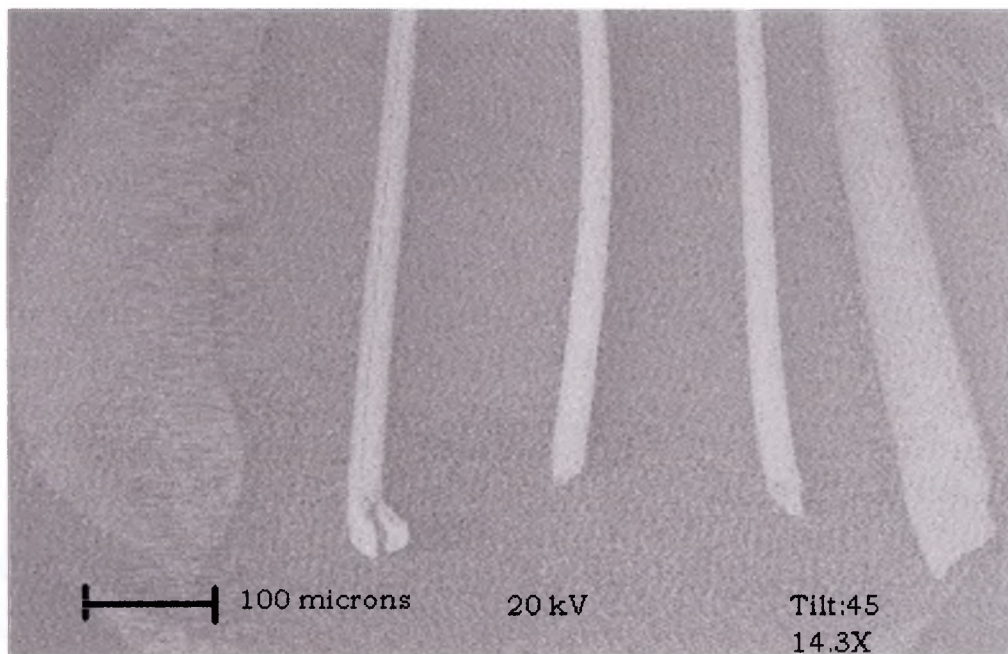
Figure 3.2.6. The effect that brightness and contrast levels have on image quality. These images were taken using 5kV with a tilt of 45° at 40X. Image a has the brightness and contrast level set to low while the image b is improved. Note that the darker regions that surround the opening where the wire is placed is due to the presence of conductive carbon impregnation in the polymer.

is too low. The settings were at their limits. An increase in accelerating voltage would have helped, except that at voltages of ten or higher, charging was noticed, even though this non-conducting sample was mounted with silver paint to prevent this from happening. This is also a good example of what good sample preparation can do for data acquisition.

As mentioned earlier in this section, backscattered images provide compositional contrast. This can be valuable information when compared next to the topographical image of secondary images. A good example of this is shown in figure 3.2.7, and 3.2.8. These sample shows several wires (Al, W with Re, Pt coated W, W, and Cu), which were provide by the Southwest Texas State University Physics Department and a patterned chip from Lucent Technology Inc. It can be seen that the secondary image always has more resolution than the backscattered image because there are more secondary electrons produced than backscattered during beam interaction as mentioned in section 2.2.3. Notice that in figure 3.2.7, the wire on the left gives almost no backscattered image, while the right most wire gives less than the three middle wires. This reveals that the left wire is composed of the lowest Z element, followed by the far right wire, and then the middle three wires are composed of the heaviest Z elements in the image. Since it was known what the wires were composed of, it is now known

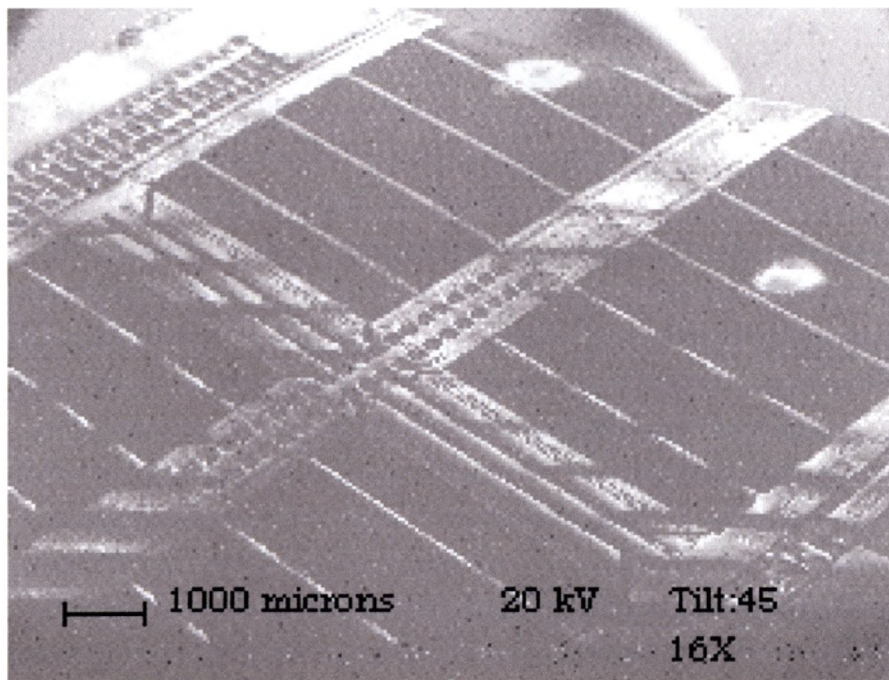


a) secondary electron image

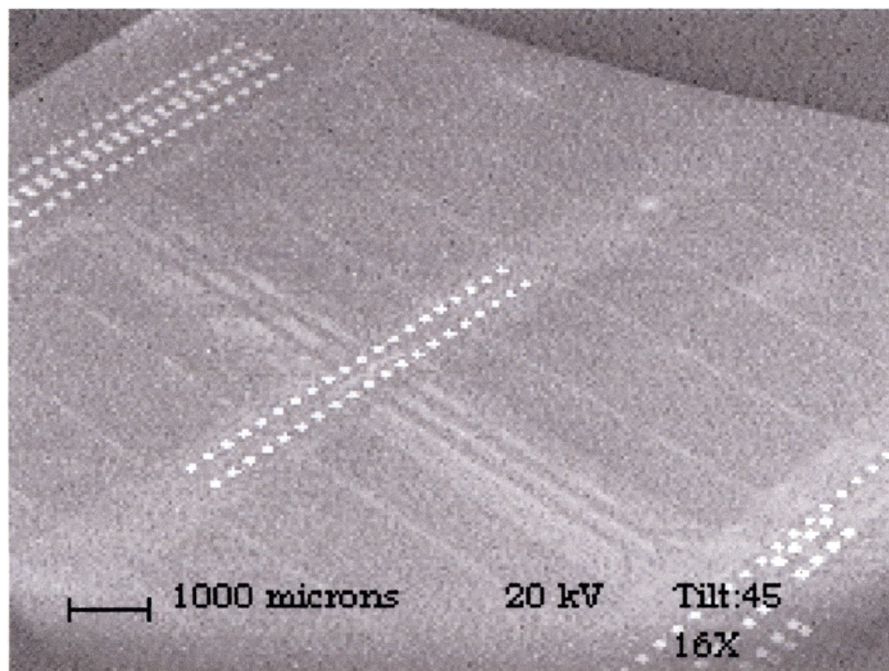


b) backscattered electron image

Figure 3.2.7. The effect that brightness and contrast levels have on image quality. These images were taken using 5kV with a tilt of 45° at 40X. Image a has the brightness and contrast level set to low while the image b is improved. Note that the darker regions that surround the opening where the wire is placed is due to the presence of conductive carbon impregnation in the polymer.



a) secondary electron image



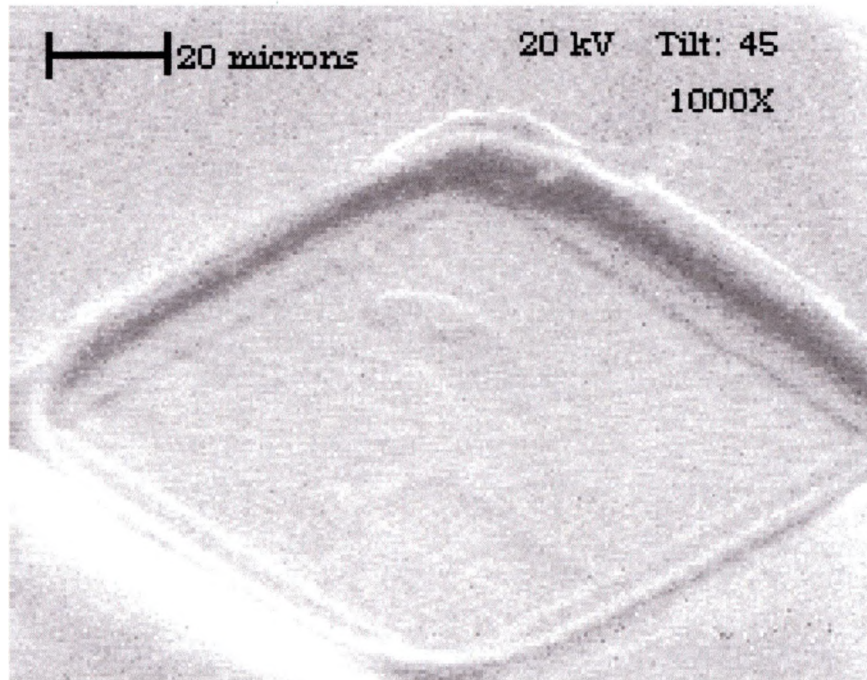
b) backscattered electron image

Figure 3.2.8. The difference of the secondary a, and backscatter image b taken using 20kV, with a tilt of 45° at 16X. Notice how image b shows compositional contrast.

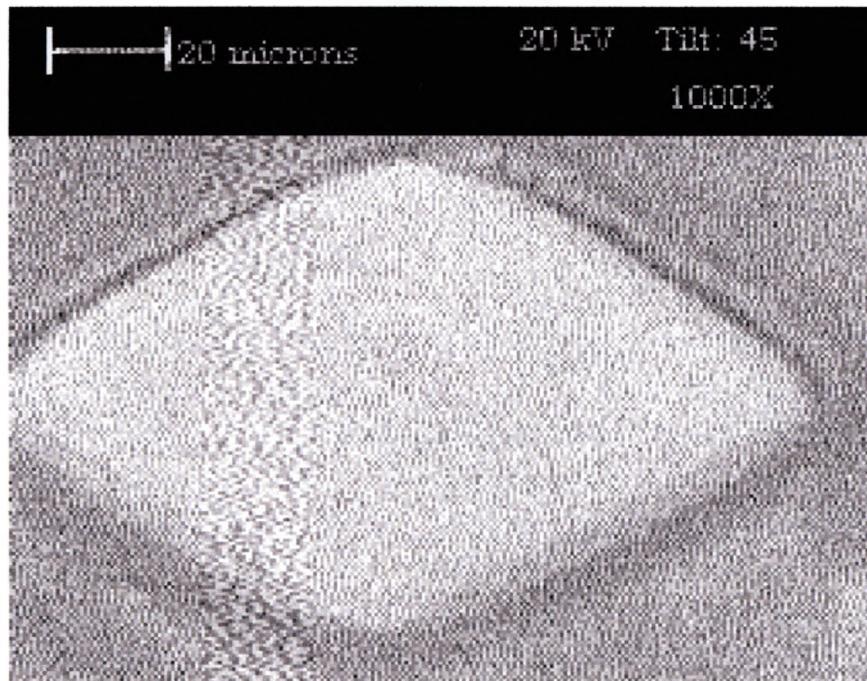
that since Al is the lowest Z of the wires in the image ($Z_{\text{Al}} = 13$), the Al is left most wire. The right most wire's backscattered image is visible but not as bright as the three middle wires, which have relatively the brightness. It can then be concluded that the Cu wire ($Z_{\text{Cu}} = 29$), is on the right and that the W wires ($Z_{\text{W}} = 74$), are in the middle. But the specific identity of W wires cannot be determined with just backscattered analysis. X-ray analysis of this sample will be discussed in section 3.3.

Figure 3.2.8 shows bright dots where higher Z elements are located. A blow up of one of the dots can be seen in figure 3.2.9. The secondary electron image shows that the dots are actually square level indentations used for wire-bonding contacts to the IC. While the backscattered image shows that the indentations consists of only one element, which is of a higher Z element than the rest of the sample, because there is no contrast in brightness inside the squares.

As can be seen in the backscattered image of the AFM tips in figure 3.2.10, suffers same effect as the secondary images mentioned earlier, of loss of brightness as tilt, is increased, although the backscattered images are effected to a smaller degree because, as mentioned in section 2.2.1 the backscattered electrons are scattered at greater angles. The AFM tip on the right is the brightest object in the backscattered images and when the tip is

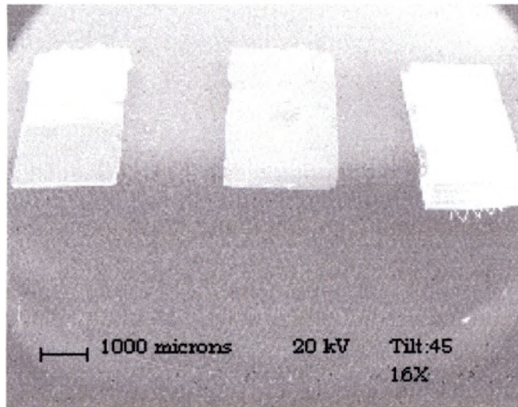


a) secondary electron image

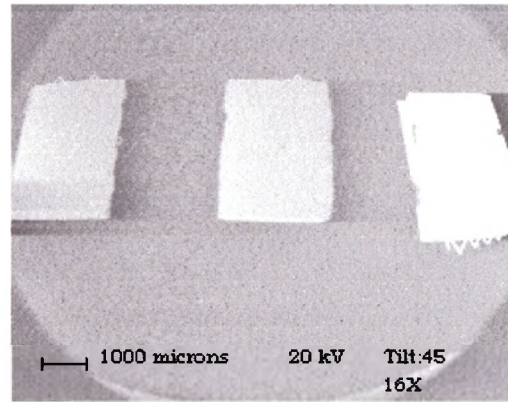


b) backscattered electron image

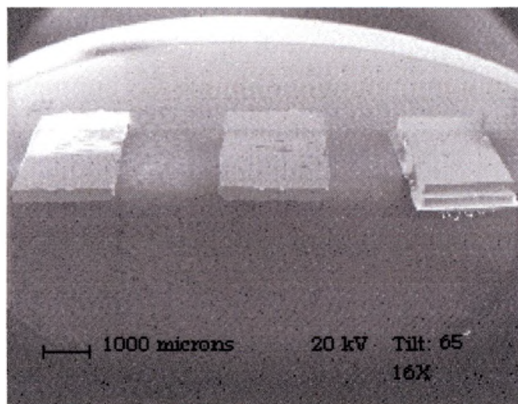
Figure 3.2.9. High magnification of one of the bright dots on the backscattered image in figure 3.2.8. Image a showing secondary image, while b shows the backscattered image using 20kV, a tilt of 45° , at 1000X.



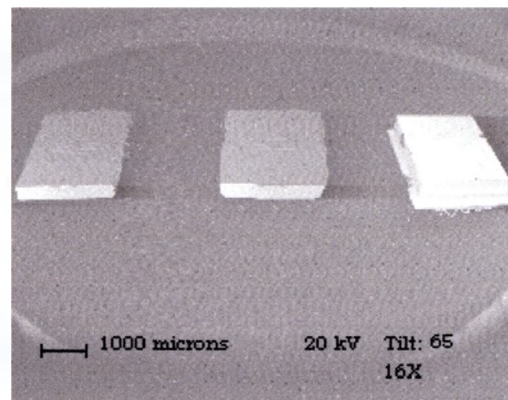
a) secondary electron image



b) backscattered electron image



c) secondary electron image



d) backscattered electron image

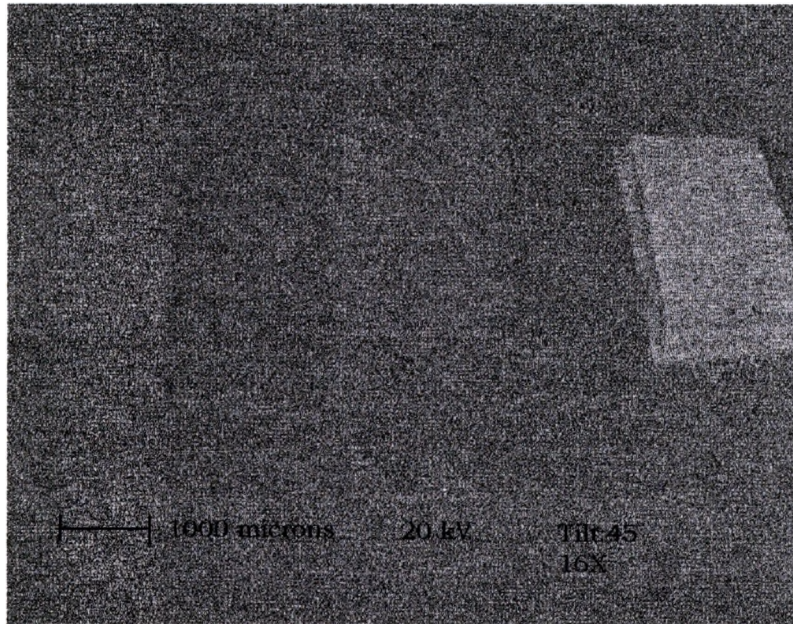
Figure 3.2.10. Comparison of tilt has on secondary images a and c, and backscattered images of b and d. Notice that tilt has more effect on the brightness of the secondary image than on the backscattered image. All of these images were taken using 20kV, at a 16X, while a and b were tilted 45° , and c and d at 65° .

tilted at a large enough angle, the front edge under the top lip of the other tips can then be seen to have a high Z composition as well. Knowing that the tip on the right was mounted upside down it can be determined that these tips either have a higher Z element coating the bottom or a light Z coating the top.

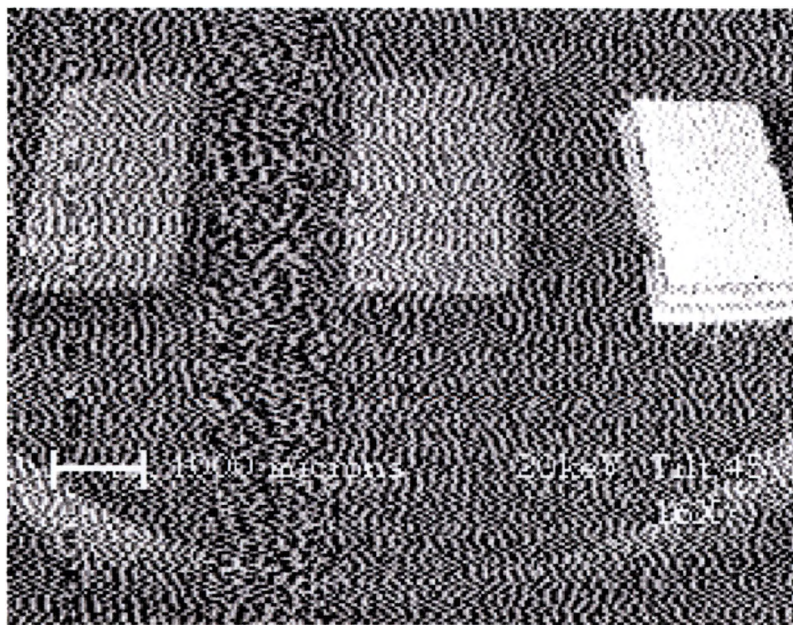
The actual elemental composition cannot be determined from backscattered electron imaging. It only shows a contrast in heavy and light elements that are present.

The rate at which the scan is taken affects the quality of the image. As discussed in chapter 3, the size of the matrix (which is selected by the operator) that the computer uses to gather and store the image determines the size and number of pixels that is used to display the image. The larger that the matrix is chosen to be, the more time is required to take the image. This results in a higher quality image. Figure 3.2.11 shows the effect of imaging AFM tips with different size matrix. A matrix of 256×200 was used for a, and 128×100 was used for b. The image in b is lower in quality as the pixel dots can easily be seen.

Both secondary and backscattered electron images exhibit topographic contrast. Secondary images are generally used for topographical imaging, and backscattered images are used to show compositional (Z) contrast. Together these two types of images can give valuable sample information. This is important since the



a) backscattered electron image



b) backscattered electron image

Figure 3.2.11. These images were taken using 20kV, with a tilt of 45° , at 16X, but image a was taken using a matrix size of 256X200, while image b used 128X100. Notice how the quality of image a is improved over image b.

primary function of the SEM is to produce images of three-dimensional objects.

3.3 EDS IMAGES

The ability to perform chemical analysis is one of the SEM's most powerful abilities. This is a simple relationship between the energy of characteristic x-rays that an element emits and its atomic number. A SEM can use this not only to detect what is in the sample, but also create an image where it is.

As discussed in section 2.4.3, the number of detected x-rays counted versus the energy of the detected x-rays can be graphed. This is called an x-ray spectral graph. The x-rays that will be graphed are the Bremsstrahlung, and characteristic, with the characteristic peaks lying on top. This can be seen in figure 3.3.1. This graph was produced using an accelerating voltage of 10 kV, with the x-ray detector's Beryllium window closed to scan one of Dr. Donald Olson's geological samples (obtained in Mexico, presumably along the route taken by the Spanish explorer Cabeza de Vaca) for elemental analysis. As can be seen, no x-rays are being created with more than the beam energy (10kV). Actually few x-rays are detected with more than 7 keV. This graph shows that the sample contains Si, S, Fe, with traces of O, and Mg. Figure 3.3.2 shows when the Beryllium window is opened and the voltage is dropped to 5 kV. Since the voltage is lower than that of

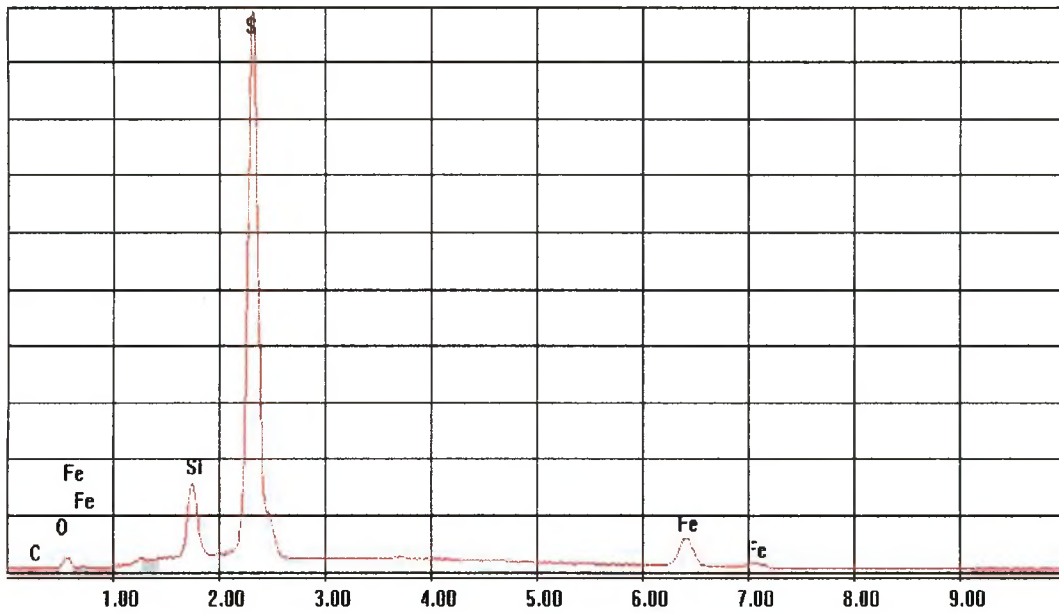


Figure 3.3.1. X-ray spectral graph, where the y-axis is x-ray counts and the x-axis is the x-ray energy, using an accelerating voltage of 10kV, with the Be window closed.

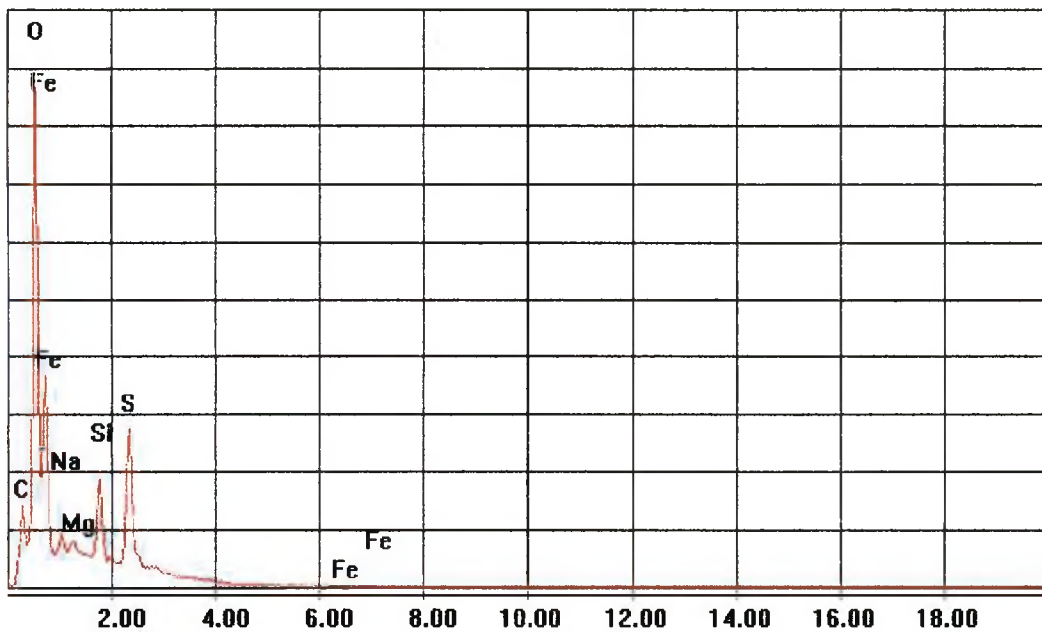


Figure 3.3.2. X-ray spectral graph, where the y-axis is x-ray counts and the x-axis is the x-ray energy, using an accelerating voltage of 5kV, with the Be window open.

the two highest Fe energy peaks ($\text{FeK}(\alpha)=6.398\text{keV}$, $\text{FeK}(\beta)=7.057\text{keV}$), they are no longer created, but now the lighter elements with x-ray energies less than 1 keV are now more visible, like C, O, other Fe peaks ($\text{FeL}(\alpha)$, $\text{FeL}(\beta)$), and Na. These graphs are set to an auto scaling. The tallest peak plus the Bremsstrahlung is scaled to just fit on the scale, and the other peaks are scaled to the height which is relative to the tallest peak. As figure 3.3.1 shows S as the tallest peak, but figure 3.3.2 shows O as the tallest peak. It can also be seen that the two figures show a different relative height difference between S and Si peaks. This is because of the difference in the height of the Bremsstrahlung curve under the peaks and that more of the lighter and fewer of the heavier x-rays are being created with the lower accelerating voltage. Also more of the lower energy x-rays are being detected with the window being opened.

Figure 3.3.3 shows the x-ray spectra of Dr Olson's second geological sample. With the window open and an accelerating energy of 10 eV was used to scan this sample since the verification that it contained the elements S, Ag, and Sb. As can be seen that it does contain the desired elements of S, Ag, along with traces of Cu, Si, and Sb. The graph shows the presence of Mg, Se, and Al, but these have such small relative peak heights, that they may just be noise instead of trace elements.

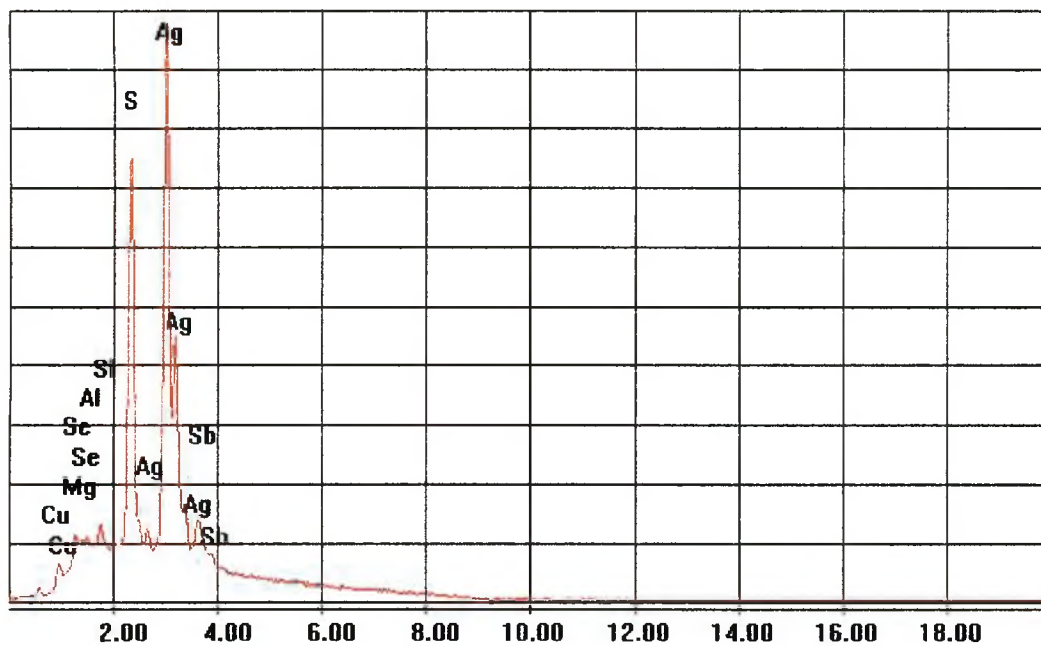


Figure 3.3.3. X-ray spectral graph, where the y-axis is x-ray counts and the x-axis is the x-ray energy, using 10 kV with the Be window open.

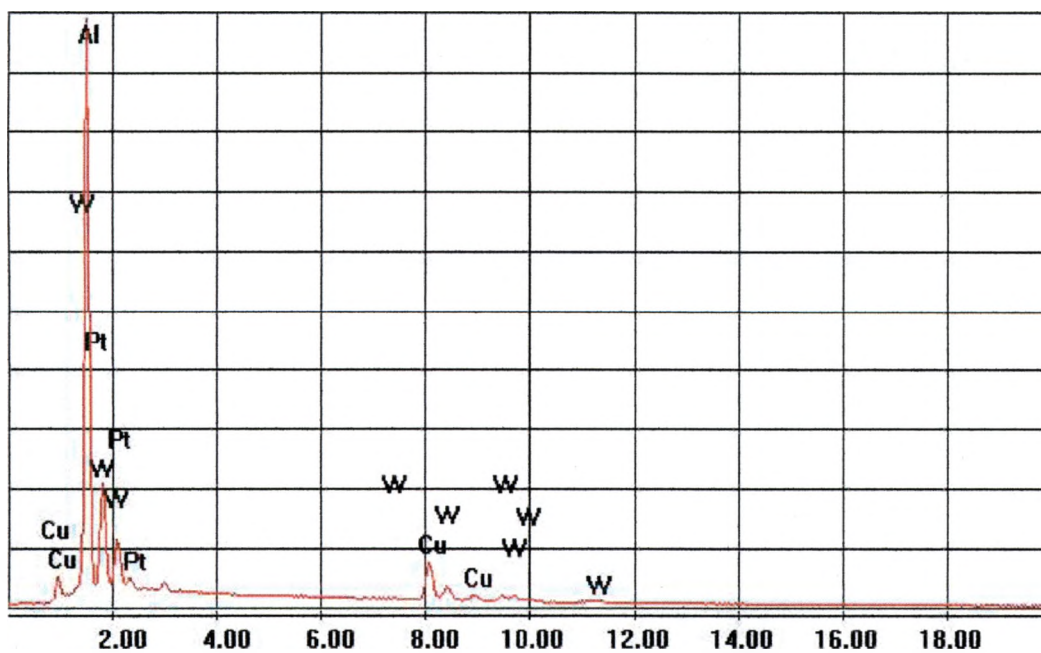
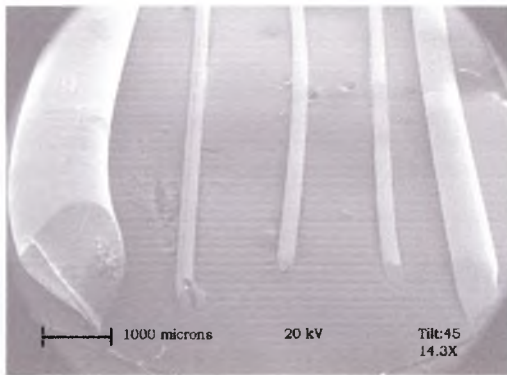


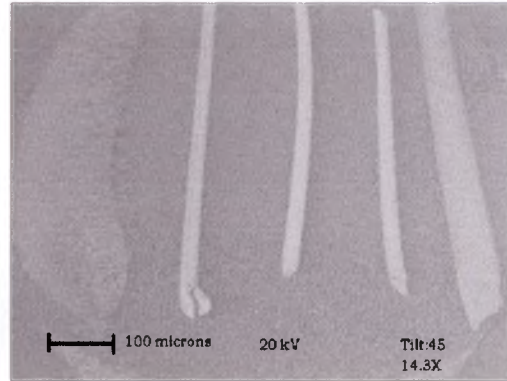
Figure 3.3.4. X-ray spectral graph, where the y-axis is x-ray counts and the x-axis is the x-ray energy, using 20 kV.

The real power of x-ray elemental analysis using a SEM is the ability to create x-ray images or maps of the sample. This not only shows the composition of the sample, but also shows the position of the elements, as well as their relative densities. Section 2.4.2 explains how these maps are created after the elemental composition has been found from an x-ray spectral graph.

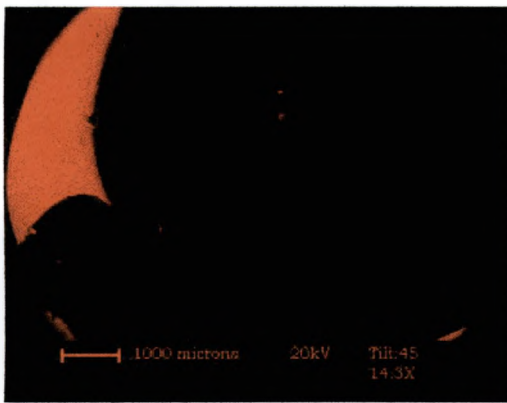
The elemental analysis of the wires that were looked at in figure 3.2.7 was conducted. Figure 3.3.4 shows the spectral graph of the image using an accelerating voltage of 20 kV. As can be seen, Al, W, Cu and Pt have been identified. But one of the wires with a diameter of 0.25 mm, was 97.3% W, know to contain some Re that was not detected. This was probably due to the fact that as W and Re lie next to each other on the periodic table, they have similar atomic numbers (Z). This causes them to have characteristic x-rays with similar energies. As little as 0.048 keV and as much as 0.337 keV separate these neighboring energy peaks. And since there is only a small amount of Re evenly mixed with the W, creating an alloy in one of the wires, the peaks are much smaller than the W peaks. As a result, the Re peaks get lost in the nearby and larger W peaks. A high magnification scan of each of the W wires at an accelerating voltage of at least 20 kV, which would increase the percentage of the Re x-rays detected, if they are present, would have to be conducted to detect the Re in the wire. The x-ray maps of the wires can be seen in



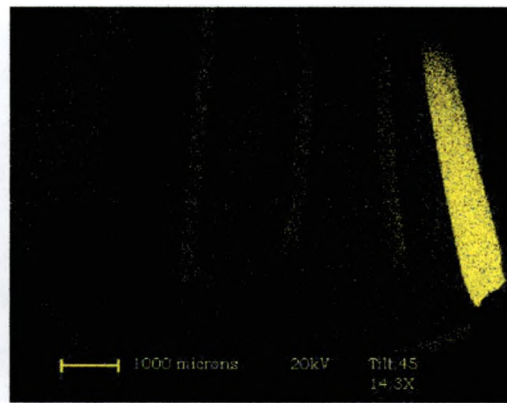
a) secondary electron image



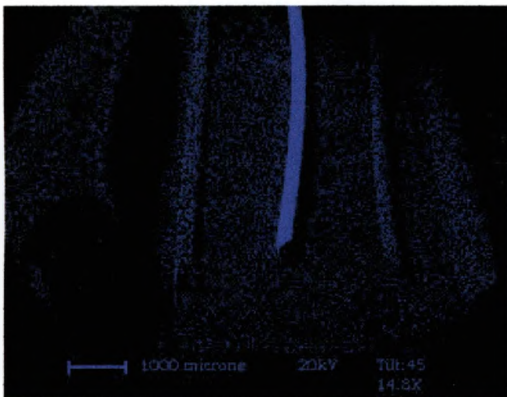
b) backscattered electron image



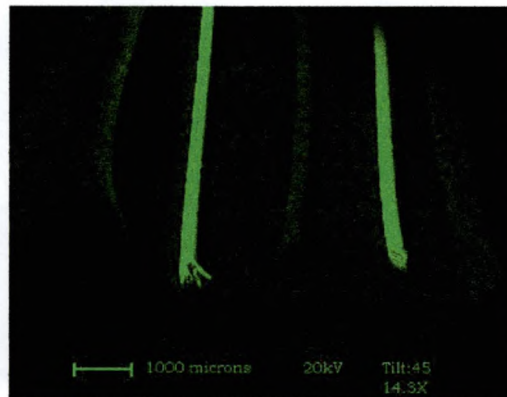
c) Al x-ray image



d) Cu x-ray image



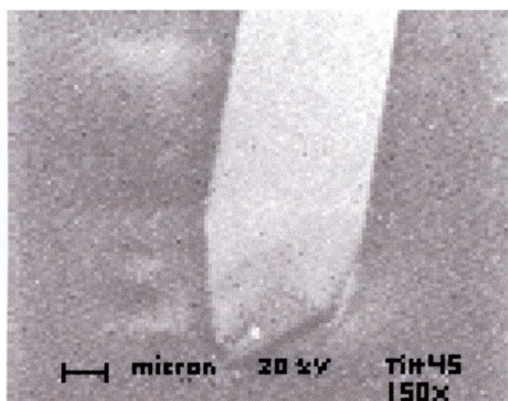
e) Pt x-ray image



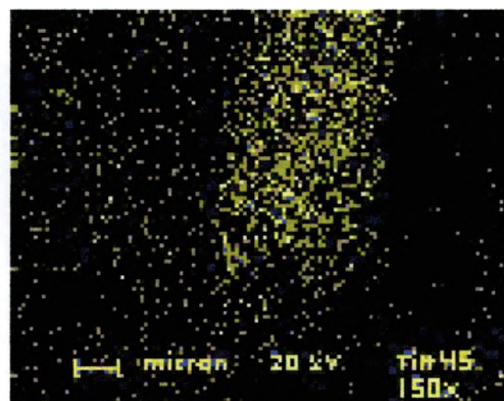
f) W x-ray image

Figure 3.3.5. Image of Al, W, Pt coated W, and a Cu wire taken using 20 kV, with a tilt of 45° , at 14.3X, where a is the secondary and b is backscattered electron, c the Al, d the Cu, e the Pt, and f the W x-ray images.

figure 3.3.5. The backscattered image shows that the far left wire is made up of the lowest Z element of the image as discussed in section 3.2. To reconfirm what was seen earlier, it can be seen that the wire on the left is Al, on the right is Cu, and in the middle are the three W wires. Al wire is useful for wire bonding contacts to IC's, while Cu wires are useful for making electromagnetic windings. It can be seen that the W wires contain trace amounts of Cu, while the outer W wires also have trace amounts of Pt. Figure 3.3.5f shows the detection of W on the Al wire. But close inspection of the Al wire in this image, shows that this small W signal is being detected along the surface next to the W wire. This is caused by the fact that during bombardment, created x-rays are emitted in all directions. W x-rays from the W wire are being emitted and bounced off of the Al wire. The middle W wire can now be identified as the pure W wire coated with Pt. This Pt coating is 5 microns thick; giving the wire a diameter of 0.254 mm. Notice how little W is detected in the Pt coated wire. This is because very few beam electrons penetrate more than the 5 microns. Figure 3.3.6 is a blow-up of Pt coated wire using the same voltage. More W is detected in this image. This is because the beam is interacting more with this particular wire than before, as the beam was being scanned over all the wires. This gives better statistical data. There also appears to be trace amounts of Al and Cu in these images which were not detected in figure 3.3.5. This was



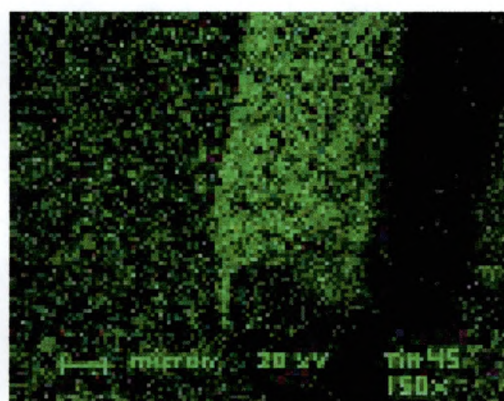
a) secondary electron image



b) Cu x-ray image



c) Pt x-ray image

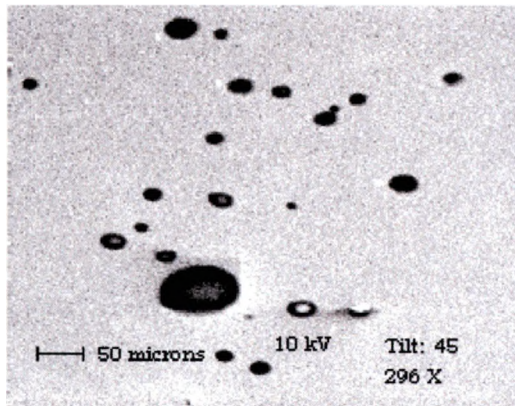


d) W x-ray image

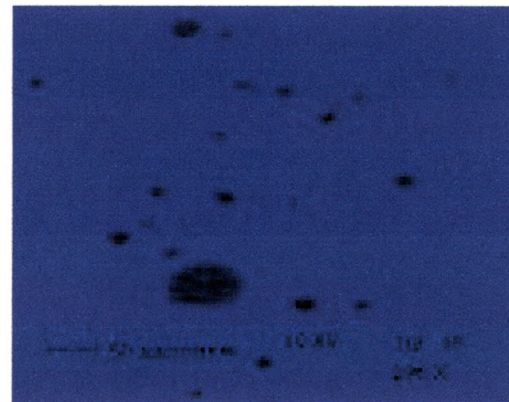
Figure 3.3.6. High magnification at 150X , while using 20 kV with a tilt of 45° , of Pt coated wire in figure 3.3.5 showing a the secondary image; b the Cu, c the Pt, and d the W x-ray images.

unexpected since A Johnson Matthey Company, the manufacture of the W wires did not include them in its contents.

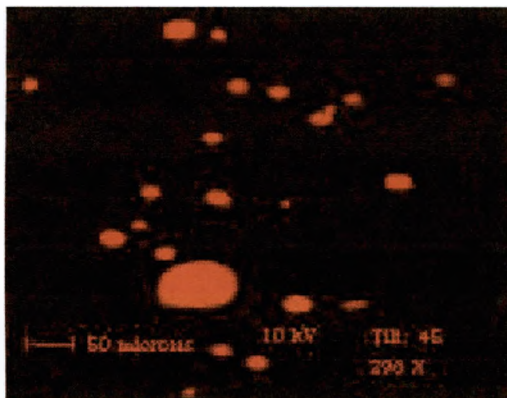
Lower magnification images of an organic solvent Isopropyl cleaned HF etched SiO_2 sample, with the hill like features on them discussed in section 3.2, appear in figure 3.3.7. As the secondary image shows, the film is covered with specks that range in size from around 10 to 50 μm . The x-ray images show that the sample contains a large amount of Si with some O evenly spread over the entire surface, with the exceptions of the specs. The evenly spread O is due to natural reoxidation, as this film was etched about two months before scanning. The specks appear to contain large amounts of O, and C, and no Si. This suggests that the dots have enough depth, which prevents the beam from penetrating, and detecting the Si underneath it. As the tilt of the sample and magnification was increased as seen in figure 3.3.8, the secondary image shows the dot to be a small hill. The Si and C maps in figures 3.3.8b, and c, show that the edges are not sharp, but fade away due to the increasing depth of the hill. At the edges, it is still shallow enough for the beam to penetrate and detect the Si. It can be seen that there is less contrast in the O between the regions inside of the bubbles and outside where the native oxide layer exists, which is shown in figure 3.3.7d, than in the Si and C, which are seen in figures 3.3.7b. This indicates that the C is on top of



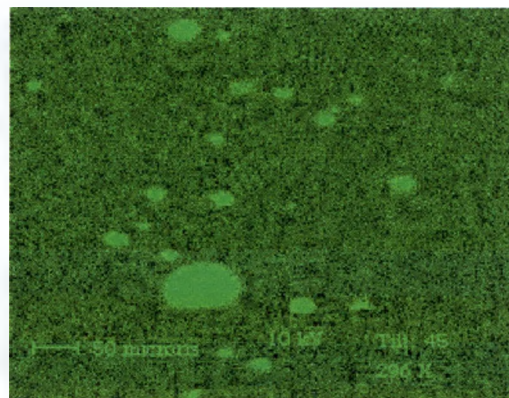
a) secondary electron image



b) Si x-ray image

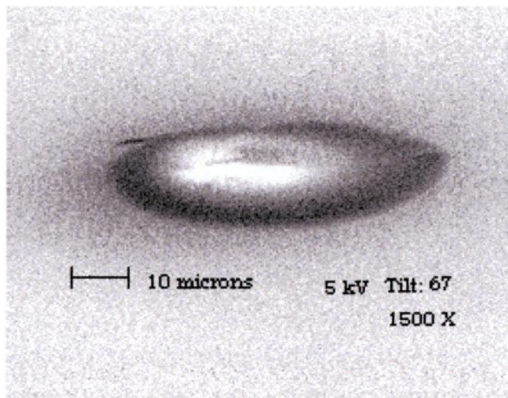


c) C x-ray image

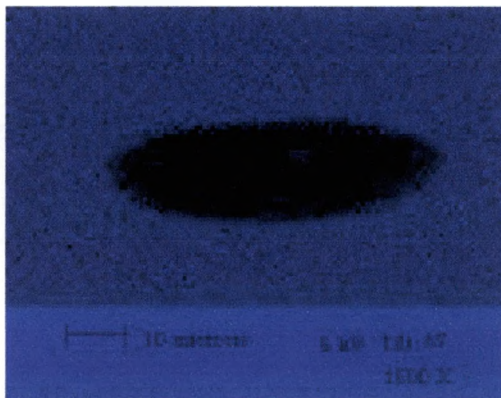


d) O x-ray image

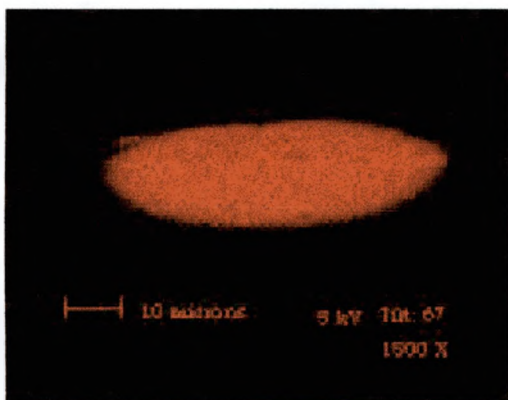
Figure 3.3.7. Secondary electron image a, and b the Si, c the C, and d the O x-ray images. These images were taken using 10 kV, with a tilt of 45° , at 296X.



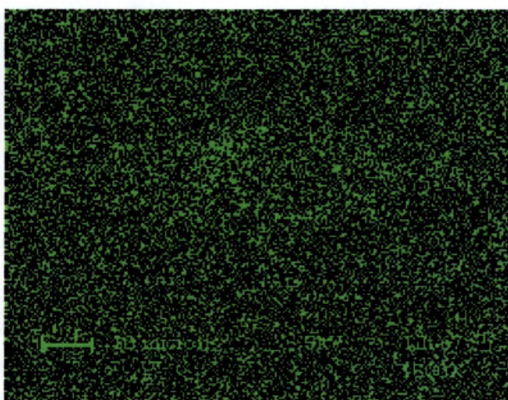
a) secondary electron image



b) Si x-ray image



c) C x-ray image



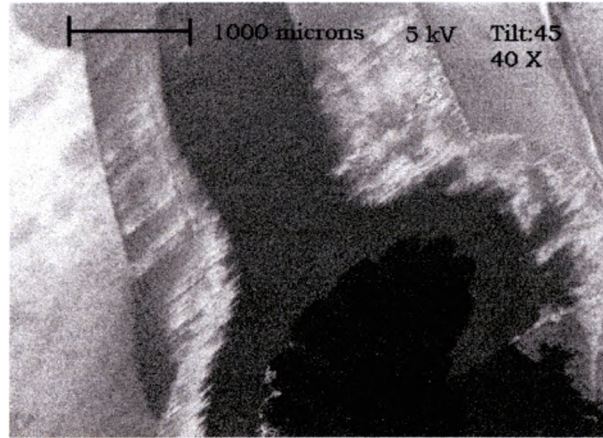
d) O x-ray image

Figure 3.3.8. High magnification image taken at 1500X using 5 kV, and a tilt of 67° , of the largest feature on figure 3.3.7. The secondary image in a, and b the Si, c the C, and d the O x-ray maps.

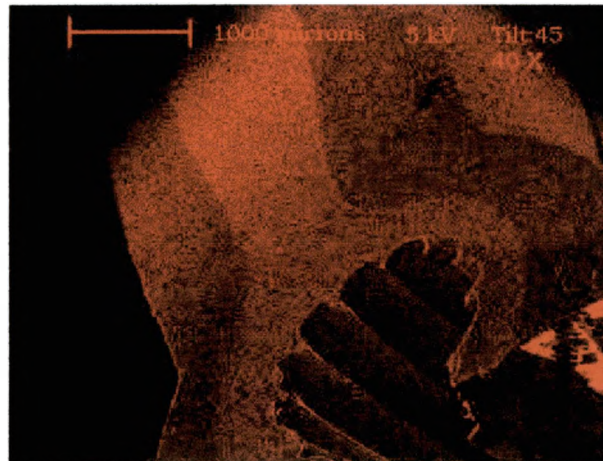
the O. This causes the O peak to fade away in figure 3.3.8d because the silicon oxide layer is enhanced, by the more grazing incidence.

The x-ray maps in figure 3.3.9, of Thermon wire insulation, show that the dark channel in the secondary image contains a higher concentration of C than the other regions. Also, it can be seen that in the region of higher C concentration, the C actually displaces the F present in the polymer.

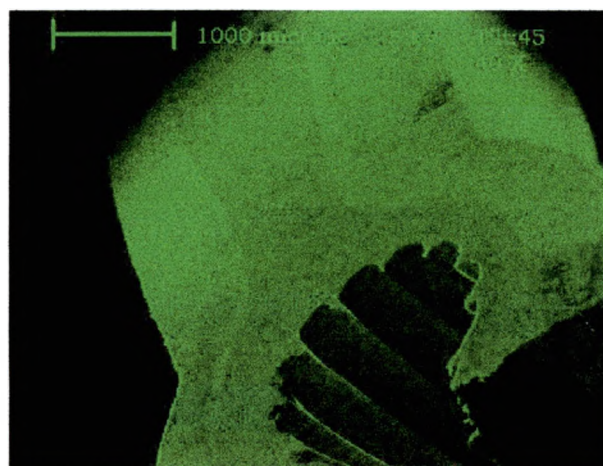
As the Lucent microelectronic chip was scanned at 20 kV, the x-ray spectrum in figure 3.3.10 a shows that the sample contains only C, O, Al, Si, small amount of Sb and trace of Zn. But since all the peaks were below 2 keV, another graph was created using 5 keV. This graph has smaller Al and Si peaks while the C and O peaks became large. This suggests that the Al and Si are probably below the surface. At the same time the N peak became distinct, as the Sb and Zn peaks got lost in the noise. With 20 kV, the Sb and Zn peaks were riding or overlapping the O peak. The x-ray maps in figure 3.3.11 shows that almost all of the x-rays are being detected from a circle in the middle of the chip. This was unexpected since the secondary and backscattered image shows a smooth and consistent image. The circle is due to low magnification and as mentioned in section 2.4.1, the acceptance



a) secondary electron image

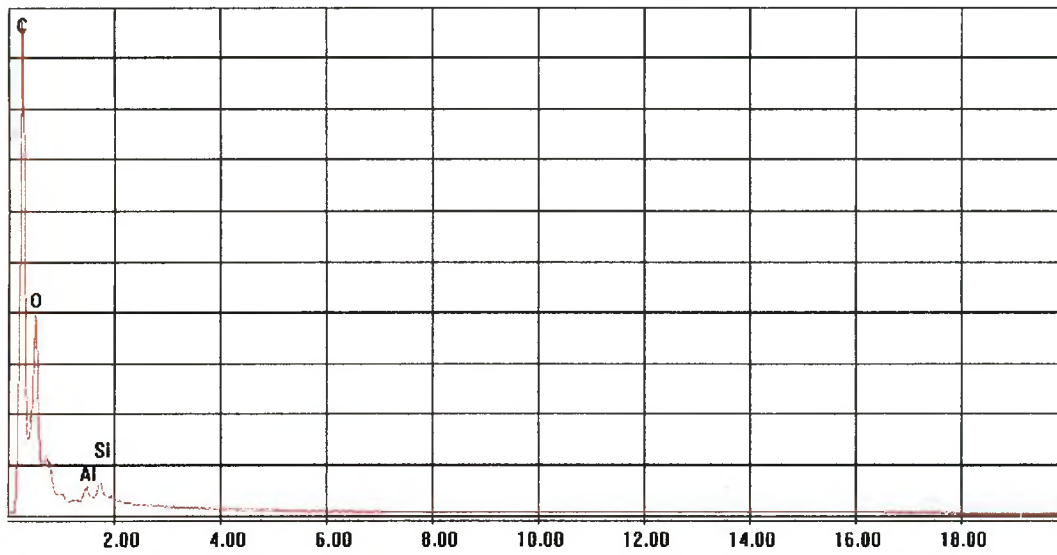


b) C x-ray image

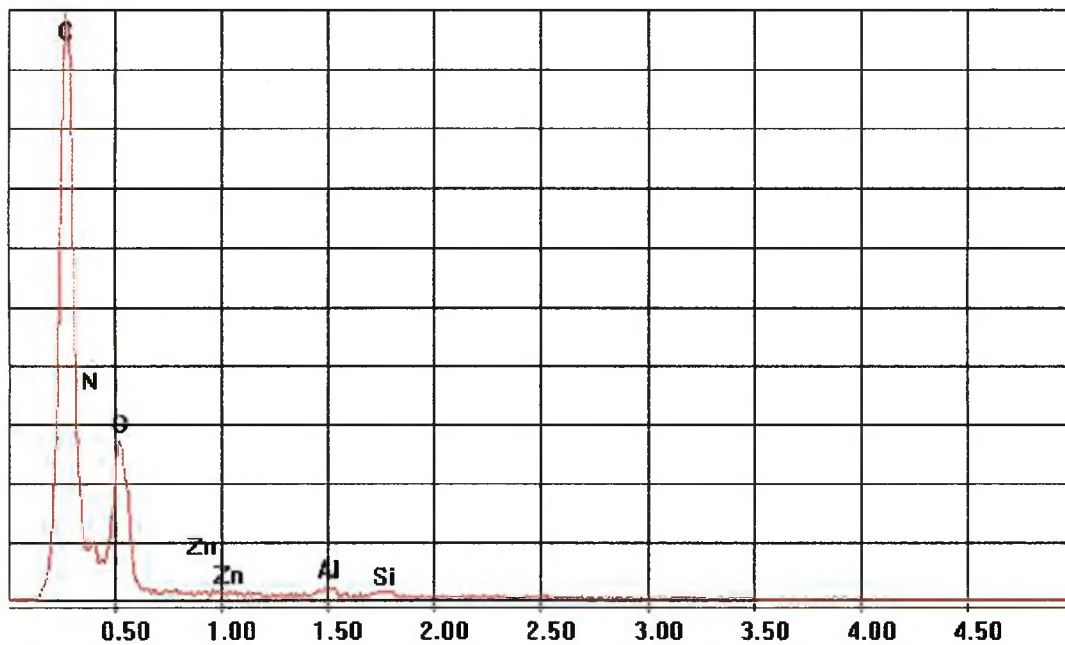


c) F x-ray image

Figure 3.3.9. The secondary image in a, and b the C, c and the F x-ray maps, using a magnification of 40X, 5kV, and a tilt of 45° of wire insulation.

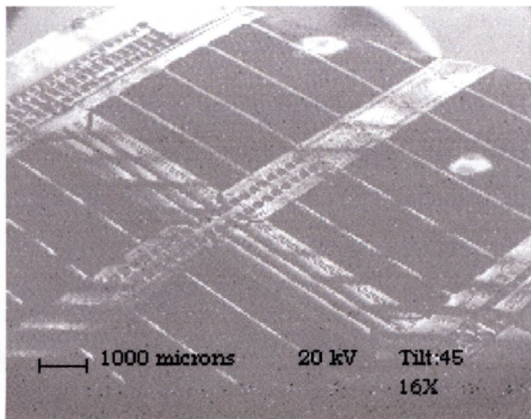


a) X-ray spectral graph created using an accelerating voltage of 20kV.

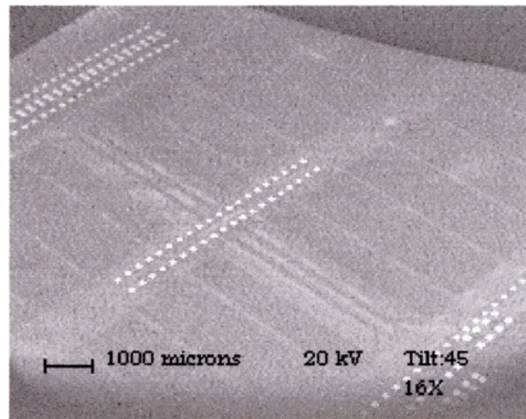


b) X-ray spectral graph created using an accelerating voltage of 5kV.

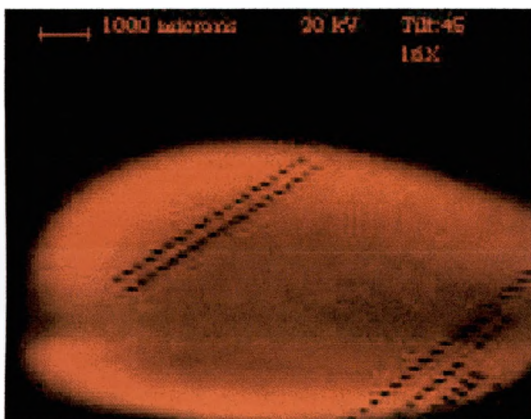
Figure 3.3.10. X-ray spectral graphs, where the y-axis is x-ray counts and the x-axis is the x-ray energy, using different accelerating voltages showing the elemental composition of a patterned electrical device.



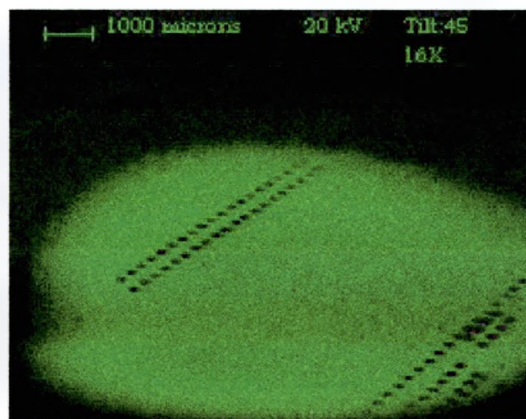
a) secondary electron image



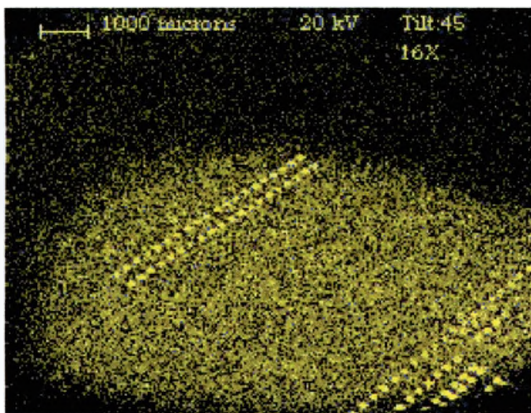
b) backscattered electron image



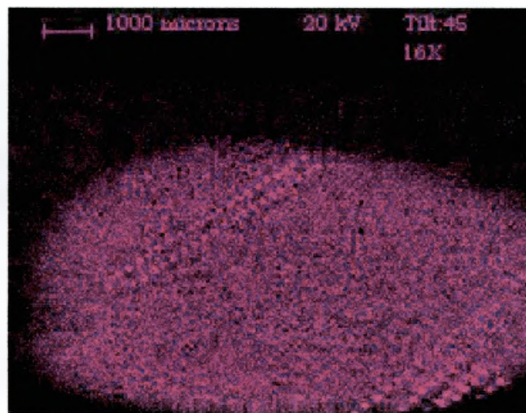
c) C x-ray image



d) O x-ray image

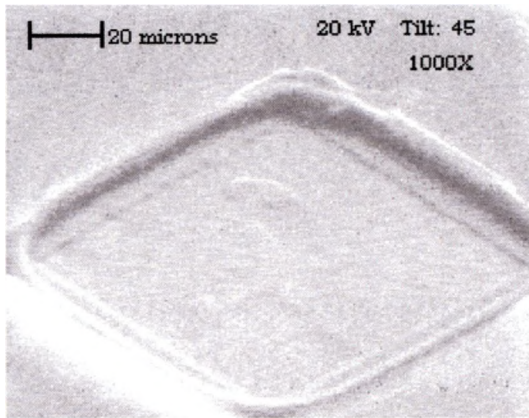


e) Al x-ray image

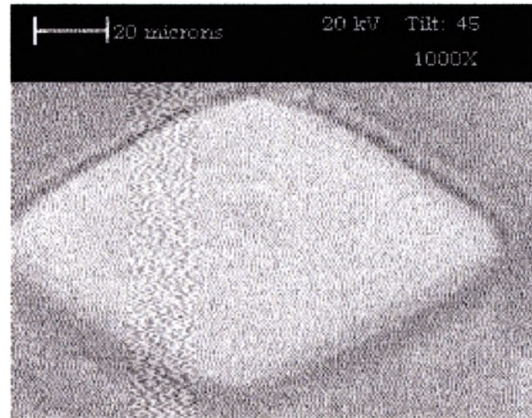


f) Si x-ray image

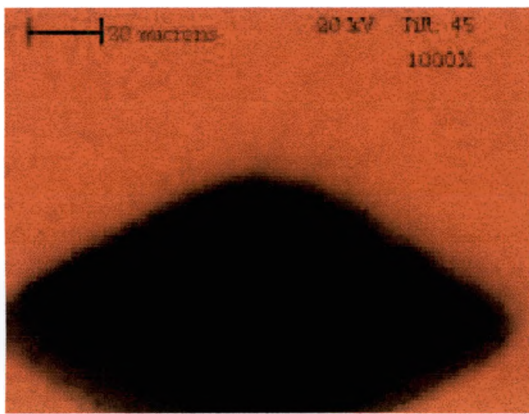
Figure 3.3.11. Images taken using 20 kV, a tilt of 45° at 16X, of a patterned electronic sample containing C, O, Al and Si showing the effect that the acceptance angle of the detector has at low magnifications.



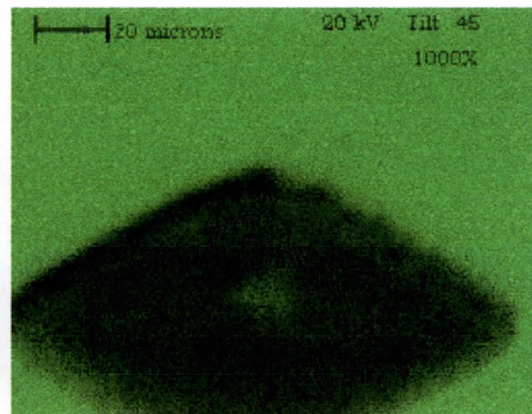
a) secondary electron image



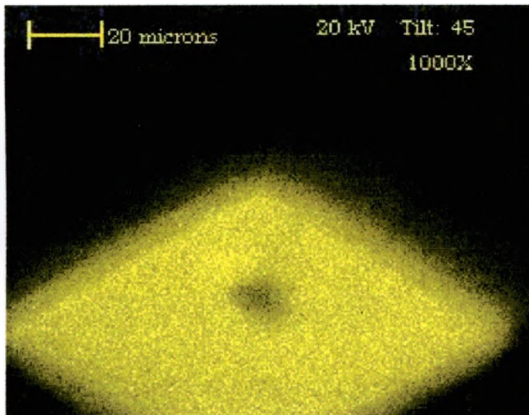
b) backscattered electron image



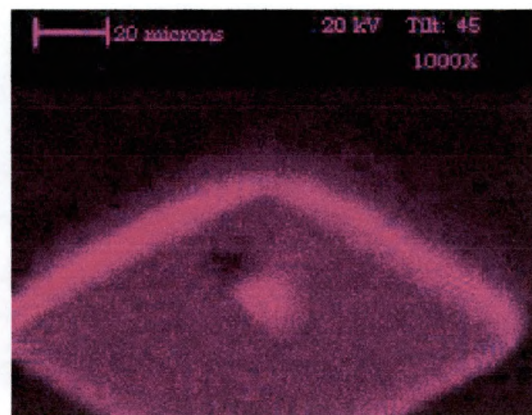
c) C x-ray image



d) O x-ray image



e) Al x-ray image



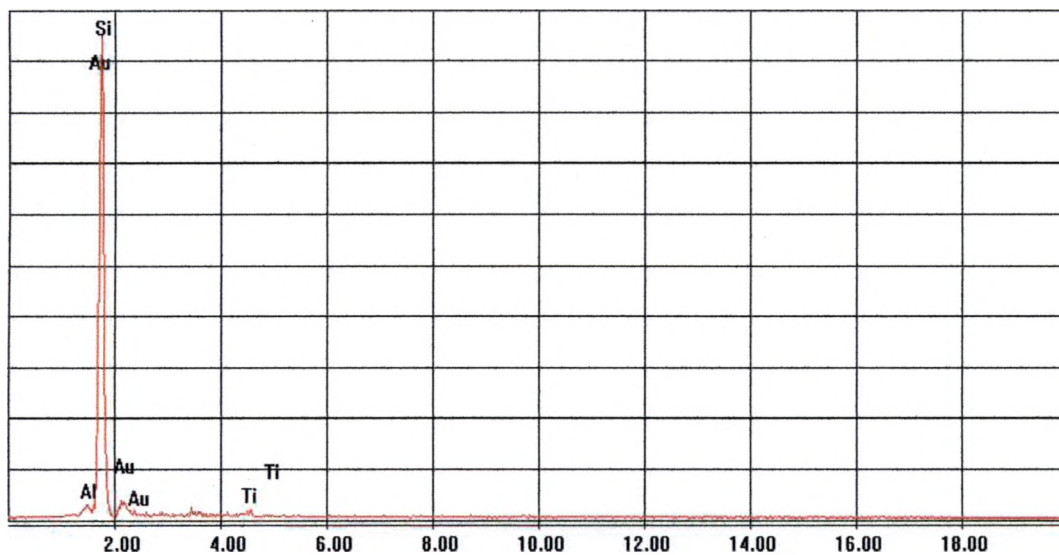
f) Si x-ray image

Figure 3.3.12. High magnification images at 1000X using 20 kV and a tilt of 45° , of small Al contact pad of figure 3.3.11.

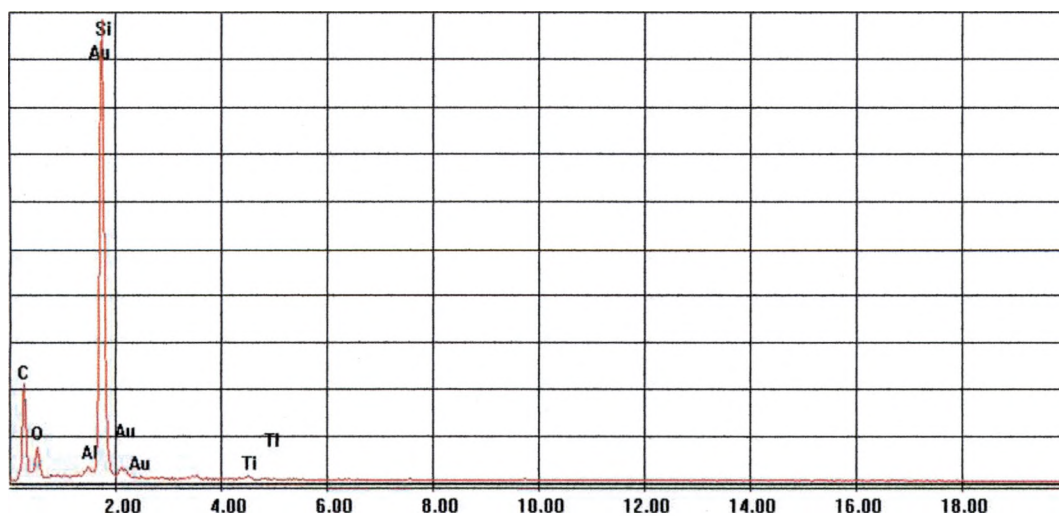
angle of the x-ray detector with a collimator in front of it. The backscattered image shows bright dots. A blow-up of one of the dots is shown in figure 3.3.12. From the secondary and backscattered image, it is seen that the feature is a depression in the sample. This supports the theory that there is some sort of covering over the sample that is exposed at these features.

The spectral graphs in figure 3.3.13, of all three AFM tips that were discussed in section 3.2, were made with an accelerating voltage of 20 keV with window closed and opened. They both show peaks of Si, Au, and Ti of the same height. As can be seen the only difference in the graphs is that with the window open C and O are detected. Once the heavier elements were found, a quick scan at 5 keV was run to find any hidden light element peaks. Figure 3.3.14 shows that the tips x-ray spectrum has a small N peak is between the C and O. If it were not there, the area around 0.4 keV would be lower. Notice how noisy or rough this image is. This is caused by a lack of good statistical counts. The noise would decrease as the length of the scan is increased. Figure 3.3.15 shows the scan that was repeated with 20 keV, having the N peak is identified.

Figure 3.3.16 shows the maps of the tips at 20 kV and 5 kV. The carbon that was detected can be seen to come from the double-sided tape used to mount the sample, not the tips, therefore the C x-ray image was not shown at 20 kV. Notice that



a) X-ray spectral graph of several coated AFM tips.



b) X-ray spectral graph, with the Be window open of several coated AFM tips.

Figure 3.3.13. Comparison of x-ray spectral graphs, where the y-axis is x-ray counts and the x-axis is the x-ray energy, created using an accelerating 20kV with the Be a) open and b) closed.

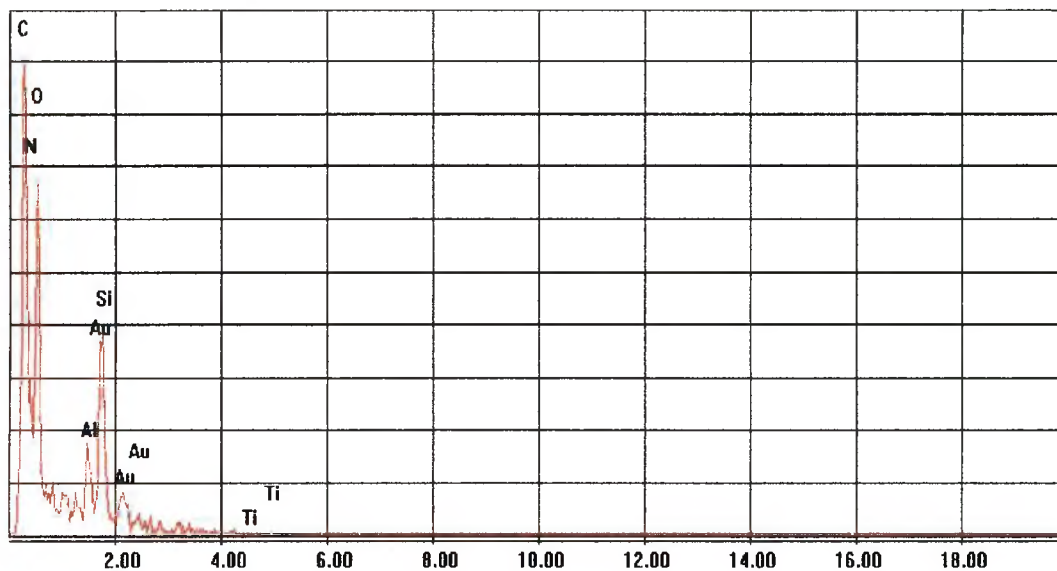


Figure 3.3.14. X-ray spectral graph, where the y-axis is x-ray counts and the x-axis is the x-ray energy, of several-coated AFM tips using an accelerating voltage of 5kV.

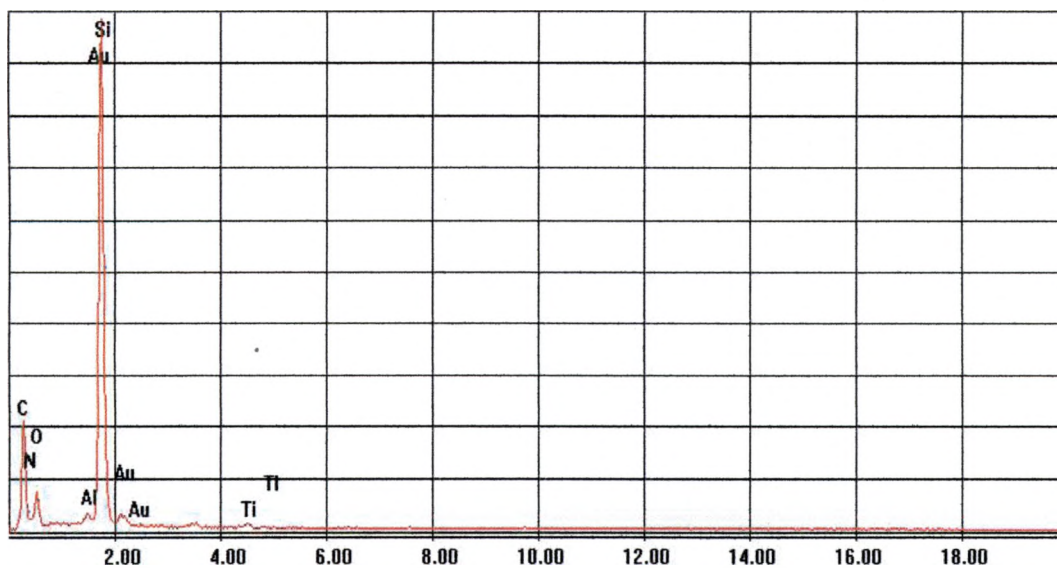
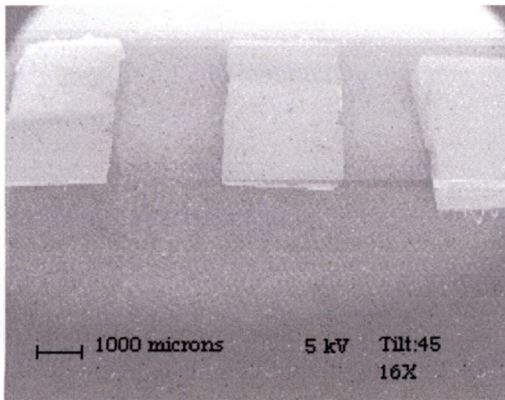
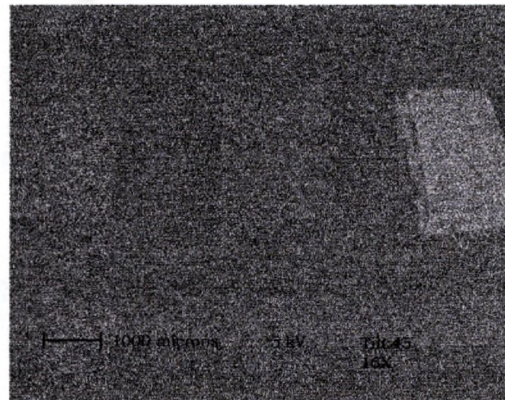


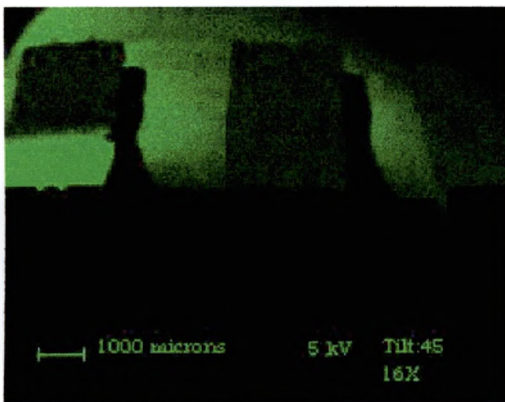
Figure 3.3.15. X-ray spectral graph, where the y-axis is x-ray counts and the x-axis is the x-ray energy, of several-coated AFM tips using an accelerating voltage of 20kV.



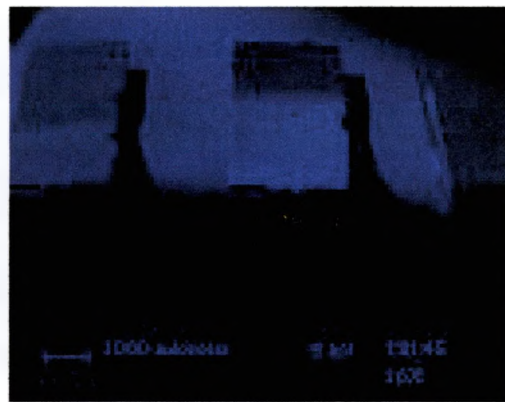
a) secondary electron image



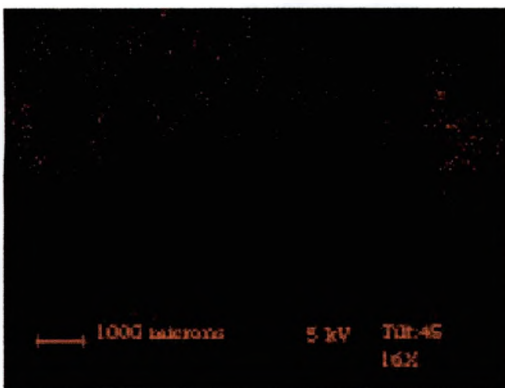
b) backscattered electron image



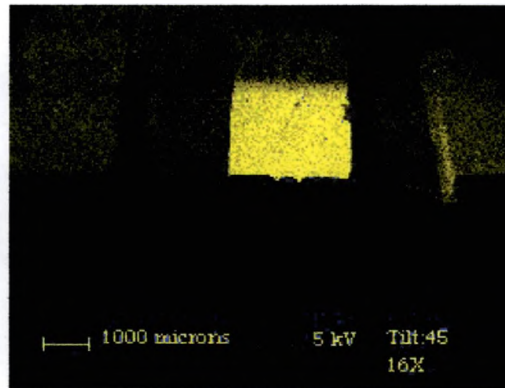
c) N x-ray image



d) O x-ray image

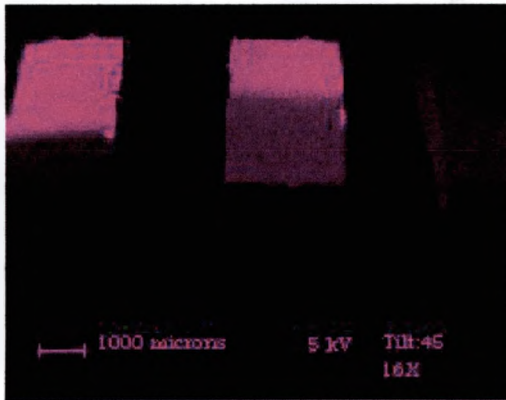


e) Ti x-ray image

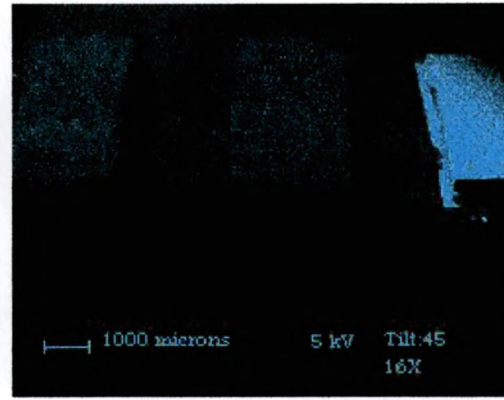


f) Al x-ray image

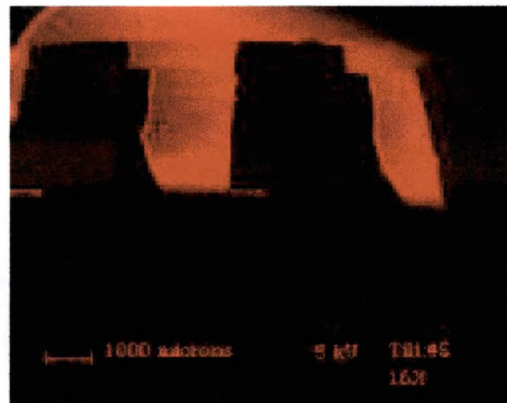
Figure 3.3.16. Images taken using 5 kV, with a tilt of 45° , at 16X of several coated AFM tips showing the effects of accelerating voltage. Figure is continued on next page.



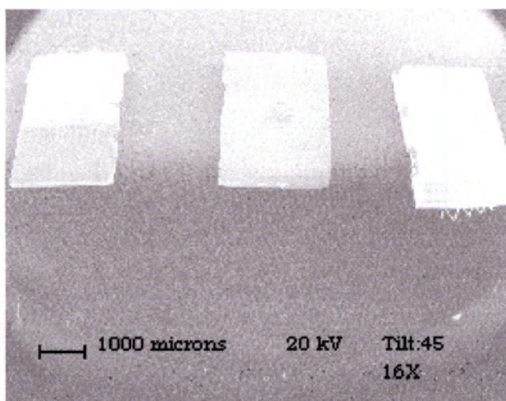
g) Si x-ray image



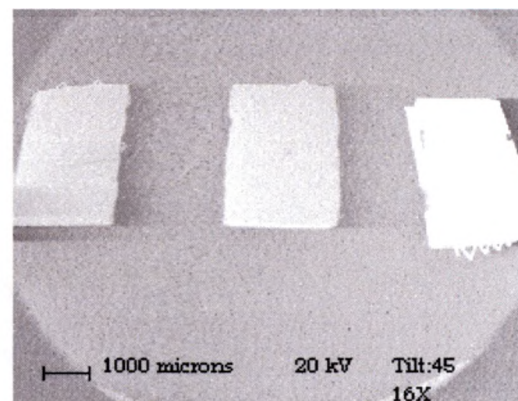
h) Au x-ray image



i) C x-ray image

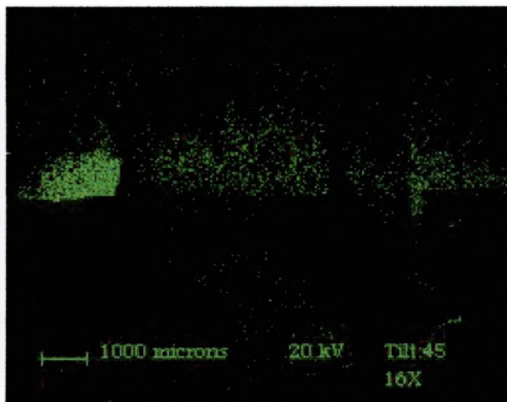


j) secondary electron image

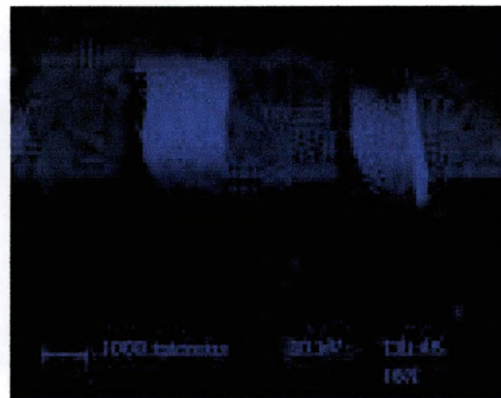


k) backscattered electron image

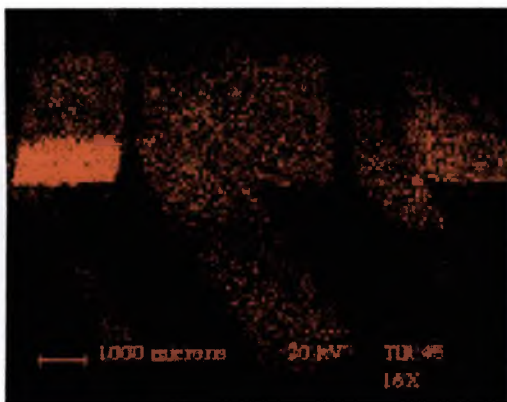
Figure 3.3.16. (Continued) Images taken using 5 kV, with a tilt of 45° , at 16X of several coated AFM tips showing the effects of accelerating voltage. Page 2 of 3.



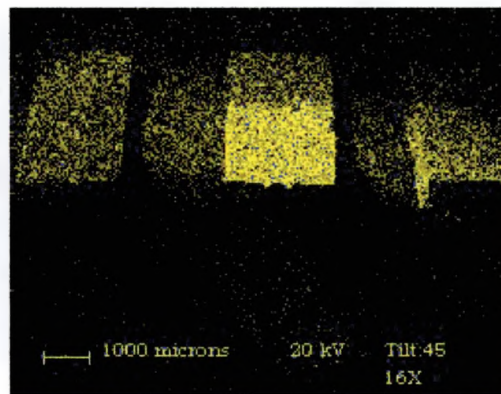
l) N x-ray image



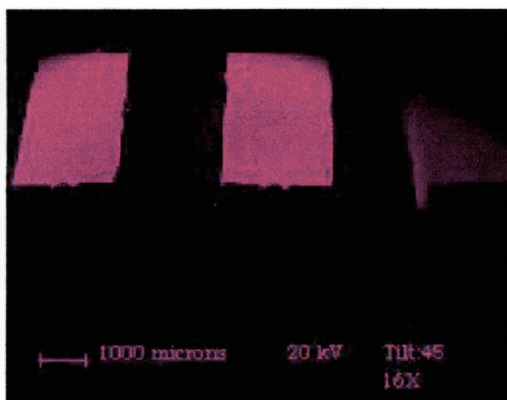
m) O x-ray image



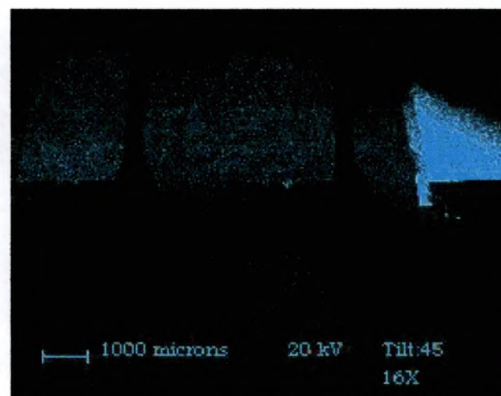
n) Ti x-ray image



o) Al x-ray image



p) Si x-ray image



q) Au x-ray image

Figure 3.3.16. (Continued) Images taken using 5 kV, with a tilt of 45° , at 16X of several coated AFM tips showing the effects of accelerating voltage. Figure is continuance from previous pages.

when 20 kV is used more Si is detected and more gold detected on the tips in the middle and to the left (as mentioned in section 3.2, the other tip is mounted upside down). This is because the higher voltage caused the beam to penetrate deeper in the sample, causing more x-rays to be emitted from deeper in the sample. But when 5kV is used the x-rays are emitted closer to the surface. This causes more N, O, and Al to be created. At a voltage this low, Ti x-rays are not created. These low magnification images show less detection of Si where the tips are coated with Al, O, Ti, and N because these surface layers keep fewer beam electrons from penetrating deep enough into the Si to create x-rays.

Figure 3.3.17 shows the spectral graph as the magnification zoomed in on the tip on the left. It shows that this tip contains Ti, N, Si and Au. The images of the middle tip are shown in figure 3.3.18, when using 5 and 20 keV. Again, notice how the higher voltage creates a deeper penetration allowing more Si, Al, O, and Au to be seen. More resolution of the actual tip can be seen. The lower voltage shows more shadowing of the tip as well.

As the AFM tips tilt was increased in figure 3.3.19, it can be seen that x-ray detection is tilt sensitive. As the angle is increased, the detection of every element drops significantly, except Si and Au. The O on the middle tip is no longer detected while the Al at the same positioning is lost in the signal from the Al sample stub.

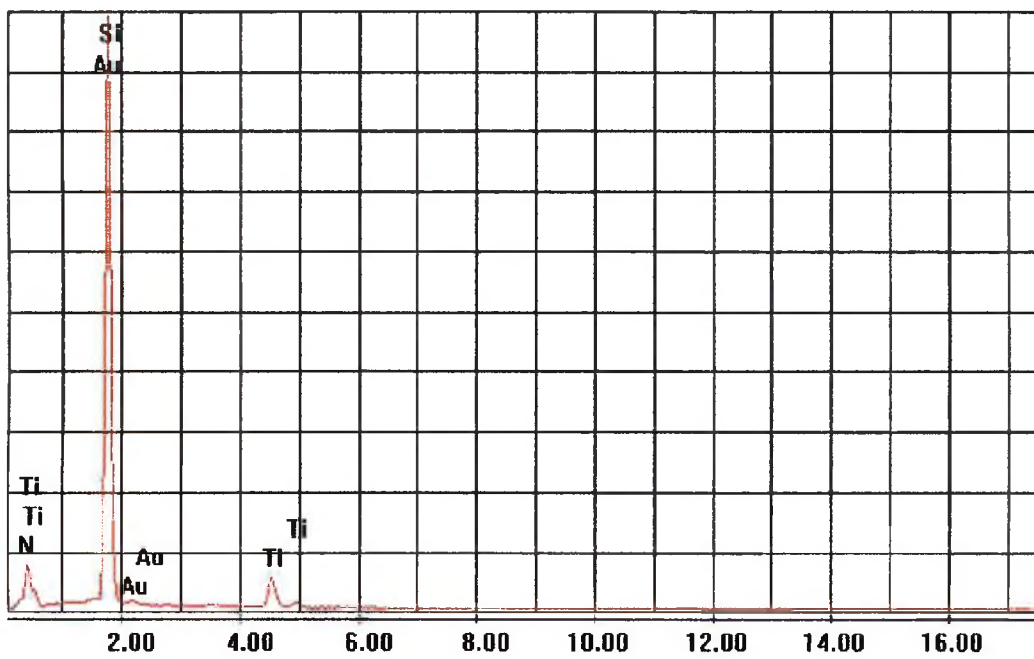
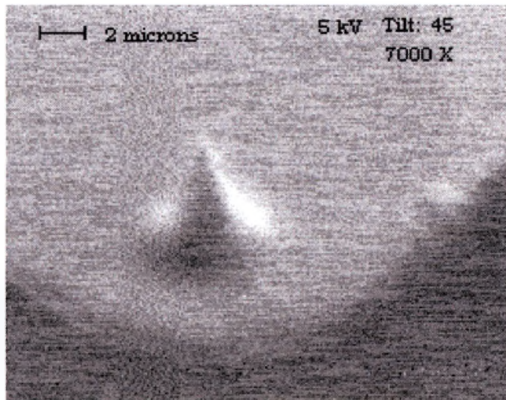
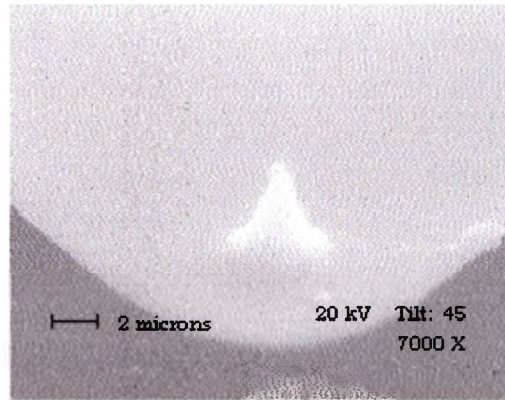


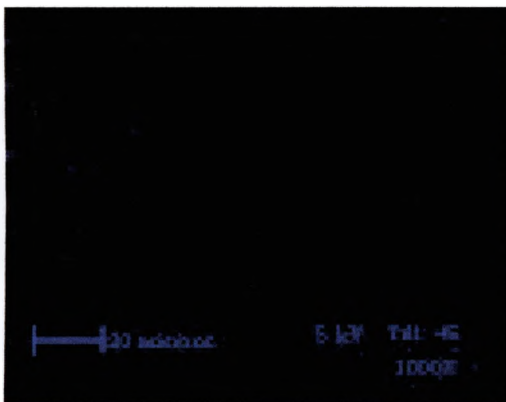
Figure 3.3.17. Spectral graph, where the y-axis is x-ray counts and the x-axis is the x-ray energy, while at high magnification of the left tip in figure 3.3.16.



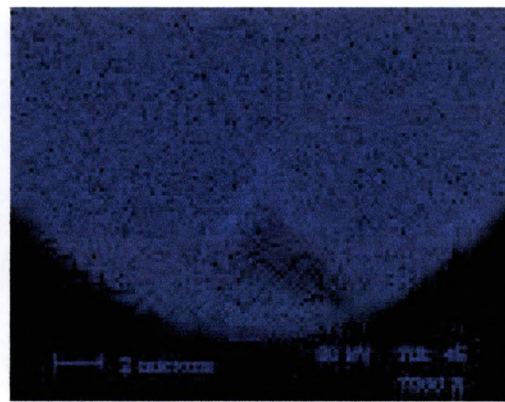
a) secondary electron image



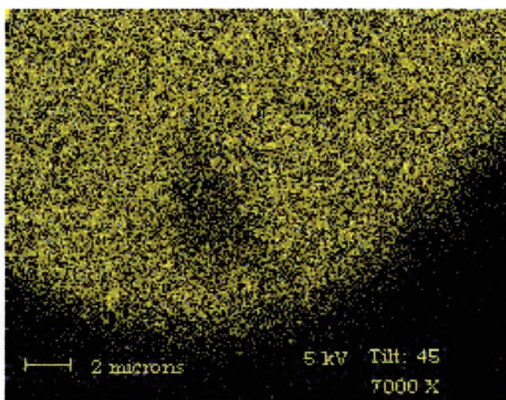
b) secondary electron image



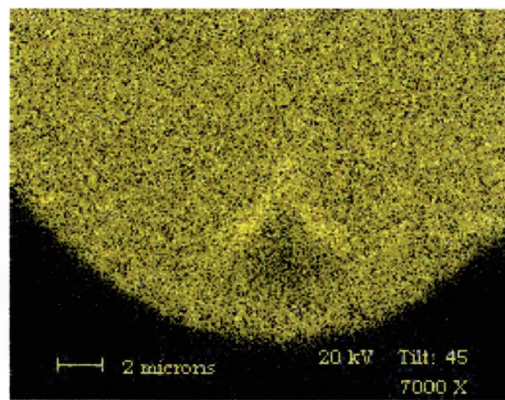
c) O x-ray image



d) O x-ray image

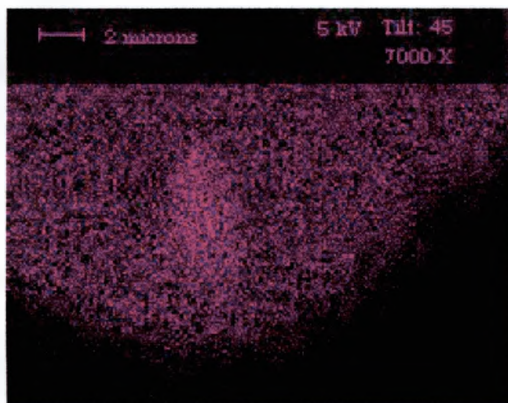


e) Al x-ray image

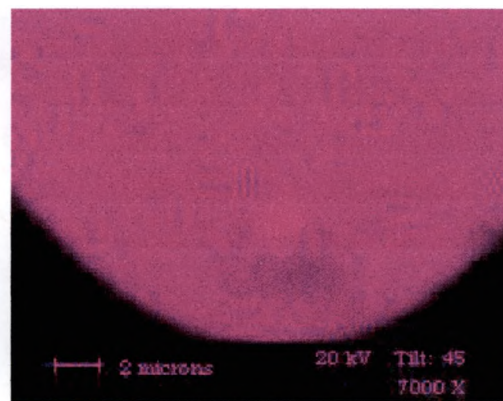


f) Al x-ray image

Figure 3.3.18. High magnification images at 7000X showing the effect accelerating voltage at 5 and 20 kV with a tilt of 45° has on the image of the middle tip in figure 3.3.16. Figure is a continued on the next page.



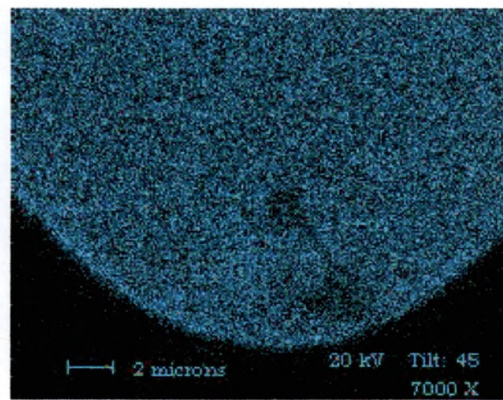
g) Si x-ray image



h) Si x-ray image

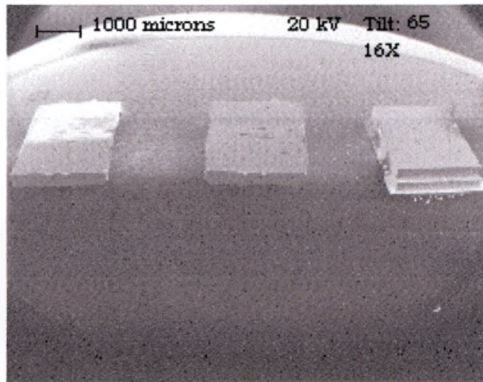


i) Au x-ray image

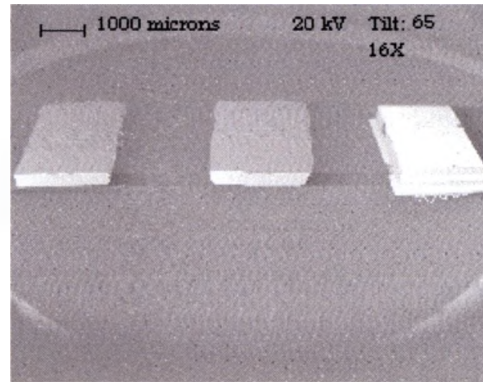


j) Au x-ray image

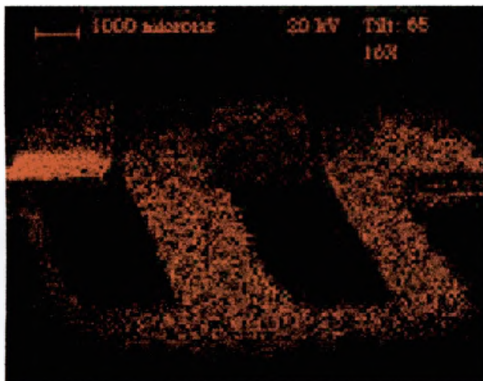
Figure 3.3.18. (Continued) High magnification images showing at 7000X the effect accelerating voltage at 5 and 20 kV with a tilt of 45° has on the image of the middle tip in figure 3.3.16. Figure is a continuance of the previous page.



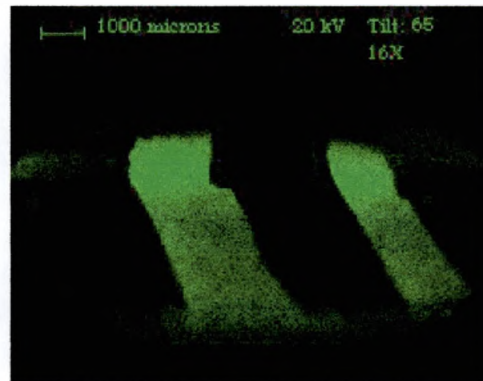
a) secondary electron image



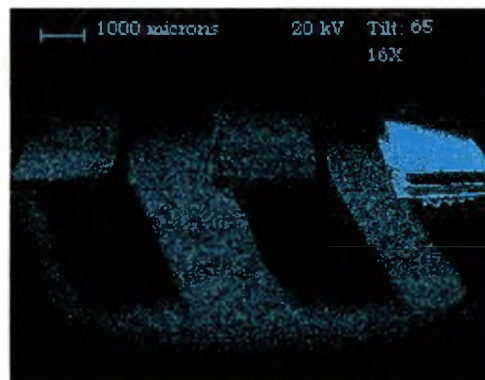
b) backscattered electron image



c) Ti x-ray image

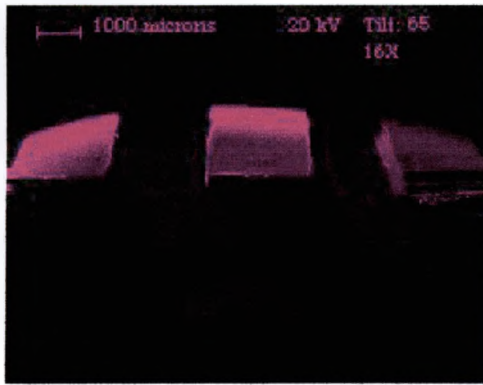


d) O x-ray image

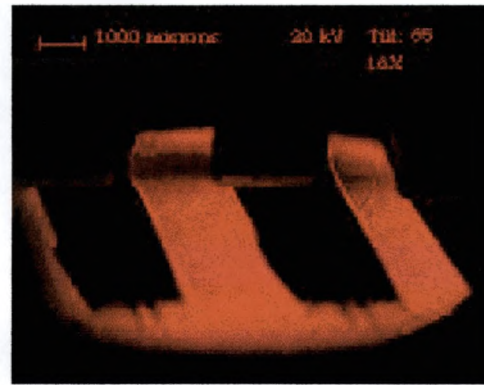


e) Au x-ray image

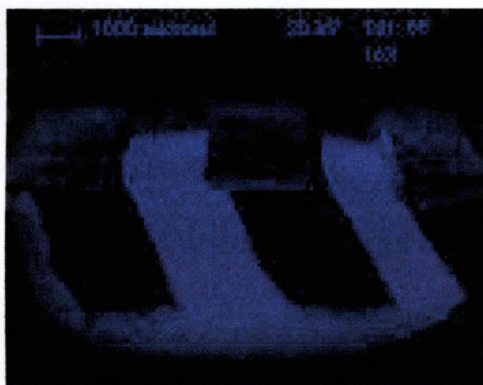
Figure 3.3.19. Images taken at 20 kV with a tilt of 6° at 16X of several coated AFM tips using more tilt than figure 3.3.16. Figure is continued on the next page.



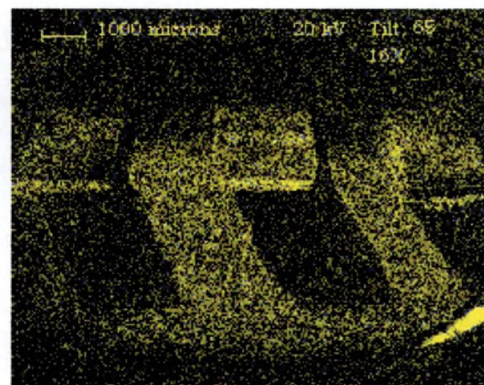
f) Si x-ray image



g) C x-ray image



h) O x-ray image



i) Al x-ray image

Figure 3.3.19. (Continued) Images taken at 20 kV with a tilt of 65° at 16X of several coated AFM tips using more tilt than figure 3.3.16. Figure is a continuation of the previous page.

At the same time, the amount of Ti and N detected on the left tip also drops. The stub that was used for mounting the tips was cut with a 45° angle with a flat top. As a result, as the sample tilt was increased, the counts from the sample drop but the counts from the part of the stub that was cut at 45° increases, showing area is emitting detected x-rays. This is why positioning to maximize x-ray counts is so important in x-ray analysis. For proper sample positioning, see appendix A.

A SEM can use this not only to detect what is in the sample, but also create an image where it is. This ability to perform chemical analysis is one of the SEM's most powerful abilities. It uses a simple relationship between the energy of characteristic x-rays that an element emits and its atomic number. This energy-dispersive spectroscopy (EDS) capability is one of the abilities that make the SEM so versatile and popular.

CHAPTER 4

CONCLUSION

In conclusion, this thesis discussed the principal, operation, systems, and techniques used to analyze samples using scanning electron microscopy. Patterned, unpatterned electronic and several various samples were examined to find their topographical and compositional characteristics. The Physics department's Amray model 1400 Scanning Electron Microscope (SEM) was used for all of the analysis. This SEM was equipped with several detectors. These include an Everhart-Thornley secondary electron detector, a GW Type 113 solid-state backscattered detector, and an EDAX ECON IV x-ray detector (refer to section 2.3 and 2.4).^{8,9}

The samples were examined under many different parameters. These include, accelerating voltage, beam current, beam diameter or spot size, scan rate, tilt and magnification.

It was found that using the highest possible accelerating voltage increases resolution. The maximum voltage is used is determined by several factors. If a sample is experiencing charging effects, the voltage should be lowered. It should also be lowered to

reduce the depth of penetration of the excitation volume if topographical elemental analysis is desired (refer to section 2.2.4). Beam diameter or spot size along with the voltage, controls the beam current. An increase in the current causes an increase in the brightness of the image. This gives a sharper image. But the smaller spot size gives higher resolution. The spots size is also used to control the dead time (refer to section 2.4.2 and appendix A) during x-ray analysis. This requires that the spot size be set for the given conditions.¹²

Tilting the sample allows for the use of the SEM's large depth of field to create help create images which appear to have 3-dimensionality. This allows for better secondary electron imaging for topographical analysis. It was also found that tilting the sample increases the number of backscattered electrons produced. But most of all, the proper tilting of the sample allows for higher quality x-ray analysis. This is because the x-rays have higher energies, which causes them to maintain straight paths after creation, and a higher percentage of them are emitted at certain angles with respect to the beam. In my analysis, I was able to show:

1. That the extrusion process creates a conductive carbon enriched channel in the Thermon polymer, which is useful for resistive heating effects.

2. Identify the elemental nature of unexpected residue left on silicon surfaces by supposedly clean Isopropyl solvent.
3. Verified the elemental composition of W wires used for thermionic emission in ion beam sources.
4. Verified the presence of Al_2O_3 , and TiN on sputter coated AFM tips.

The Scanning Electron Microscope is a powerful instrument that permits the observation and characterization of materials at a local surface. Irradiating a finely focused beam of electrons that are rastered across the sample surface performs this analysis. As the beam is scanned over the sample, the beam electrons interact with the sample atoms. This produces different types of signals; which include secondary electrons, backscattered electrons, and x-rays. By examining these signals, many characteristics of the sample can be determined. These include, surface topography, and composition. Therefore this instrument has clear usefulness in microelectronic failure analysis applications.⁴

Since the images produced by a SEM have such a high depth of field, and shadowing, they are highly three-dimensional. This allows for easy interpretation of its data by the human eye and brain. Along with its high resolution, which is much higher than an optical microscope and its compositional abilities, makes the SEM a popular instrument.^{3,4}

A SEM's versatility for the examination and analysis of a solid material's microstructure characteristics makes it a very useful tool in the microelectronic industry.

APPENDICES

APPENDIX A

SEM Operation Procedures

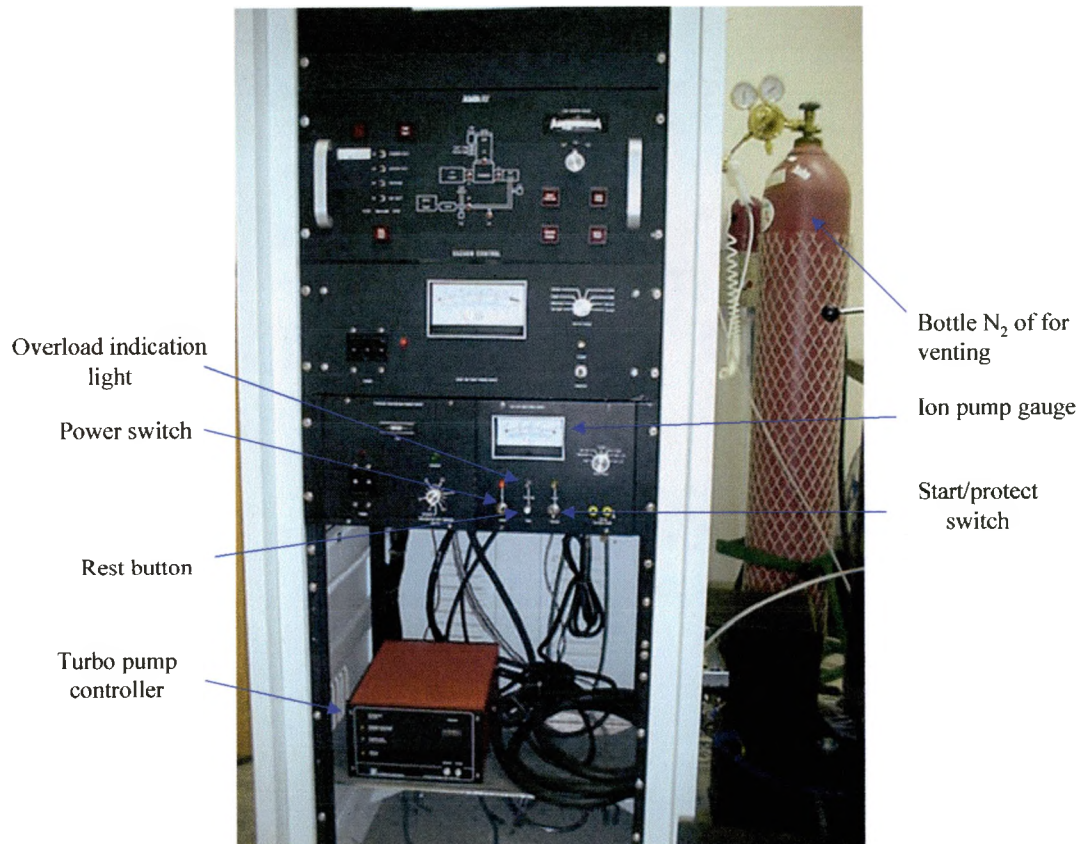
VACUUM CONTROL CONSOLE
SHOWING N₂ CHAMBER VENTING BOTTLE

Figure A.1. Vacuum control console

CHAMBER VACUUM CONTROL

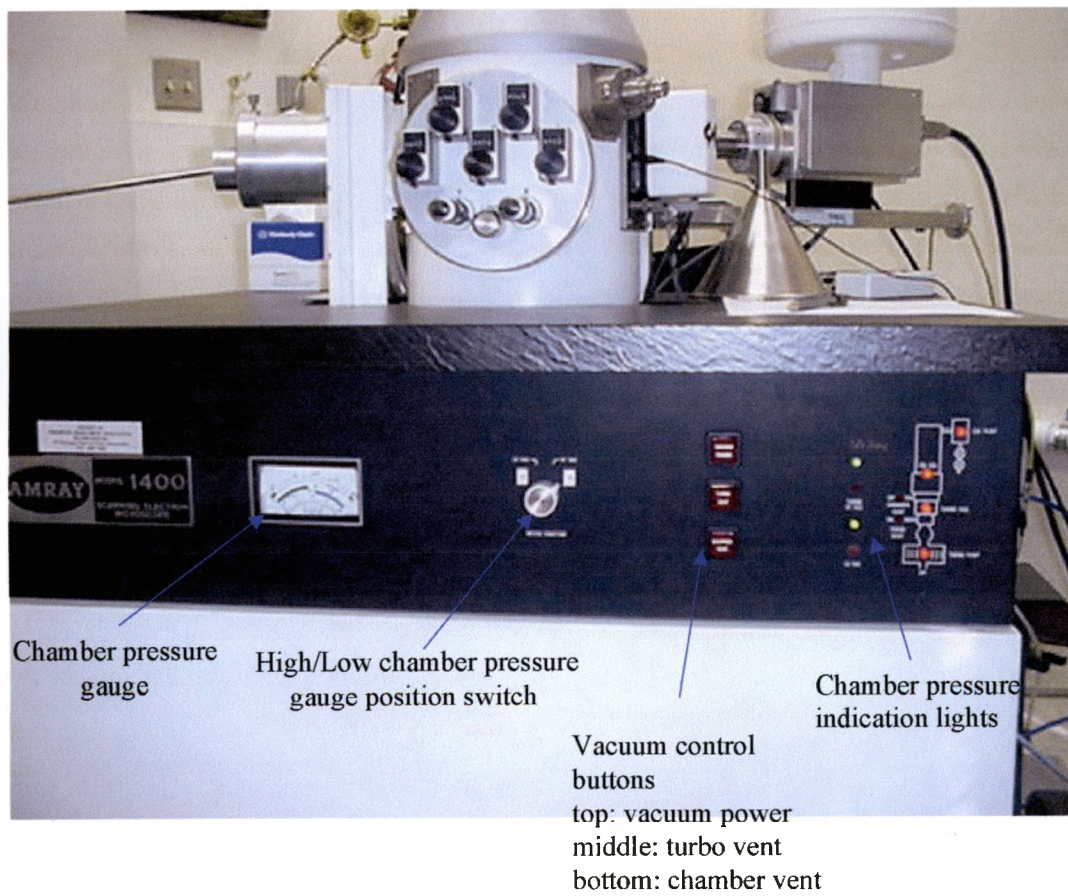


Figure A.2. Chamber control vacuum

SEM COLUMN SHOWING LN₂ DEWAR

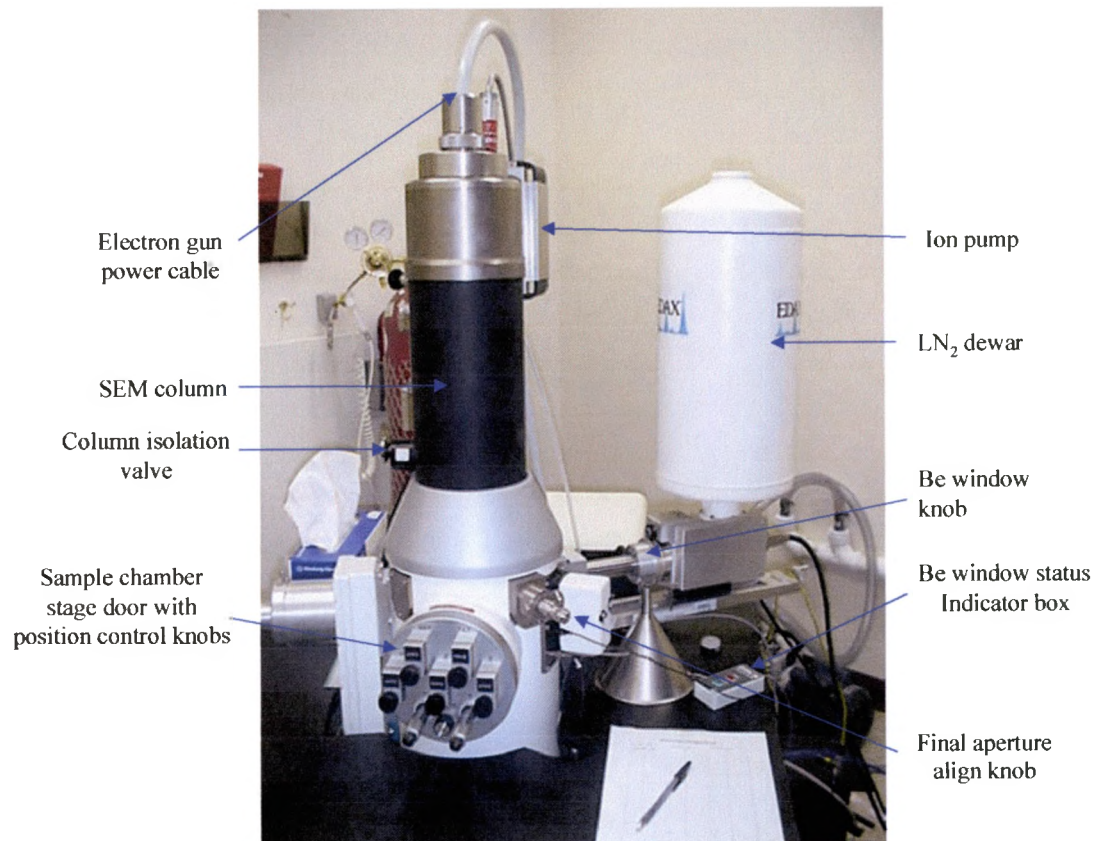


Figure A.3. SEM column with attached LN₂ dewar.

OPEN SEM CHAMBER WITH SAMPLE STAGE EXTENDED

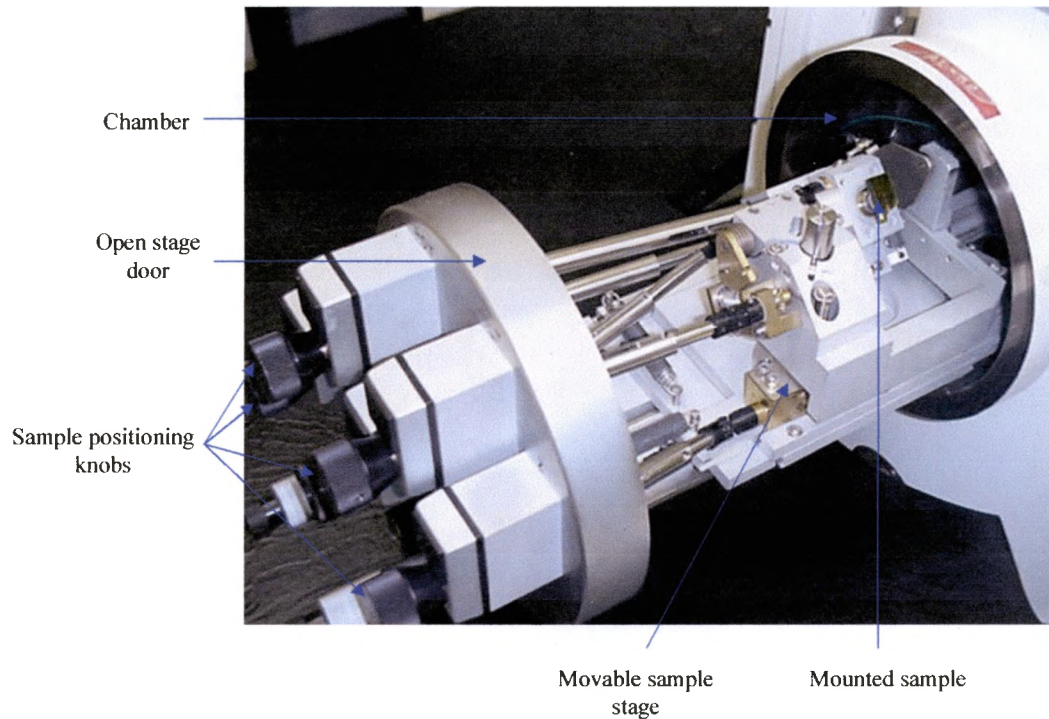


Figure A.4. Sample stage extended. Note the mounted sample.

VIEW OF CHAMBER INTERIOR SHOWING PARTS OF THE X-RAY AND E-T DETECTORS

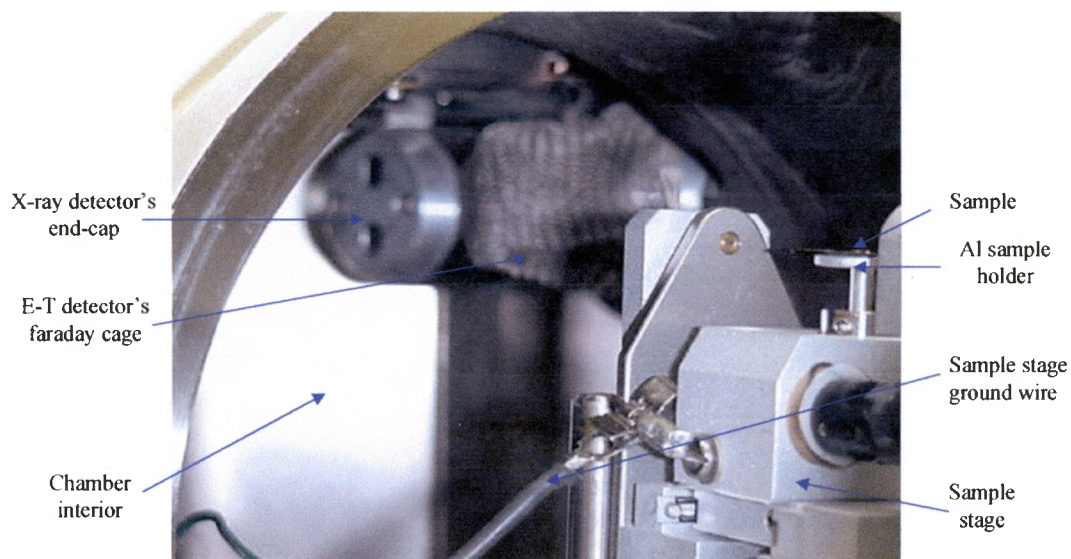


Figure A.5. Interior of chamber, showing parts of the E-T and x-ray detectors.

SEM IMAGE CONTROL AND DISPLAY CONSOLE

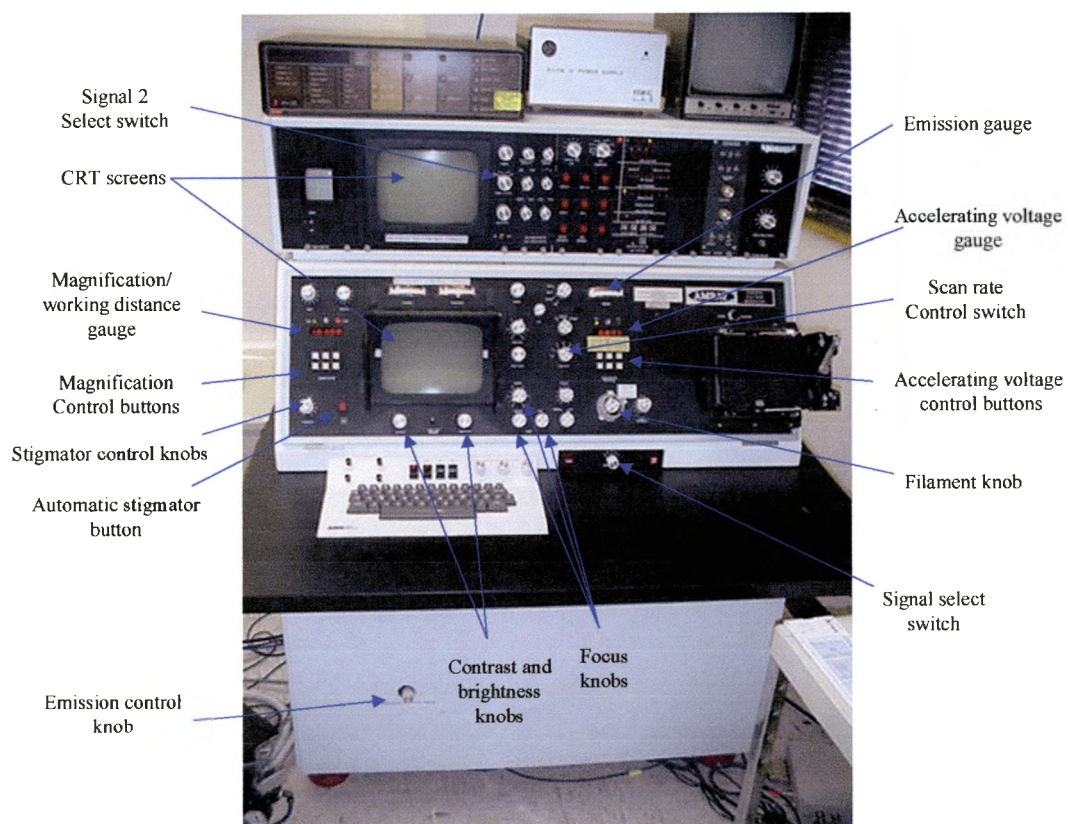


Figure A.6. SEM image control and display console.

SEM Operation Procedures

I. Turn on SEM

1. Check the systems vacuum.
 - i. Ion pump gauge on the bottom of the vacuum control console should be around 0.5mA.

If the gauge is reading zero, the ion pump power supply's power is off or the overload light should be on. In either case, the pump will have to be restarted. See appendix B for the ion pump restart procedures.
 - ii. The chamber pressure gauge on the SEM unit should be in the green or pegged when the gauge knob is turned to the high vac setting. (The gauge should only be turned on to check the pressure and immediately turned off or it can be damage.)
 - iii. The green lights next to the chamber pressure gauge should be on.
2. Check EDAX LN₂ dewar for LN₂. (If less than 4 inches from bottom, fill doer with LN₂, and fill out the EDAX LN₂ Fill log.)
3. Turning on the computer

- i. Turn on the computer by turning the key.
 - ii. Log onto the computer, using student as the username and physics as the password.
 - iii. Open and minimize the program iDX
 - iv. Open the program eDX ZAF.
4. Make sure the column isolation valve is close. The valve knob is located on the left side of the column. The valve is closed when the knob is pushed in all the way.
 5. If the accelerating voltage gauge, which is located in the middle of the control console, has no reading, make sure that the filament is set to zero. The filament control knob is just above the desk top of the secondary control console and to the left of the camera. Set the accelerating voltage to 5keV.
 6. Check the emission gauge, and NEVER let it rise above 100. This gauge is located above the accelerating voltage gauge. The emission control knob is located on the front panel below the desktop. If you are sitting, the knob is just above your left ankle. Turning the knob counter-clock wise, lowers the emission, and clock-wise raises the emission.

7. Turning on the Filament. (If the filament is set at 50 units, skip steps i through v)
 - i. Turn the filament knob from 0 to 10 units
 - ii. Turn the filament knob from 10 to 20 units
 - iii. Turn the filament knob from 20 to 30 units
 - iv. Turn the filament knob from 30 to 40 units
 - v. Turn the filament knob from 40 to 50 units
 - vi. Turn the filament knob from 50 to 60 units
 - vii. Turn the filament knob from 60 to 70 units
 - viii. Turn the filament knob from 70 to 80 units
 - ix. Turn the filament knob from 80 to 81 units

The emission should NEVER be turned up no more than 10 units/minute! A larger or faster increase can destroy the LaB₆ filament.

8. Set the emission at 100.

II. Vent Chamber to load or change the sample. (If the sample to be examined is already in the chamber, step II should be omitted.

1. Make sure the column isolation valve is closed. The valve knob is located on the left side of the column. The valve is closed when the knob is pushed in all the way, and the red col isol light of the SEM schematic on the SEM unit should flash. (This light has also been

known to flash when the valve is not fully closed.

Therefore it should not be trusted. So make sure that the valve is fully depressed.

2. Hit the red chamber vent button next to the chamber pressure gauge on the SEM unit. (When the button has been activated, it should light up, and you can hear the vent valve open.)
3. The main valve on the N₂ bottle behind the SEM unit needs to be opened. (The chamber should open on its own in no more than two minutes. If it opens faster, the black valve on the N₂ bottle needs to be closed a small amount.)
4. The main valve on the N₂ bottle needs to be closed to prevent the gas from leaking out.
5. The chamber stage can now be easily pulled out. If an alarm sounds or if it only pulls out about an inch and no more, the Z or the Z' knob on the front of the chamber stage needs to be turned counter-clock wise several turns because the stage is hitting one of the detectors, and needs to be lowered.
6. The stage only needs to be pulled far enough to remove the Al sample stub, or the stage will be pulled off of its tracks, and will have to be in them.

7. The sample and stub can be removed by lifting it out with a pair of tweezers. If the stub will not lift out, the hex head set screw on the left side of the stub holder needs to be loosened.
8. The desired sample on a stub can now be placed in the stage. (The sample position and or orientation should be recorded.)
9. While the stage is out, check that all positioning knobs work properly.
10. The stage should now be pushed back in the closed position. While applying a little pressure on chamber to keep it closed, push the red chamber vent button (which should be lit up). The light should go off and the mechanical pump should turn on. The green light on the turbo pump control box should come on. (The turbo pump control box is on the bottom of the control tower.) This light indicates that the turbo pump is turning and accelerating.
11. The green light on the turbo control box should turn off and the yellow light should come on after a few minutes. This light indicates that the pump is at normal operating speed. (75,000 RPMs)

III. Sample positioning

1. Check the chamber pressure gauge on the SEM unit should be in the green or pegged when the gauge knob is turned to the high vac setting, (The gauge should only be turned on to check the pressure and immediately turned off or it can be damage.) that the green lights next to the chamber pressure gauge come on. Then it is safe to open the column isolation valve when the green lights are on. Now the valve knob on the left side of the column needs to be pulled out to open. (When the valve is opened, an image should appear on the CRTs because the SEM is imaging.)
2. Decrease the magnification all the way, by hitting the down arrows next to the magnification gauge to the left of the CRT on the secondary election image control console.
3. Set the spot size to zero, by turning the spot size knob on the secondary election image control console.
4. A good CRT image should be obtained and kept as soon as possible. The following is a list of the most common steps that should followed to get a good image.

- i. Adjust the brightness and contrast: The brightness and contrast knobs on the secondary control console so that their gauges read zero. This step should be repeated anytime that is needed.
- ii. Adjusting the focus: The image needs to be focused by turning the focus knobs on the secondary control console, in the direction makes the image clear. When the magnification is to be increased, it should be done in steps, so that the image is not lost. Once the proper focus has been achieved, changing the magnification will not affect the focus; therefore to achieve the highest level of focus, the magnification should be set higher to focus and then zoom back down to the desired imaging magnification. (If the image moves in the X and or Y direction while the focus knob is being turned, the final aperture needs to be aligned. It is aligned by setting the magnification to 1 kX and while wiggling the medium focus, turn the X aperture align knob on the SEM column in the direction which causes a decrease in the image

movement, until there is no more movement.

Repeat this procedure with the Y aperture align knob. Increase the magnification to 3 kX and repeat the procedure for X, and Y. This can be repeated at higher magnifications for which is necessary. If only part of the image can be focused, the stigmator (stig) needs to be adjusted. The stig is adjusted by pushing the red stigmator button, which puts two lines (one horizontal and one vertical) and turn the X and Y stigmator knobs to move the lines so that they cross on a region of the image that is in focus.

5. Select the desired accelerating voltage for imaging. BUT do not let the emission rise above 100. Every time the voltage is changed, the coarse focus should be rastered from 1 to 10 and back to dissipate the hysteresis which builds up on the scan coils, and the beam needs to be aligned, by moving the x beam align knob until the image is at a maximum brightness, and then repeated for the y beam align knob. But do not forget to adjust the brightness and contrast during this procedure.

6. Need to adjust the position of the sample to a location where imaging is desired. The position control knobs control the position of the sample. These knobs are located on the front of the sample stage. To move the sample, these knobs are turned clock-wise or counter clock-wise while watching the image on the CRTs. These knobs include X, Y, Z, Tilt, Y', Z', and Rotation.

Below is a description of the control of each knob:

- i. X moves the sample to the left or right along the x-axis (X ranges from 0 to 25 mm)
- i. Y moves the sample up or down along the y-axis (Y ranges from 0 to 30 mm)
- iii. Z raises or lowers the sample along the z-axis (Z ranges from 0.0 to 267.3, but the gauge is off by 405.7)
- iv. Tilt tilts the sample around the x-axis (Tilt ranges from 0 to 70° , but the gauge is off by -10°)
- v. Y' moves the sample up or down, but in a reference frame of the tilted axis (Y' ranges from 0.0 to 126.5, but the gauge is off by 3.0)

- vi. Z' raises or lowers the sample, but in a reference frame of the tilted axis (Z' ranges from 0.0 to 73.5, but the gauge is off by -1)
 - vii. Rotation rotates the sample 360° along the Z' -axis
7. The toggle switch by the magnification gauge should be toggled to the W.D. position. Now the magnification gauge reads the W.D. (working distance) this is the distance (in mm) from the sample to the SEM's final aperture. The W.D. should be around 16 if elemental compositional data is desired and should continue with the procedure for maximizing x-ray counts below, if not then the working distance can be adjusted to control the depth of field of the image, and the spot size can also be adjusted when no elemental analysis is to be conducted to increase image resolution.

Procedure for Maximizing X-ray Counts

To maximize the x-ray counts make sure that eDX ZAF program is maximized on the monitor since the x-ray counts per second (CPS) are read off of the on the bottom left corner of the computer monitor. Now the optimal position of the sample must be found. This is the position in which the largest amount of x-rays

given off by the sample, are released towards the x-ray detector and not to other locations in the chamber.

1. Make sure that the desired accelerating voltage for imaging is selected.
2. Refer to section III, number 6 above for sample positioning control.
3. Adjust the X, Y, and Y' knobs on the chamber stage, to position the sample to a location where imaging is desired, while watching the image on the CRTs.
4. The tilt knob needs to be adjusted. The sample needs to be tilted while watching the CPS. A maximum position can be found and should be at an angle of about 45° (The tilt gauge is off by -10° , so it will read 35° when it is actually at 45°) for maximization.
5. Now the sample height needs to be adjusted by the Z and the Z' knobs. Toggle the switch by the magnification gauge to the W.D. position. As the sample is raised, it is brought closer the x-ray detector, so the counts will change. If the sample is to far from the detector, most of the x-rays released by the sample will under shoot the detector. But if the sample is to close to the detector, they will over shoot it. So there is a maximum position that should be found, It should be around 16 mm.

5. Increase magnification so that the desired area is displayed on the CRT screens.
6. Steps 4 – 6 may need to be repeated several times to obtain the best position for the sample, because the counts may change when the magnification changes.

Procedure for X-ray Spectrum Creation

1. Now push the enable button on the EDSG box to the left of the computer monitor.
2. The start button on the top left of the monitor with the little stopwatch should be clicked on with the mouse.
3. Select the spot size that makes the dead time between 25 and 30, on the bottom center of the computer monitor of the iDX screen.
4. If elements below Na are to be analyzed, the Be window must be opened. First push the lock button on the shaft below the LN₂ doer, and turn the knob to the open position (a red light on the Be window status box on the SEM table top should come on).
5. Step 10 may need to be repeated if the window was opened.
6. Now the x-ray spectrum that was discussed in section 2.?, can be created. First the spectrum needs to be cleared by clicking on the button with the little broom on it. Now a new

spectrum can be taken by clicking on the start button. The longer it runs the less noise the spectrum will have. To stop the scan, clicking the start button.

7. Click the peak identification button (button with the ? over the three peaks). Click the delete all button to clear all the elements in the two little widows. Now place the cursor on top of a peak of the spectrum and click on it. One or several elements should appear in the bottom window in the peak identification menu. Click on the element with the best fit and the click on the add button, the selected element should now appear in the top window.
8. Repeat step 7 until all peaks have been identified. This spectral graph may then be saved and printed for future use.

Procedure for Computer Image Creation

1. Once the spectral graph has been created and identifying the samples elements minimize eDX ZAF and maximize iDX.
2. To create an image on the computer, only the image appearing on the bottom CRT can be transferred to the computer. The signal select switch controls what image is displayed on this screen. Position A displays the secondary and B displays the backscattered images.

3. Once the desired image is on the bottom CRT, make sure that enable button on the EDSG box to the left of the computer monitor is light, which indicates that the signal is being transferred to the computer. A matrix of 125 X 200 or smaller should be selected by clicking on the down arrow beneath the matrix window on the right side of the screen and selecting one of them. Now the electron image collection button (the button with e^- on it) needs to be click on to start taking an image. The brightness and contrast below the bottom CRT screen will probably need to be adjusted for the computer image.
4. Once the contrast and brightness are set, the electron image collection needs to be clicked to stop the collection. A higher matrix should now be selected (the larger the matrix, the higher the quality of the image, but more time is required) and a new image collected as discussed in step 3.
5. To create x-ray images, click on the region of interest (ROI) button to the right of the peak identification button.
 - i. Type in the symbol of an element, which was found in the x-ray spectrum.
 - ii. Find that elements characteristic x-ray energy by looking it up on the table on the wall, and type in a starting energy and an ending energy. These energies

should be selected so that most of the peak will be covered.

- iii. Repeat steps i and ii until all ROI for the desired elements that are to be mapped, have been selected.
6. The x-ray collection button (button with the x) should be clicked. The collection can be stopped, by clicking on the collection button again, or it will stop when all frames have been completed, depending on the selected matrix, this could take several hours.
 7. These images can be saved and printed for latter use. But before they are saved, all the parameters should be entered into the image parameters in the edit menu. To print all of the images, they must be selected by clicking on them while the Ctrl button is pressed.

APPENDIX B

ION PUMP RESTART PROCEDURES

1. Make sure the filament is turned to ZERO.
2. Turn the accelerating voltage down until it reads OFF.
3. Make sure that the column isolation valve is closed.
4. Check the chamber pressure gauge. If the chamber is at high pressure, go to next step. If it is not, make sure that the chamber has not been vented. If so, make sure that the N₂ gas bottle is closed, then close chamber and apply pressure keeping it closed and push the chamber vent button. If chamber has not been vented, check the turbo pump and its controller to make sure that they are on. If they are on maintenance will be needed before continuing.
5. Flip the gun ion pump power supply from protect to start, then push the rest button, turn meter range to keep the reading from going off scale. After a minute, flip toggle back to protect. This is to prevent overheating of the pump as the power supply runs current through it.
6. If the power supply stays on and does not overload for the next several hours, check every 30 minutes that the supply

has not overloaded, and is working properly. If it overloads then move to step 7, if it doesn't, the steps below can be skipped and the SEM can now be turned back on.

7. Open column isolation valve to allow turbo pump the pump the gun area.
8. Close the column isolation valve and repeat steps 5 – 7 after 30 minutes if the ion pump gauge is above 100mA, 15 minutes, if the gauge is reading between 20 and 100mA, and 10 minutes if it reads less than 20mA. This is to allow the pump to cool down and prevent over heating as the power supply runs current through it.

APPENDIX C

Faraday cup Construction procedure

- 1 Drill a 5/64-inch deep hole in an aluminum sample stub with a 5/64-inch bit as shown in figure A.7.
- 2 Clean stub and a Ted Pella, Inc. platinum 100 μm aperture with the following procedure:
 - i. Turned sonic to degas for 5 minutes at 40°C.
 - ii. Place stub and aperture in beaker of 100 mL of Micro and sonic for 5 minutes at 40°C.
 - iii. Rinse in 18 M Ω H₂O at 22°C twice.
 - iv. Place stub and aperture in beaker of 100 mL of acetone and sonic for 5 minutes at 40°C.
 - v. Place stub and aperture in beaker of 100 mL of isopropyl and sonic for 5 minutes at 40°C.
 - vi. Repeat step v.
 - vii. Remove stub and aperture from beaker and allow them to dry.
- 3 Carefully place the aperture on top of the drilled hole so that the sides of the hole are covered, leaving only the hole of the aperture as the only opening of the cup.

- 4 Place a drop of Ted Pella, Inc. Colloidal silver paint on the stub and carefully brush some paint around the aperture without moving the aperture or getting paint over the hole. This could cover the hole and block it.
- 5 Let paint dry before placing it in the SEM.

FARADAY CUP

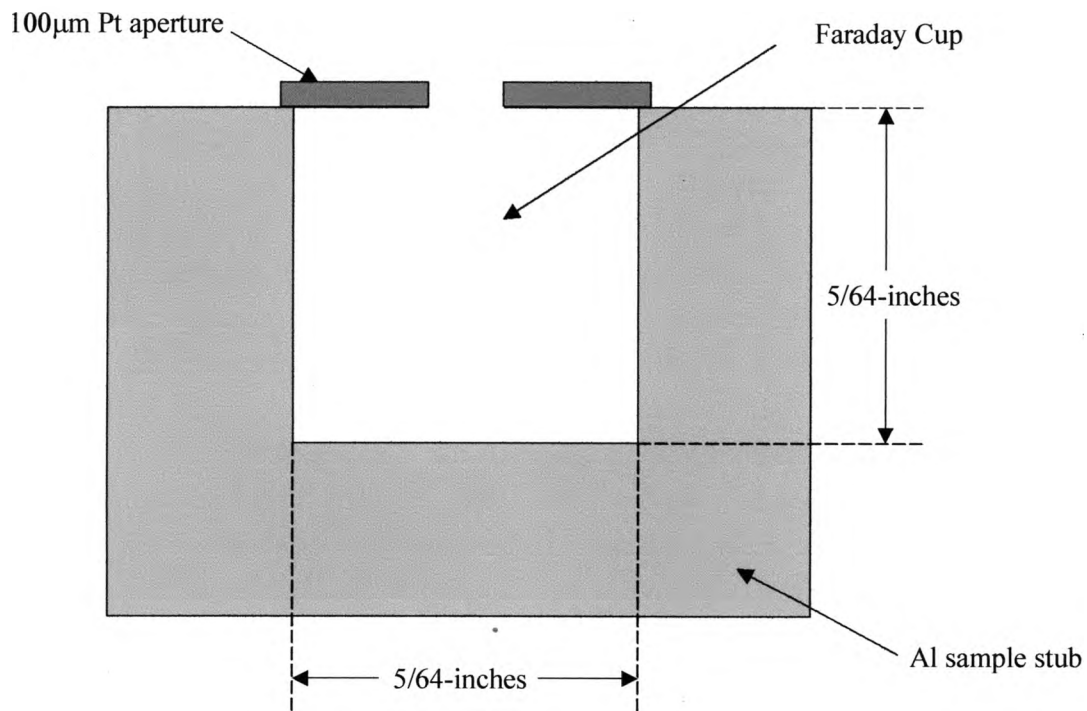


Figure A.7. Diagram of a cross-section of a Faraday cup for measuring SEM beam current.

APPENDIX D

BEAM CURRENT OF AMRAY MODEL 1400 WITH LaB₆ FILAMENT**Table A.1. Beam current obtained for given accelerating voltages and spot sizes.**

Accelerating Voltage(kV)	Spot Size	Beam Current(nA)	Accelerating Voltage(kV)	Spot Size	Beam Current(nA)
5	0	8.45	20	0	115.00
5	1	3.48	20	1	21.30
5	2	1.39	20	2	6.00
5	3	0.62	20	3	2.75
5	4	0.30	20	4	1.22
5	5	0.15	20	5	0.61
5	6	0.07	20	6	0.33
5	7	0.03	20	7	0.19
10	0	51.30	20	8	0.10
10	1	8.85	20	9	0.04
10	2	3.80	30	0	130.80
10	3	1.65	30	1	23.25
10	4	0.75	30	2	7.41
10	5	0.35	30	3	3.18
10	6	0.19	30	4	7.44
10	7	0.08	30	5	0.70
10	8	0.03	30	6	0.43
15	0	102.00	30	7	0.25
15	1	14.00	30	8	0.14
15	2	4.24	30	9	0.08
15	3	1.78	30	10	0.03
15	4	0.84			
15	5	0.48			
15	6	0.28			
15	7	0.16			
15	8	0.08			
15	9	0.03			

BIBLIOGRAPHY

- ¹D. C. Joy, *SEM Microcharacterization of Semiconductors* (Academic Press, San Diego, 1989).
- ²Oliver C. Wells, *Scanning Electron Microscopy* (McGraw-Hill Book Company, New York, 1974).
- ³J.W. S. Hearle, J. T. Sparrow, and P. M. Cross, *The Use of the Scanning Electron Microscope* (Pergamon Press Ltd., New York, 1972).
- ⁴Barbra L. Gabriel, *SEM: A User's manual for Materials Science* (American Society For Metals, Metals Park, Ohio, 1985).
- ⁵Joseph I. Goldstein, *Scanning Electron Microscopy and X-ray Microanalysis*, 2nd ed. (Plenum Press, New York, 1992).
- ⁶S. J. B. Reed, *Electron Microprobe Analysis and Scanning Electron Microscopy in Geology* (Cambridge University Press, New York, 1996).
- ⁷P. J. Goodhew, F. J. Humphreys, *Electron Microscopy and Analysis*, 2nd ed. (Taylor and Francis, New York, 1988).
- ⁸GW Electronics Incorporated Operation and Installation, Manual , 1981.
- ⁹Edax Service/Installation Manual , 1999.
- ¹⁰Varian Basic Vacuum Practice Report.
- ¹¹O'Hanlon, *A User's Guide to Vacuum Technology*, 2nd ed. (John Wiley and Sons, New York, 1989).
- ¹²Joel Brochure Report No. 1205G011, 1998.

VITA

Michael L. Matheaus was born on July 16, 1970 in Seguin, Texas to Frank and Jeanette Matheaus. After graduating from Navarro High School, Geronimo, Texas, in 1988, he enrolled at Southwest Texas State University in San Marcos Texas. During the summer of 1991 he started taking flying lessons and that fall entered the Air Force Reserve Officer Training Corps training program at SWT. In December of 1996 he received his Bachelor of Science Degree in Mathematics. He continued his education in the physics masters program at SWT in the spring of 1997. During the fall of 1998 he was assigned teaching duties. During the summer of 1999 he worked as a research assistant to Dr. Carlos Gutierrez. As a research assistant, some of his work was published as a coauthor in the May/June issue of Journal of Vacuum Science Technology.

Permanent Address: 1201 Haberle Rd.

Seguin, Texas 78155

This thesis was typed by Michael L. Matheaus.